*Ph.D. thesis*

# Luminescent lanthanide complexes

## for the sensing of relevant biomarkers

**Cycle XXXI**


| | |
|---|---|
| **Ph.D. candidate** | Georgina Faura Muñoz |
| **Supervisor** | Andrea Melchior |
| **Co-supervisor** | Marilena Tolazzi |


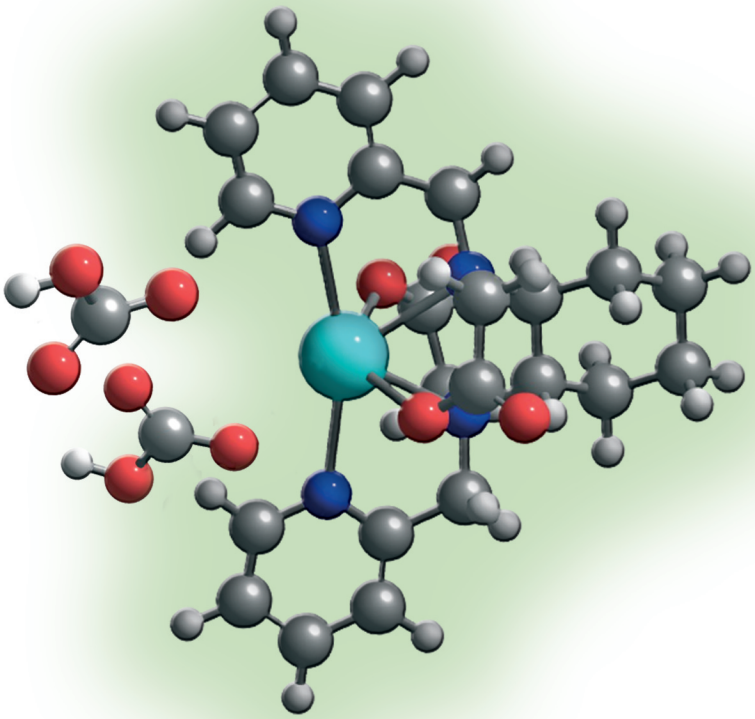


UNIVERSITÀ DEGLI STUDI DI UDINE

hic sunt futura

UNIVERSITÀ DEGLI STUDI DI UDINE
hic sunt futura

www.uniud.it

Doctor of Philosophy degree in
Environmental and Energy Engineering Science

Cycle XXXI

Title of the thesis

# "Luminescent lanthanide complexes for the sensing of relevant biomarkers."

Ph.D. candidate
Georgina Faura Muñoz

Supervisor
Prof. Andrea Melchior

Co-supervisor
Prof. Marilena Tolazzi

**2019**

*Nothing in life is to be feared, it is only to be understood.*
*Now is the time to understand more, so that we may fear less.*

***Marie Salomea Skłodowska Curie***

# Table of contents

# Acknowledgements

First of all, I would like to thank my supervisor Andrea Melchior and my co-supervisor Marilena Tolazzi, who gave me the opportunity to develop this Ph.D. thesis in the Thermodynamics and Modelling Research Group in University of Udine. Thank you for giving me the chance to mature and develop personally and professionally.

Secondly, I would like to thank very much the evaluation committee of this thesis for their insightful suggestions and comments.

I also would like to thank all the co-authors which contributed to the publications and communications related to this thesis. This manuscript would not have been possible without your hard and brilliant work and feedback. Special thanks to the Luminescent Materials Laboratory of University of Verona for receiving me in your research group and teaching me a lot about lanthanides and luminescence.

Thank you Pierluigi Polese for helping me (and everyone around him) in an endless list of things!

Thanks to all the PhD students that have been in the Thermodynamics and Modelling research group, to Cristian and Sara, for introducing me into the group and the labs, and accompanying me through the hard first months in Italy… without speaking Italian at all! Thank you Daniele, for always making me laugh in the hardest moments and making me see things from a positive point of view. Thank you Matteo, for supporting me in the last steps through this difficult and important part of my career. I also want to send my best wishes to Martina, the new Ph.D. candidate in our research group.

The path has felt much smoother with the company and support of the colleagues in University of Udine. I would like to specially thank Merlyn and our enjoyable 'slow-food' lunches together, Bruno 'the extra-kind newbie boy' who shared flat for a short time with me and Gerard, Ruben and Ehsan for your infinite kindness in and out of work.

Special thanks to Rabail and Hassib and the deep talks about the ‘little’ things that really matter, Maria for your unflagging support in the professional and personal field, Hari and the endless sushi lunches, Yamanappa and the coolest NMR videos in YouTube, Ashraf for your kind and wise words (and the *roti*!), Salvo for the infinite laughs (you are crazy and we both love that xD), Rosario for the nerd-touch I needed to survive here in Udine and Rossella, for the best coffee breaks in Yellow Pecora. And also to the rest of colleagues that, in one way or another, made me learn a lot about life.

Thank you all for the *apperitivi*, for the scientific and personal support, for the lunches and dinners together, for the good and bad moments, for the beers, for the laughs and, in short, for being there!

I could not finish this section without thanking all my family and friends in Spain (and Switzerland, and France, and United States, and Japan, and Germany…), who gave me so much support even from the distance… Candi, Pere, Ana, Anna, Irene, Marc, Mercè, Pili, Thomas, Maria, Ruby, Sergio, Sira, David, Ferran, Roger, Cristina, Mariona… (please, don’t kill me if I forgot someone!) I miss you all so much!

And a special THANK YOU for Gerard, who followed me to Italy from my second Ph.D. year and shared with me, more than nobody else, both the beers and the tears.

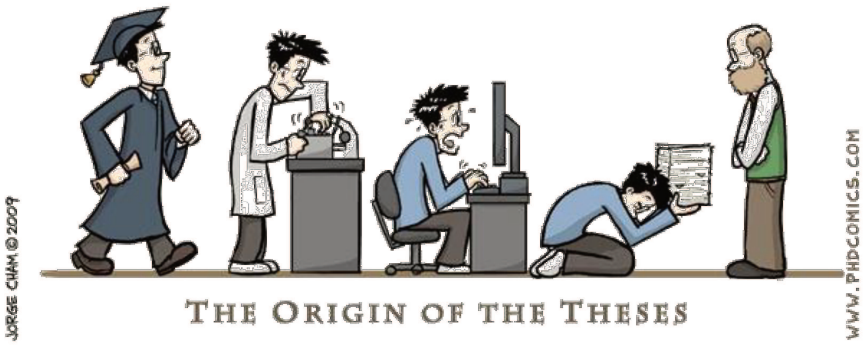

# Co-Authorship Statement

This thesis contains information included in papers previously published (reported in the Annex). The articles were collaborations of our research group, Thermodynamics and Modelling (Polytechnic Department of Engineering and Architecture, University of Udine), with Lorenzo di Bari's research group (Chemistry and Industrial Chemistry Department of the University of Pisa, Italy) and/or Fabio Piccinelli's Luminescent Materials Laboratory (Department of Biotechnology of the University of Verona, Italy).

Potentiometric, calorimetric (ITC titrations) and spectrophotometric (UV-Vis titrations) studies, along with computational studies (DFT) on the structure of the complexes, have been performed in University of Udine.

The synthesis of the ligands and most of the luminescent studies have been performed in University of Verona, where I had the opportunity to perform some luminescence experiments during a doctoral stay in their research group.

The circularly polarized light luminescence (CPL) studies have been performed in the University of Pisa.

# Abbreviations

| | |
|---|---|
| **BGS** | British Geological Survey |
| **Bic** | Bicarbonate |
| **Cit** | Citrate |
| **CPL** | Circularly polarized light |
| **CRT** | Cathodic Ray Tube |
| **DACH** | 1,2-diaminocyclohexane |
| **DFT** | Density Functional Theory |
| **DOE** | Department Of Energy |
| **EA** | Elemental analysis |
| **emf** | Electromotive force |
| **EPA** | Environmental Protection Agency |
| **ESI-MS** | Electrosptray ionization mass spectrometry |
| **EST** | Equilibrium speciation tool |
| **$IC_{50}$** | Half maximal inhibitory concentration |
| **ITC** | Isothermal titration calorimetry |
| **Lac** | Lactate |
| **LASER** | Light Amplification by Stimulated Emission of Radiation |
| **LED** | Light-Emitting Diode |
| **Ln** | Generic lanthanide |
| **LT** | Luminescent titration |
| **MRI** | Magnetic Resonance Imaging |
| **NMR** | Nuclear Magnetic Resonance |
| **PAPC** | Polyamino-Polycarboxylate |
| **PC** | Personal computer |
| **PET** | Positron Emission Tomography |

| | |
|---|---|
| **rac** | Racemic |
| **TBP** | tri-n-butylphosphate |
| **TV** | Television |
| **UV** | Ultraviolet light |
| **Vis** | Visible light |

# Abstract

Biomarkers are particular physiological characteristics which may indicate the presence of a disease in the organism. The abnormal concentration of certain anions in specific *locus* in the organism could be related to some illnesses or undesirable physiological conditions and, consequently, would act as a biomarker for the diagnosis and/or monitoring of these diseases. Luminescent trivalent lanthanide complexes have been extensively used as optical probes for this kind of biomarkers due to their peculiar spectroscopic properties.

In this work a library of lanthanide polyamino-polycarboxylate complexes with either pyridine or quinoline chromophore moieties with a 1,2-diaminocyclohexane backbone are studied. The formed complexes differ in charge, steric hindrance and lipophilicity, which strongly affect the stability and mobility/location of the complexes in the organism for the eventual performance of *in vitro* experiments in terms of cell viability and cell association.

All the complexes have been found to be highly stable in water at physiological pH, with the luminescent species being the predominant ones in all cases. In addition, it has been proved that some of the complexes are promising luminescent sensors for the detection of lactate, bicarbonate and citrate, which are relevant biomarkers for the diagnosis of some diseases. Moreover, preliminary simulations have been performed on the speciation of the most promising complex ($[Tb(bpcd)]^+$) in the presence of all the three anions at specific physiological concentrations. The complex appeared to have especial affinity for the citrate anion. All these results are of main importance in order to efficiently orientate forthcoming studies under more complex conditions (i.e. matrixes containing more potentially-interfering species) or on the use of these probes in *in vitro* experiments.

# Reading notes

**Chapter 1 Introduction to lanthanides -** Global introduction to lanthanides, their coordination chemistry and their luminescent properties.

**Chapter 2 Aim of this thesis**

**Chapter 3 Instrumentation and techniques -** Techniques and its principles, reagents and protocols used and treatment of the data.

**Chapter 4 Complexation and protonation -** Explanation on the choice of the ligands, results and discussion related to its equilibrium constants, structure and luminescence. Partial conclusions.

**Chapter 5 Luminescent sensing of relevant biomarkers -** This chapter is introduced by a short background about sensing of biomarkers. Then, it is separated in three main blocks: sensing of lactate, sensing of bicarbonate and sensing of citrate. Each block presents its own in-detail introduction/state of the art, results and discussion, and partial conclusions.

**Chapter 6 General conclusions and future outlook**

# Chapter 1

# Introduction to lanthanides

## 1.1. About lanthanides and their relevance

### 1.1.1. A brief history

From the end of the 18th century many complex oxides (formerly called 'earths') containing lanthanide mixes have been obtained from diverse minerals. In 1794, the Finnish chemist, physicist and mineralogist Johan Gadolin extracted one of these oxides from a black mineral (subsequently called gadolinite). From then, many lanthanide oxides have been separated from this mineral among others (Table 1.1.). However, at that time it was usual to fall into misidentifications due to the unreliable atomic masses. It was not until the 20th century when the English physicist Henry Moseley analysed the X-Ray spectra of elements and showed, by means of atomic number, that there were 15 elements from lanthanum to lutetium (Figure 1.1.). The last lanthanide found, the radioactive promethium, was discovered after Second World War.[1]

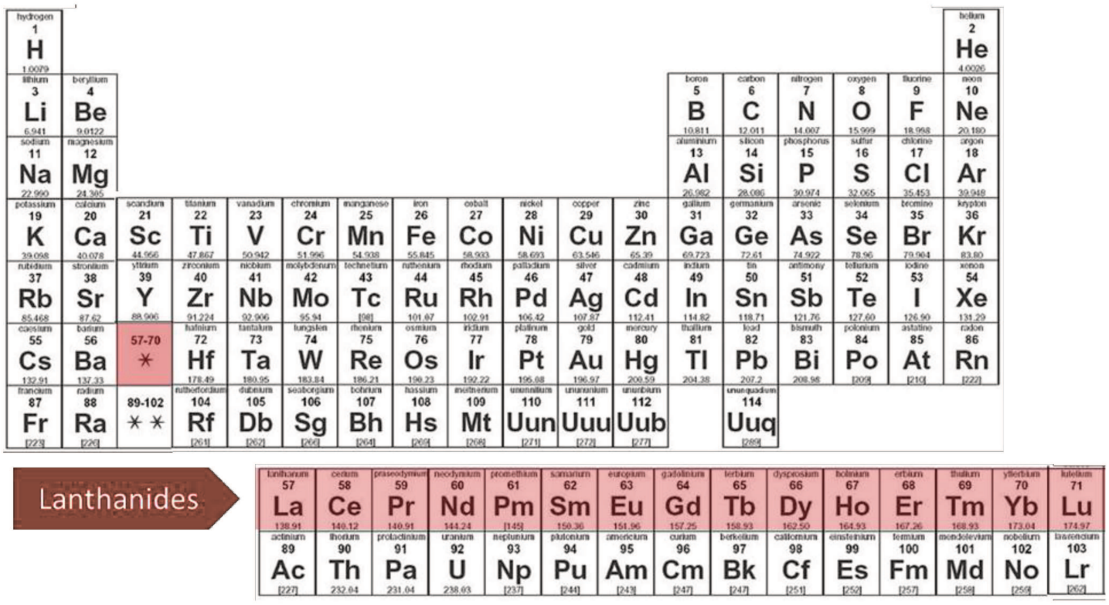


***Figure 1.1.*** *Situation of the lanthanide series in the periodic table.*

The term ‘rare earth’ has been commonly used since then to refer to lanthanides. This ‘earths’ were described as ‘rare’ due to the difficult identification and separation of these elements, chemically similar among them.[1]

### 1.1.2. Sources and supply risk

Lanthanides are still called ‘rare earths’ (Section 1.1.1.), even if they are not rare at all.[2–4] In fact, even the two least abundant non-radioactive lanthanides, in terms of crustal concentration (thulium and lutetium), are nearly 100 times more common than gold (Figure 1.2.).[5] This persistent misnomer is currently owed to their high supply risk (Figure 1.3.a), attributed to the heterogeneous distribution of its production among countries[4,6,7] (Figure 1.3.b) and the difficulty in extracting and purifying them from both, natural[1,6,8] (Table 1.1.) and anthropogenic[2,9–12] (Table 1.2.) sources.

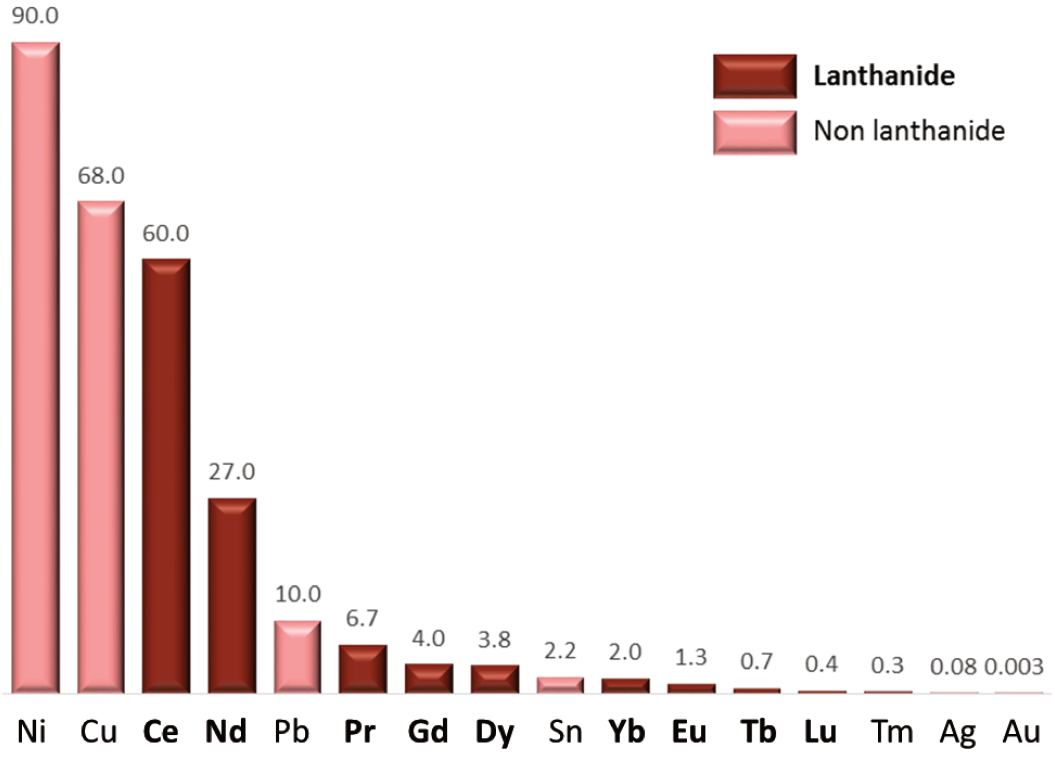


***Figure 1.2.*** *Abundance (in ppm) of some elements in Earth’s crust. From EPA (2012), USA.*

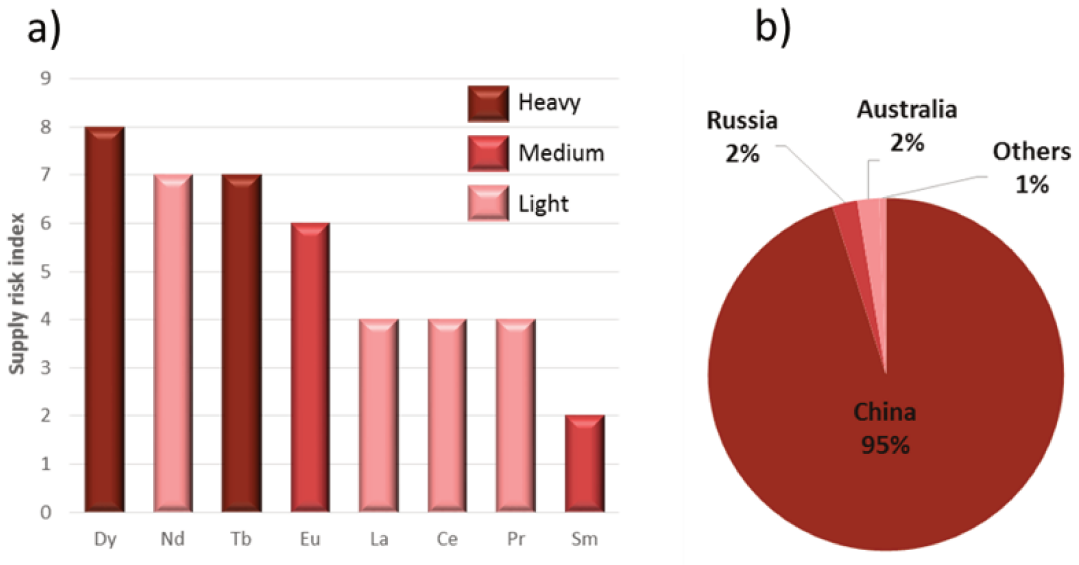


***Figure 1.3.*** *a) Supply risk estimated for some lanthanides between the years 2015-2030. DOE (2010), US. b) Production of rare earths around the world. From BGS (2013), UK.*

***Table 1.1.*** *Lanthanide minerals.*[1,6,7,13]

| Mineral | Main lanthanides |
|---|---|
| **Cerite** | La, Ce, Pr, Gd, Tb… |
| **Monazite** | Mostly all (except Pm) |
| **Bastnäsite** | Mostly all (except Pm) |
| **Laterite** | Mostly all (except Pm) |
| **Allanite (Orthite)** | La, Ce… |
| **Samarskite** | Ce, Nb… |
| **Gadolinite** | La, Ce,, Nd, Tb, Dy, Er |
| **Xenomite** | All (except Pm) |
| **Fergusonite** | Ce, Nd, Dy, Er… |
| **Euxenite** | Ce, Nb, Dy, Er… |
| **Polycrase** | Ce, Nb, Dy, Er… |
| **Blomstrandine** | Nb, Dy, Er… |
| **Pm** | Not naturally found on Earth. |
| **Lu** | Radioactive. |

***Table 1.2.*** *Lanthanides that may be present in some recycled end-of-live products.*[2,6,10]

| Recycled material | Lanthanides present |
|---|---|
| **NdFeB magnets**[a] | Pr, Nd, Gd, Tb, Dy |
| **SmCo magnets**[b] | Sm |
| **Plasma displays** | Eu, Gd |
| **LEDs** | Ce, Eu, Gd |
| **CRT screens** | Ce, Sm, Nd, Eu, Tb |
| **Fluorescent lamps** | La, Ce, Eu, Gd, Tb |
| **Oil refining catalyst** | La, Ce |
| **Auto catalysts** | La, Ce, Pr, Nd |
| **Batteries** | La, Ce, Pr, Nd, Sm |
| **Glass additives** | La, Ce, Pr, Nd |

[a] Hard disks, speakers, headphones, electric motors…

[b] Electric motors, NMR spectrometers…

The demand for lanthanides has increased dramatically due to their unique properties, which are of great importance in many sectors (refer to Section 1.1.3.). The United States once was self-sufficient in lanthanides, but over the last 30 years they become import-dependent, together with Europe.[4,5,14–16] Definitely, that turns the lanthanide issue into an important political and economic problem, as the most of the rare earth production is centred in China (Figure 1.3.b).[4,6,7] Therefore, the challenging recovery of lanthanides (and actinides) from end-of-life products (also called urban mining) and industrial waste streams has become an issue of concern to the scientific community, which has been increasing its efforts in this field during the last years.[2,6,11,17]

Industrial waste streams may also be considered. They present less than a 1% rare-earth oxide concentration but, as the waste volumes are huge, the total amount of *f*-block metals in this sources is significant.[9] The recycling of lanthanides and actinides cannot replace the mining of rare earth ores, but it can complement it, which would help balance the oversupply of lanthanum and cerium from some minerals for the production of the valuable neodymium,[10] indispensable for the miniaturization of everyday life electronic devices, such as mobile phones or hard disks.

### 1.1.3. Applications of lanthanides

Due to their particular nuclear, metallurgical, chemical, catalytic, electrical, magnetic, and optical properties (mostly determined by their unique intra-4*f* transitions), lanthanides have widespread importance in many sectors and are critical to hundreds of applications (Table 1.3).[3–6,10,18] In addition, several lanthanide applications are highly specific and (for the moment) irreplaceable. For instance, europium is used in computer monitors and televisions as the red phosphor. Nevertheless, fibre-optic cables present long distance performance thanks to some erbium-doped fibre lengths, which act as LASER amplifiers. Even if both lanthanides are very expensive (250 – 1700 $/kg for Eu, ~700 $/kg for Er), they cannot be replaced by cheaper materials, as they alone present the required optical properties.[5]

*Table 1.3. Some applications of lanthanides.*[5–7,10]

| Element | Applications |
|---|---|
| **La** | Fuel catalyst, fuel cells and batteries, optical lenses, night vision instruments, carbon-arc lamps, cigarette lighters, optical fibres, X-ray films, LASERs… |
| **Ce** | Automobile and petroleum refining catalyst, metallurgical industry, glass polishing, carbon-arc lamps, self-cleaning ovens, cigarette lighters, military applications… |
| **Pr** | Aircraft engines, cigarette lighters, carbon-arc lamps, fibre optic, glass colouring… |
| **Nd** | Magnets (cell phones, computers, air bags, MRI…), colouring pigments, surgical LASERs, cigarette lighters… |
| **Pm** | Not naturally found on Earth. |
| **Sm** | Durable permanent magnets, thermos-resistant (aerospace and military applications), carbon-arc lamps, neutron absorber… |
| **Eu** | LASERs, TV and PC monitors… |
| **Gd** | Magneto-optic recording, MRI, radiation detector, temperature and oxidation-resistant alloys, TV phosphors… |
| **Tb** | Fuel cells, fluorescent lamps, magneto-optic recording… |
| **Dy** | Motors (Next-generation vehicle, energy-conserving home electronics, wind power generators…), miniaturization of electronics, LASER… |
| **Ho** | Scarce. No commercial uses yet (unusual magnetic properties). |
| **Er** | Fibre optic, medical LASERs, pink glass colorant, metallurgy, nuclear industry… |
| **Tm** | The rarest. Very expensive. X-ray phosphors. |
| **Yb** | High electrical resistance under stress (stress monitoring). |
| **Lu** | Radioactive. Catalyst… |

## 1.2. Properties of lanthanides

### 1.2.1. Electronic configuration of lanthanides

Lanthanides are characterized by filling the 4*f* orbitals gradually along the series. The first two lanthanides, lanthanum (La) and cerium (Ce), present an exception to the Aufbau principle, by filling the 5d orbital before the 4f (Table 1.4.). This happens since the 5*d* subshell presents lower energy than the 4*f* in the case of these two atoms. From praseodymium (Pr) to lutetium (Lu), orbitals are filled following the Aufbau principle, except in the case of the eighth lanthanide, gadolinium (Gd), whose energy necessary to add an electron to the 5*d* orbital is lower than the necessary to 'break' the stable half-filling of the 4*f* orbital.[1]

Mostly all trivalent lanthanide (Ln(III)) ions are paramagnetic, as they present unpaired 4*f* electrons. La(III) and Lu(III) are exceptions, presenting $4f^{0}$ and $4f^{14}$ electronic configurations respectively (Table 1.4.). The seven unpaired electrons confer Gd(III) ($4f^{7}$) a high magnetic moment, which makes Gd(III) complexes very interesting for magnetism-related applications, such as MRI.[19]

### 1.2.2. 4*f* shielding and lanthanide contraction

The 4*f* electrons are more internal than the lower energy 5*s* and 5*p* ones. This results in the shielding of the 4*f* valence electrons from the ligands (they do not participate in bonds) and the marked independence of the spectroscopic and magnetic properties of lanthanides from the environment. Furthermore, the 4*f* orbital does not shield sufficiently the positive charges generated with increasing atomic number (z) along the lanthanide series. This generates a contraction of the outer orbitals (greater than expected) and the consequent more-than-expected decrease on the atomic and the Ln(III) ionic radii with increasing z (Table 1.5.). Some authors also attribute part of this so-called lanthanide contraction to relativistic effects (around 10% influence in the contraction).[1,20,21]

***Table 1.4.*** *Ground state electronic configurations of the lanthanide (Ln) atoms and their most common ions shown in correct order of orbital filling.*[22]

| Element | Ln | $Ln^{3+}$ | $Ln^{4+}$ | $Ln^{2+}$ |
|---|---|---|---|---|
| **La** | $[Xe]\ 5d^1\ 6s^2$ * | $[Xe]$ | | |
| **Ce** | $[Xe]\ 4f^1\ 5d^1\ 6s^2$ * | $[Xe]\ 4f^1$ | $[Xe]$ | |
| **Pr** | $[Xe]\ 4f^3\ 6s^2$ | $[Xe]\ 4f^2$ | $[Xe]\ 4f^1$ | |
| **Nd** | $[Xe]\ 4f^4\ 6s^2$ | $[Xe]\ 4f^3$ | $[Xe]\ 4f^2$ | $[Xe]\ 4f^4$ |
| **Pm** | $[Xe]\ 4f^5\ 6s^2$ | $[Xe]\ 4f^4$ | | |
| **Sm** | $[Xe]\ 4f^6\ 6s^2$ | $[Xe]\ 4f^5$ | | $[Xe]\ 4f^6$ |
| **Eu** | $[Xe]\ 4f^7\ 6s^2$ | $[Xe]\ 4f^6$ | | $[Xe]\ 4f^7$ |
| **Gd** | $[Xe]\ 4f^7\ 5d^1\ 6s^2$ * | $[Xe]\ 4f^7$ | | |
| **Tb** | $[Xe]\ 4f^9\ 6s^2$ | $[Xe]\ 4f^8$ | $[Xe]\ 4f^7$ | |
| **Dy** | $[Xe]\ 4f^{10}\ 6s^2$ | $[Xe]\ 4f^9$ | $[Xe]\ 4f^8$ | $[Xe]\ 4f^{10}$ |
| **Ho** | $[Xe]\ 4f^{11}\ 6s^2$ | $[Xe]\ 4f^{10}$ | | |
| **Er** | $[Xe]\ 4f^{12}\ 6s^2$ | $[Xe]\ 4f^{11}$ | | |
| **Tm** | $[Xe]\ 4f^{13}\ 6s^2$ | $[Xe]\ 4f^{12}$ | | $[Xe]\ 4f^{13}$ |
| **Yb** | $[Xe]\ 4f^{14}\ 6s^2$ | $[Xe]\ 4f^{13}$ | | $[Xe]\ 4f^{14}$ |
| **Lu** | $[Xe]\ 4f^{14}\ 5d^1\ 6s^2$ | $[Xe]\ 4f^{14}$ | | |

* Aufbau-anomalous electronic configurations

***Table 1.5.*** *Atomic and ionic radii of lanthanides and Yttrium (Å) reported by Shannon (1976).*[23] *Also a new set of ionic radii in aqueous solution obtained from EXAFS experimental data is reported (values marked with *).*[24] *CN: coordination number*

| Atom | CN | Ln | $Ln^{3+}$ | Atom | CN | Ln | $Ln^{3+}$ |
|---|---|---|---|---|---|---|---|
| **La** | 8 | 1.300 | 1.160 | **Tb** | 8 | 1.134 | 0.994 |
| | 9 | 1.356 | 1.216 | | 9 | 1.192 | 1.052 |
| | 10 | 1.41 | 1.27 | | | | 1.090* |
| | | | 1.250* | | | | |
| **Ce** | 8 | 1.283 | 1.143 | **Dy** | 8 | 1.167 | 1.027 |
| | 9 | 1.336 | 1.196 | | 9 | 1.223 | 1.083 |
| | 10 | 1.39 | 1.25 | | | | 1.075* |
| | | | 1.220* | | | | |
| **Pr** | 8 | 1.266 | 1.126 | **Ho** | 8 | 1.155 | 1.015 |
| | 9 | 1.319 | 1.179 | | 9 | 1.212 | 1.072 |
| | | | 1.200* | | 10 | 1.26 | 1.12 |
| | | | | | | | 1.055* |
| **Nd** | 8 | 1.249 | 1.109 | **Er** | 8 | 1.144 | 1.004 |
| | 9 | 1.303 | 1.163 | | 9 | 1.202 | 1.062 |
| | 10 | 1.41 | 1.27 | | | | 1.040* |
| | | | 1.175* | | | | |
| **Pm** | 8 | 1.233 | 1.093 | **Tm** | 8 | 1.134 | 0.994 |
| | 9 | 1.284 | 1.144 | | 9 | 1.192 | 1.052 |
| | | | | | | | 1.025* |
| **Sm** | 8 | 1.219 | 1.079 | **Yb** | 8 | 1.125 | 0.985 |
| | 9 | 1.272 | 1.132 | | 9 | 1.182 | 1.042 |
| | | | 1.140* | | | | 1.010* |
| **Eu** | 8 | 1.206 | 1.066 | **Lu** | 8 | 1.117 | 0.977 |
| | 9 | 1.260 | 1.120 | | 9 | 1.172 | 1.032 |
| | | | 1.120* | | | | 0.995* |
| **Gd** | 8 | 1.193 | 1.053 | **(Y)** | 8 | 1.159 | 1.019 |
| | 9 | 1.247 | 1.107 | | 9 | 1.215 | 1.075 |
| | | | 1.105* | | | | |

# 1.3. Coordination chemistry of Ln(III) in aqueous solution

## 1.3.1. Coordination chemistry

The most common oxidation state of lanthanides in aqueous solution is 3+. Lanthanide trivalent cations ($Ln^{3+}$) are small and present high charge density (they are hard acids); the heavier they are, the greater is its charge density, which causes heavier $Ln^{3+}$ to usually form complexes with higher stability than lighter ones.[1,25–28] As an example, we present the stability constants of some $Ln^{3+}$ with the broadly used ligands ethylene-diaminetetraacetic acid (EDTA) and diethylenetriaminepentaacetic acid (DTPA) (Figure 1.4.) in Table 1.6., where we observe an increasing trend on the stability constants with increasing atomic number.

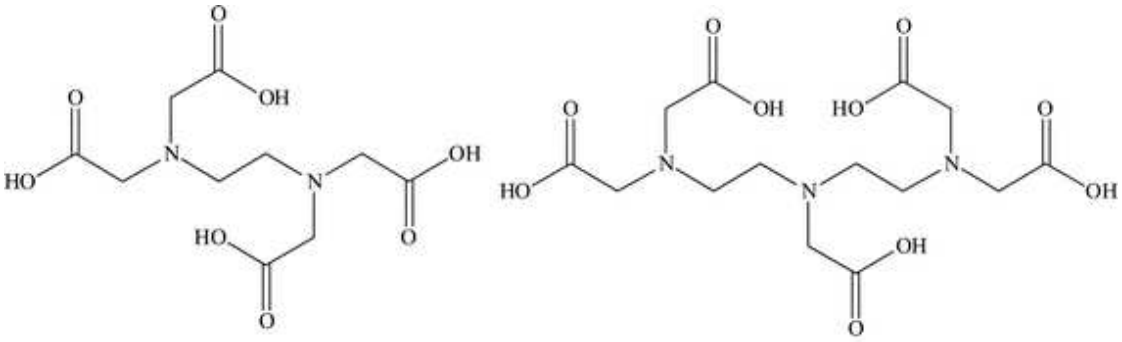


**$H_4$EDTA** **$H_5$DTPA**

***Figure 1.4.*** *$H_4$EDTA and $H_5$DTPA.*

***Table 1.6.*** *Stability constants (logβ) of some $Ln^{3+}$ in aqueous solution (at T = 298.15 K and μ = 0.1 M NaCl) with $EDTA^{4-}$ and $DTPA^{5-}$. Charges omitted for clarity.*

| Ligand | La | Ce | Pr | Nd | Sm | Eu | Gd | Tb | Dy | Ho | Er | Tm | Yb | Lu |
|---|---|---|---|---|---|---|---|---|---|---|---|---|---|---|
| **EDTA** | 15.46 | 15.94 | 16.36 | 16.56 | 17.10 | 17.32 | 17.35 | 17.92 | 18.28 | 18.60 | 18.83 | 19.30 | 19.48 | 19.80 |
| **DTPA** | 19.48 | 20.33 | 21.07 | 21.60 | 22.34 | 22.39 | 22.46 | 22.71 | 22.82 | 22.78 | 22.74 | 22.72 | 22.62 | 22.44 |

***μ:*** *Ionic strength, properly defined in Chapter 3.*

As hard acids, $Ln^{3+}$ present a strong affinity towards hard bases like neutral (i.e. ethers)[29] or negatively-charged (i.e. carboxylates)[30] O-donors and N-donors[29,31].[32–34] Due to that, the most popular ligands for the formation of strong Ln(III) complexes are polyamino-polycarboxylates (PAPC), which present both, negatively-charged O- and neutral N-donor atoms.[25,31,32,34–42] (Figures 1.5. and 1.6.) Thus, PAPC are broadly used in applications where higly stable Ln(III) complexes are needed, such as biomedical applications,[37,43–45] where ligands have to overcome the high stability of Ln(III) hydrates (Section 1.3.3.) and the presence of toxic free $Ln^{3+}$ in the body has to be avoided[34,46].

The stability of a complex is quantitatively related to its formation constant ($\log\beta$, properly defined in Section 3.2.1.2.), which is at the same time related to its free energy of formation ($\Delta G^0$, properly defined in Section 3.2.5.). $\Delta G^0$ depends on the formation enthalpy ($\Delta H^0$) and entropy ($\Delta S^0$) of the complex (Equation 3.13.). As hard acids, $Ln^{3+}$ ions usually present low enthalpies (either positive or negative) and high entropy values.[1,47] In other words, the formation of Ln(III) complexes is entropically driven. Thus, given the formation of a Ln(III) complex in water, represented in Equation 1.1., it is not difficult to deduce that a multidentate ligand (L, N=1, where N is associated to the number of ligand molecules, free or not) would displace more water molecules from the first coordination sphere than a monodentate one (N>1), which would cause at the same time the rising of *n* (associated to the number of 'free' water molecules) and, consequently, there would be a greater increment in entropy.[1,30,48] The low enthalpy values can be explained by the high stability of the Ln(III) hydrate complexes (Section 1.3.3.), which is similar to that of the Ln(III) complex.[30] Moreover, the formed complex presents a lower overall charge density, which reduces the additional ordination of the solvent in the second coordination sphere.

$$[Ln(H_2O)_x]^{3+}_{(aq)} + NL^{y-}_{(aq)} \rightleftharpoons [Ln(L)_N(H_2O)_{x-n}]^{(3-y)}_{(aq)} + nH_2O_{(l)} \qquad \textit{Equation 1.1.}$$

Actually, it is well known that polydentate ligands present higher stability than an equivalent amount of monodentate ligands presenting the same number and type of donor atoms.[49–51]

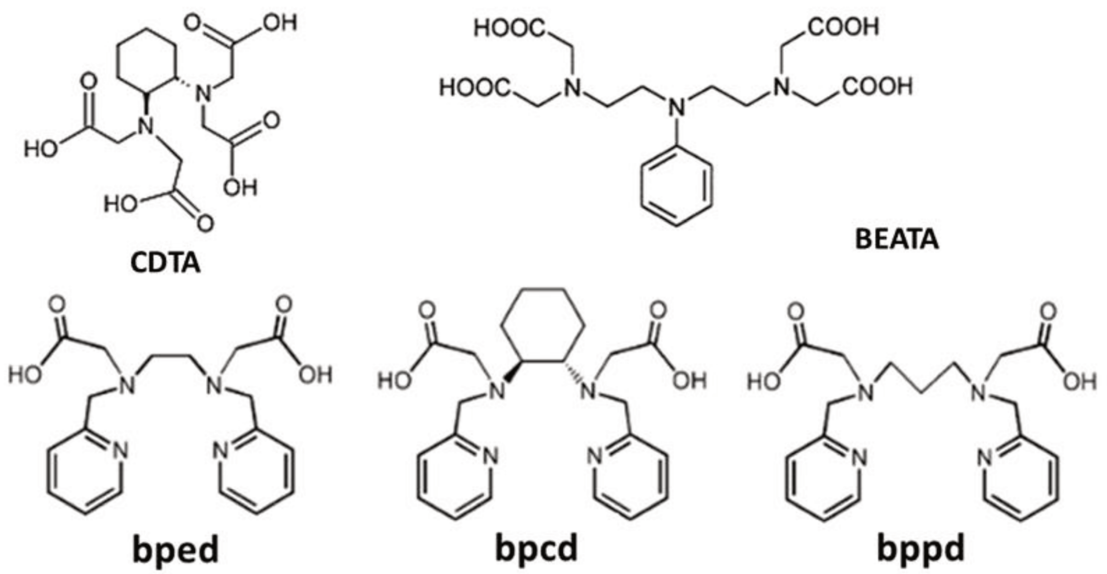


***Figure 1.5.*** *Open-chained PAPC ligands.* ***CDTA:*** *trans-1,2-diaminocyclohexane-N,N,N',N'-tetraacetic acid.* ***BEATA:*** *N,N-bis(2-aminoethyl)aniline-N,N,N',N'-tetraacetic acid.* ***bped:*** *N,N'-bis(2-pyridylmethyl)ethylenediamine- N,N'-diacetate.* ***bpcd:*** *N,N'-bis(2-pyridylmethyl)-trans-1,2-diaminocyclohexane-N,N'-diacetic acid.* ***bppd:*** *bis(2-pyridylmeth- yl)-1,3-diaminopropane diacetate.*

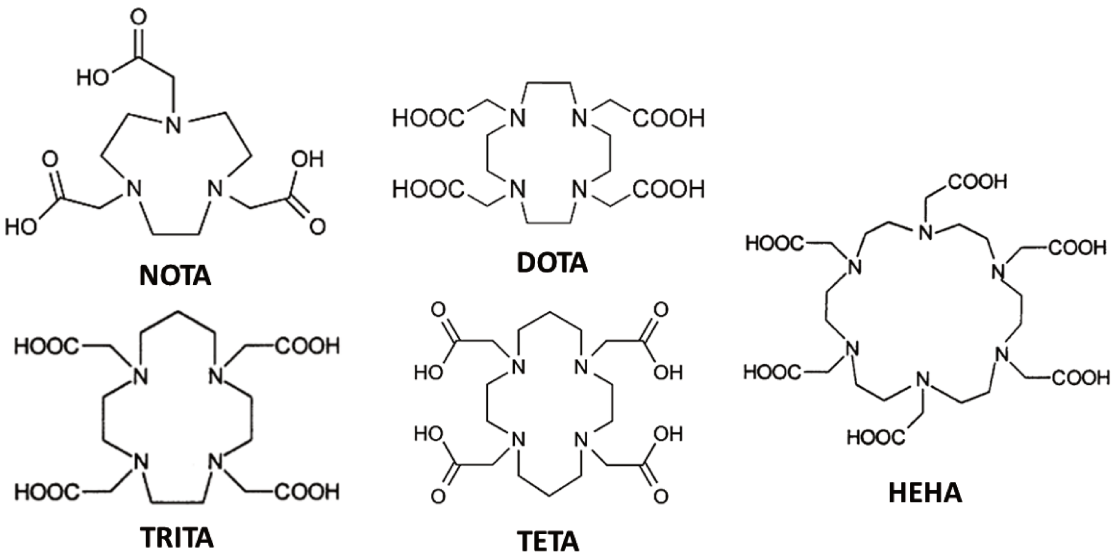


***Figure 1.6.*** *Macrocyclic PAPC ligands.* ***NOTA:*** *1,4,7-triazacyclono- nane-1,4,7-triacetic acid* ***TRITA:*** *1,4,7,10-tetraazacyclotetradecane-1,4,7,10-tetraacetic acid.* ***DOTA:*** *1,4,7,10-tetraazacyclododecane-1,4,7,10-tetraacetic acid.* ***TETA:*** *1,4,8,11-tetraaza-cyclotetradecane-1,4,8,11-tetraacetic acid.* ***HEHA:*** *1,4,7,10,13,16-hexaazacyclooctadecane-N, N', N'', N''', N'''', N''''-hexaacetic acid.*

Thus, the high thermodinamical stability of Ln(III) complexes with PAPC is also enhanced due to the multidentate nature of these ligands, which acts also as a chelating agent: polydentate ligands coordinate to the metal occupying at least two positions in the first coordination sphere, giving rise to cyclic structures which confer additional stability to the complex. The complexes presenting these cyclic structures are called chelated complexes, and the ligand that chelates the metal is called chelating agent.[30,47]

### 1.3.2. Coordination numbers, bonding and geometry

Lanthanide coordination numbers (CN) are diverse and may be rather large, presenting values usually from 6 to 12, but also lower values (2-3)[1] are known.[1,21,52–54] CN also depends on the $Ln^{3+}$ radius and strongly on the ligand. In other words, CNs depend mainly on steric factors rather than crystal field effects, principally due to the shielding of the 4*f* valence electrons, which lightly contribute in the formation of the bonds.[46,54] Therefore, lanthanide complexes have a strong ionic character and, consequently, their bonds are rather labile and largely electrostatic.[32,46]

Thus, the prediction of the geometry and the speciation of lanthanide complexes is not trivial; there are not strong directional forces that dictate unambiguous coordination geometries and some factors, such as steric effects, and electrostatic attraction/repulsion, may become of main importance.[1,46,52,55] For instance, regarding electrostatic effects, for small ligands (namely water, hydroxide or halides) the CN depends on the amount of ligands fitting around the metal without repulsing each other (first-order effects). On the other hand, and regarding steric effects, large ligands difficult large CNs due to their bulky surroundings (second-order effects).[1,45]

### 1.3.3. $Ln^{3+}$ in water

When the number of donor atoms of the complexing ligand is low, the complex may complete its coordination sphere with solvent molecules (e.g. water). $Ln^{3+}$ ions easily form hydrated complexes, as they present very high hydration free energies (table 1.7.).[1]

In former studies, the CN of lanthanides with water in aqueous solution was thought to be 9 for the early lanthanides (La-Sm) and 8 for the later ones (Dy-Lu), with intermediate lanthanides (Eu, Gd and Tb) showing either of both or mixtures in equilibrium (the so-

called gadolinium break).[1,23] But recent studies[24] affirm that n = 9 for all $[Ln(H_2O)_n]^{3+}$ in aqueous solution, except for Ln = Lu (n = 8).

***Table 1.7.*** *Hydration free energies ($-\Delta G^0_{hyd}$ (kJ/mol))[38] of $Ln^{3+}$ ions.*

| | La | Ce | Pr | Nd | Sm | Eu | Gd | Tb | Dy | Ho | Er | Tm | Yb | Lu |
|---|---|---|---|---|---|---|---|---|---|---|---|---|---|---|
| $-\Delta G_{hyd}$ kJmol | 3300 | 3359 | 3392 | 3419 | 3490 | 3522 | 3539 | 3561 | 3600 | 3612 | 3632 | 3673 | 3702 | 3718 |

## 1.4. Luminescence of trivalent lanthanide complexes

### 1.4.1. Luminescence

Due to the Laporte-forbidden *f-f* transitions, lanthanides present particularly small absorption coefficients.[59] Thus, a photosensitation of the lanthanide luminescence is needed. To do so, an adequate ligand has to be chosen, presenting an organic antenna chromophore near the lanthanide cation capable to absorb the exciting light and efficiently transfer the energy to the metal centre. This process is called the antenna effect, and it is fundamental in the design of bright luminescent lanthanide complexes.[1,55,57,60]

In order to quantify the photosensitizing efficiency of the ligand, the term quantum yield ($\Phi$) is used. The total quantum yield ($\Phi_{tot}$) is the product of i) the intersystem crossing ($\Phi_{ISC}$), ii) the energy transfer ($\Phi_{ET}$) and iii) the lanthanide luminescence ($\Phi_{Ln}$) (Equation 1.2.).[46]

$$\Phi_{tot} = \Phi_{ISC} \cdot \Phi_{ET} \cdot \Phi_{Ln} \qquad \textit{(Equation 1.2.)}$$

The generally accepted photosensitation mechanism in lanthanide complexes is shown, in a simplified way, in Figure 1.7., where the $\Phi$ components are represented in their corresponding steps. It is important that the lower triplet state of the antenna presents higher energy ($\Delta E \geq 1850$ cm$^{-1}$) than the highest luminescent state of the lanthanide cation, in order to avoid back energy transfer to the antenna's triplet state. But, at the same time, the gap has to be as low as possible in order to assure the highest $\Phi$.[61]

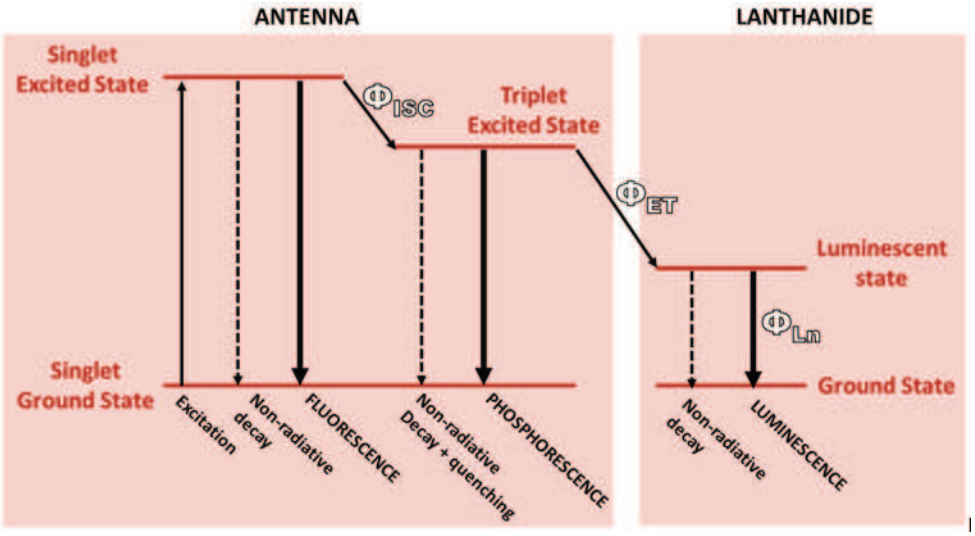


***Figure 1.7.*** *Energy conversion process (antenna effect) in luminescent lanthanide complexes.*

High $\Phi_{tot}$ values are also related to a large energy gap between the highest ground state level and the lowest excited energy level (radiative energy level) of the lanthanide ion. As it can be seen in the adapted Dieke's diagram in Figure 1.8. (modified from literature)[62], the lanthanide ions presenting the largest gaps are Eu(III), Gd(III) and Tb(III). Consequently, they present the strongest luminescence among the lanthanides and their luminescent complexes are less affected by the quenching effect caused by the O-H vibrations of water molecules.[63] This is of main importance when working in bioapplications such as the sensing of biomarkers, as they have to show good performance in aqueous solution. Among those three Ln(III), Eu(III) and Tb(III) are the most used for luminescent applications, as Gd(III) emits into the UV region (310nm), which incites undesired background fluorescence from biological matrices and hinders its use in bioapplications. On the other hand, Eu(III) and Tb(III) emit into the visible spectra.[46,55,57,63]

Absorption and luminescence spectra are unusually sharp for lanthanide complexes due to the formally forbidden nature of the *f-f* electronic transitions, and they remain mostly unaffected by the environment (Figure 1.9.).[46,55,64,65] Ln(III) also exhibit long luminescence lifetimes ($10^{-6} \rightarrow 10^{-3}$ s, organic dyes usually present $10^{-9}$ s lifetimes). This fact is especially interesting for its use in bioapplications, as the undesired short-lived background luminescence from the biological matrix may be avoided by using time-delayed spectroscopic techniques (Figure 1.10.).[46,60,63,64]

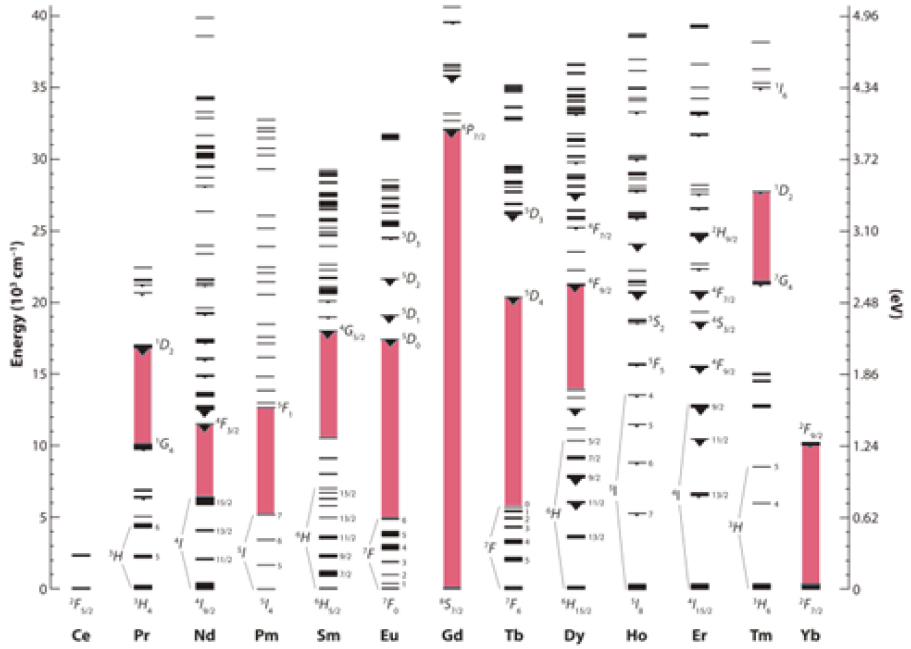


***Figure 1.8.*** *Modified Dieke energy diagram of some $Ln^{3+}$, from literature*[62]*. Largest energy gaps shaded in red.*

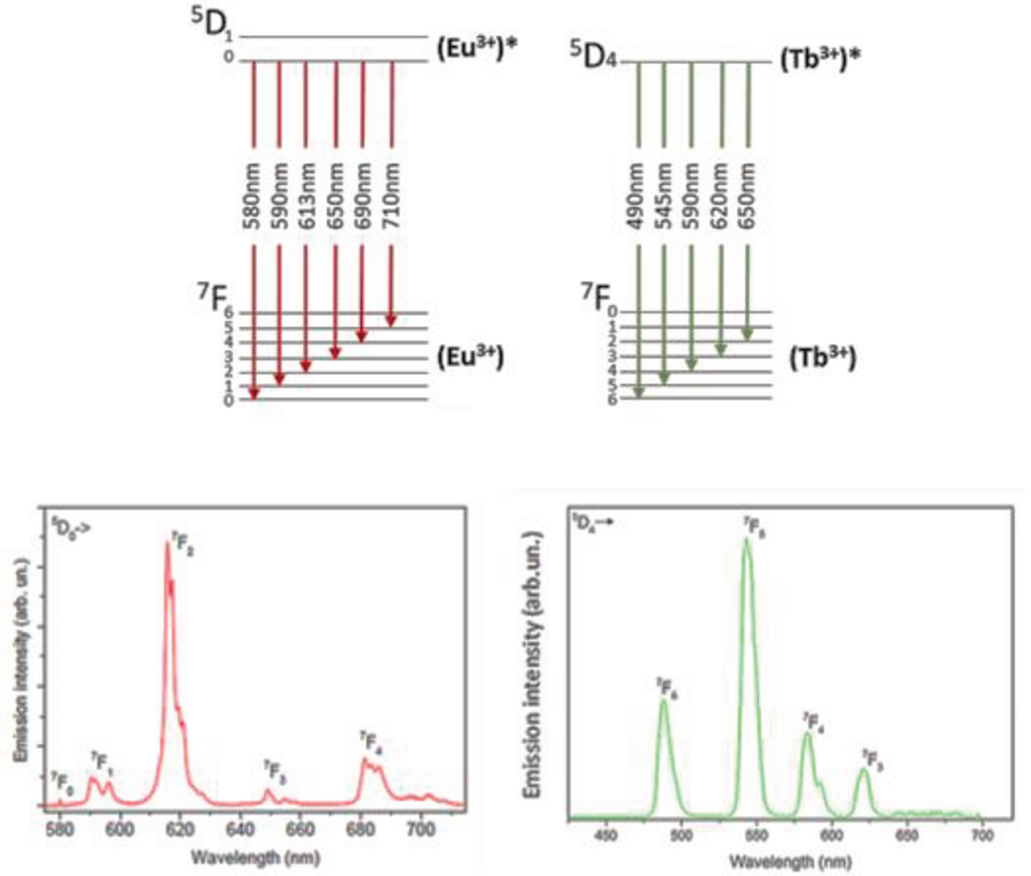


***Figure 1.9.*** *Eu(III) and Tb(III) 4f-4f transitions and their typical emission wavelengths (top, redrawn*[46]*); emission spectra of Eu(III) (bottom left) and Tb(III) (bottom right).*

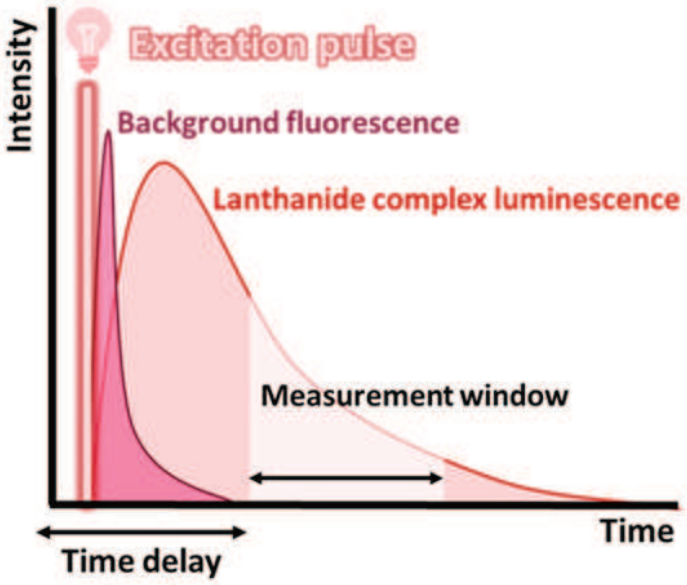


***Figure 1.10.*** *Graphic explanation of the time-delayed (or time-gated) measures, redrawn*[64].

## 1.4.2. Luminescent sensing of biomarkers

Biomarkers are defined as '*a characteristic that is objectively measured and evaluated as an indicator of normal biologic processes, pathogenic processes, or pharmacologic responses to a therapeutic intervention*'. One of these 'characteristics' may be the concentration of certain molecules in the organism which, in abnormal concentrations, may indicate the presence of a disease. Thus, they are very useful for the screening, early diagnosis and monitoring of many illnesses.[66]

Luminescent trivalent lanthanide complexes have been extensively used as probes for biomarkers due to their exceptional optical properties which have been already discussed. For instance, the determination of pH in cells and tissues is of main importance in analytical, biomedical and diagnostic studies, as it is a crucial feature for many physiological activities. In luminescent Ln(III) complexes, protonation or deprotonation of the antenna moieties can lead to perceptible changes in the energy absorption and/or transfer to the metal, which generates a noticeable change on the emission intensity (Figure 1.11.). Most pH luminescent sensors are developed regarding that pH dependence,[60,67,68] and many recent examples of pH sensors and pH-regulated Ln(III) complexes for imaging applications can be found in literature [69–72].

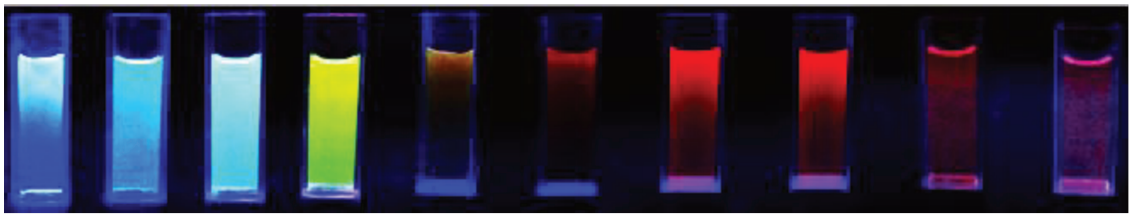

***Figure 1.11.*** *Emission colour changes of a mixture of an Eu(III) and Tb(III) complex in water from pH 3 (left) to pH 12 (right).*[69]

Several recent studies found in literature present also the development of Ln(III) complexes for the sensing of amino acids, proteins and nucleic acid probes, which are definitely relevant for the study of metabolic reactions, enzymatic activity, anticancer reactions and gene therapy among others.[67,73–76] Also numerous luminescent Ln(III) complexes have been designed for the detection and quantification of many metal ions[77–79] and some anions, such as phosphate,[80–83] lactate,[28,66,84] or bicarbonate,[85,86] due to its importance for the early diagnosis of some diseases. These anionic biomarkers are usually detected via the substitution of the water molecules found in the first coordination sphere by the target anion, which causes the rising of the luminescent signal,[84,87,88] but they may also be based on, for instance, the change in the distance between the antenna moiety and the metal centre[64].

The luminescent sensing of biomarkers will be further discussed in Chapter 5.

## 1.5. References


[1] S. Cotton, *Lanthanide and Actinide Chemistry*, John Wiley & Sons, Ltd, **2006**.

[2] C. Tunsu, M. Petranikova, M. Gergorić, C. Ekberg, T. Retegan, *Hydrometallurgy* **2015**, *156*, 239–258.

[3] F. Xie, T. A. Zhang, D. Dreisinger, F. Doyle, *Miner. Eng.* **2014**, *56*, 10–28.

[4] A. Golev, M. Scott, P. D. Erskine, S. H. Ali, G. R. Ballantyne, *Resour. Policy* **2014**, *41*, 52–59.

[5] G. B. Haxel, J. B. Hedrick, G. J. Orris, *United States Geol. Surv. Fact Sheet* **2002**, *087*, 4.

[6] T. Dutta, K. H. Kim, M. Uchimiya, E. E. Kwon, B. H. Jeon, A. Deep, S. T. Yun, *Environ. Res.* **2016**, *150*, 182–190.

[7] C. Hurst, *Inst. Anal. Glob. Secur.* **2010**, 43.

[8] F. J. Alguacil, F. Rodríguez, *Rev. Metal.* **1997**, *33*, 187–196.

[9] K. Binnemans, P. T. Jones, B. Blanpain, T. Van Gerven, Y. Pontikes, *J. Clean. Prod.* **2015**, *99*, 17–38.

[10] K. Binnemans, P. T. Jones, B. Blanpain, T. Van Gerven, Y. Yang, A. Walton, M. Buchert, *J. Clean. Prod.* **2013**, *51*, 1–22.

[11] Y. Wu, X. Yin, Q. Zhang, W. Wang, X. Mu, *Resour. Conserv. Recycl.* **2014**, *88*, 21–31.

[12] I. De Michelis, F. Ferella, E. F. Varelli, F. Vegliò, *Waste Manag.* **2011**, *31*, 2559–2568.

[13] "Mineralogy database," can be found under https://www.mindat.org/, **2018**.

[14] ad-hoc Working group on defining critical raw materials, *Eur. Commision* **2014**, 1–205.

[15] European Comission, "Critical Raw Materials," can be found under http://ec.europa.eu/growth/sectors/raw-materials/specific-interest/critical_es, **n.d.**

[16] N. T. Nassar, X. Du, T. E. Graedel, *J. Ind. Ecol.* **2015**, *19*, 1044–1054.

[17] I. Anastopoulos, A. Bhatnagar, E. C. Lima, *J. Mol. Liq.* **2016**, *221*, 954–962.

[18] K. Wang, H. Adidharma, M. Radosz, P. Wan, X. Xu, C. K. Russell, H. Tian, M. Fan, J. Yu, *Green Chem.* **2017**, 4469–4493.

[19] P. Caravan, J. J. Ellison, T. J. McMurry, R. B. Lauffer, *Chem. Rev.* **1999**, *99*, 2293–2352.

[20] P. S. Bagus, Y. S. Lee, K. S. Pitzer, *Chem. Phys. Lett.* **1975**, *33*, 408–411.

[21] P. Pyykkö, *Chem. Rev.* **1988**, *88*, 563–594.

[22] K. T. Rim, K. H. Koo, J. S. Park, *Saf. Health Work* **2013**, *4*, 12–26.

[23] R. D. Shannon, *Acta Crystallogr. Sect. A* **1976**, *32*, 751–767.

[24] P. D'Angelo, A. Zitolo, V. Migliorati, G. Chillemi, M. Duvail, P. Vitorge, S. Abadie, R. Spezia, *Inorg. Chem.* **2011**, *50*, 4572–4579.

[25] P. Di Bernardo, A. Melchior, M. Tolazzi, P. L. Zanonato, *Coord. Chem. Rev.* **2012**, *256*, 328–351.

[26] Z. Li, Y. Zhang, B. Shuter, N. M. Idris, *Langmuir* **2009**, *25*, 12015–12018.

[27] P. Thakur, J. L. Conca, L. J. Van De Burgt, G. R. Choppin, *J. Coord. Chem.* **2009**, *62*, 3719–3737.

[28] G. Tian, L. R. Martin, L. Rao, *Inorg. Chem.* **2010**, *49*, 10598–10605.

[29] S. Kannan, M. A. Moody, C. L. Barnes, P. B. Duval, *Inorg. Chem.* **2008**, *47*, 4691–4695.

[30] H. Kitano, Y. Onishi, A. Kirishima, N. Sato, O. Tochiyama, *Radiochim. Acta* **2006**, *94*, 541–547.

[31] M. G. B. Drew, M. R. S. Foreman, M. J. Hudson, K. F. Kennedy, *Inorganica Chim. Acta* **2004**, *357*, 4102–4112.

[32] P. Di Bernardo, A. Melchior, M. Tolazzi, P. L. Zanonato, *Coord. Chem. Rev.* **2012**, *256*, 328–351.

[33] D. L. Ramasamy, V. Puhakka, E. Repo, S. Khan, M. Sillanpää, *Chem. Eng. J.* **2017**, *324*, 104–112.

[34] A. Bianchi, L. Calabi, F. Corana, S. Fontana, P. Losi, A. Maiocchi, L. Paleari, B. Valtancoli, *Coord. Chem. Rev.* **2000**, *204*, 309–393.

[35] A. De Bettencourt-Dias, P. S. Barber, S. Viswanathan, *Coord. Chem. Rev.* **2014**, *273–274*, 165–200.

[36] R. Ferreirós-Martínez, D. Esteban-Gómez, C. Platas-Iglesias, A. de Blas, T. Rodríguez-Blas, *Dalton Trans.* **2008**, 5754–65.

[37] R. Janicki, A. Mondry, P. Starynowicz, *Coord. Chem. Rev.* **2017**, *340*, 98–133.

[38] M. Regueiro-Figueroa, D. Esteban-Gõmez, A. De Blas, T. Rodríguez-Blas, C. Platas-Iglesias, *Chem. - A Eur. J.* **2014**, *20*, 3974–3981.

[39] M. D. Ogden, S. I. Sinkov, G. P. Meier, G. J. Lumetta, K. L. Nash, *J. Solution Chem.* **2012**, *41*, 2138–2153.

[40] N. Chatterton, C. Gateau, M. Mazzanti, J. Pécaut, A. Borel, L. Helm, A. Merbach, *Dalton Trans.* **2005**, 1129–1135.

[41] Y. Inomata, T. Sunakawa, F. S. Howell, **2003**, *648*, 81–88.

[42] C. C. McLauchlan, J. Florián, D. S. Kissel, A. W. Herlinger, *Inorg. Chem.* **2017**, *56*, 3556–3567.

[43] F. Caillé, C. S. Bonnet, F. Buron, S. Villette, L. Helm, S. Petoud, F. Suzenet, É. Tóth, *Inorg. Chem.* **2012**, *51*, 2522–2532.

[44] J. M. Couchet, J. Azéma, C. Galaup, C. Picard, *J. Lumin.* **2011**, *131*, 2735–2745.

[45] E. Brunet, O. Juanes, R. Sedano, J. C. Rodríguez-Ubis, *Tetrahedron Lett.* **2007**, *48*, 1091–1094.

[46] M. C. Heffern, L. M. Matosziuk, T. J. Meade, *Chem. Rev.* **2014**, *114*, 4496–4539.

[47] A. Braibanti, V. Carunchio, *I Complessi Metallici in Soluzione*, Roma, **1999**.

[48] G. R. Choppin, P. Thakur, J. N. Mathur, *Comptes Rendus Chim.* **2007**, *10*, 916–928.

[49] J. J. R. Frausto da Silva, *J. Chem. Educ.* **1983**, *60*, 390.

[50] E. G. Moschetta, K. M. Gans, R. M. Rioux, *J. Catal.* **2014**, *309*, 11–20.

[51] J. M. Idée, M. Port, C. Robic, C. Medina, M. Sabatou, C. Corot, *J. Magn. Reson. Imaging* **2009**, *30*, 1249–1258.

[52] G. Kauffman, *Coordination Chemistry of the Lanthanide Elements — One Hundred Years of Development and Understanding*, **1967**.

[53] S. A. Cotton, *Comptes Rendus Chim.* **2005**, *8*, 129–145.

[54] P. Caravan, T. Hedlund, S. Liu, S. Sjoberg, C. Orvig, *J. Am. Chem. Soc.* **1995**, *117*, 11230–11238.

[55] M. H. V. Werts, *Sci. Prog.* **2005**, *88*, 101–131.

[56] W. W. Lukens, M. Speldrich, P. Yang, T. J. Duignan, J. Autschbach, P. Kögerler, I. F. Galvan, N. Ferre, L. M. Frutos, L. Gagliardi, et al., *Dalt. Trans.* **2016**, *45*, 11508–11521.

[57] K. Binnemans, *Chem. Rev.* **2009**, *109*, 4283–4374.

[58] C. F. Ramogida, J. F. Cawthray, E. Boros, C. L. Ferreira, B. O. Patrick, M. J. Adam, C. Orvig, *Inorg. Chem.* **2015**, *54*, 2017–2031.

[59] A. Aebischer, F. Gumy, J.-C. G. Bünzli, *Phys. Chem. Chem. Phys.* **2009**, *11*, 1346–1353.

[60] J. C. G. Bünzli, *Chem. Rev.* **2010**, *110*, 2729–2755.

[61] M. Mihorianu, M. Leonzio, M. Monari, L. Ravotto, P. Ceroni, M. Bettinelli, F. Piccinelli, *ChemistrySelect* **2016**, *1*, 1996–2003.

[62] M. D. Chambers, D. R. Clarke, *Annu. Rev. Mater. Res.* **2009**, *39*, 325–359.

[63] J. Vuojola, T. Soukka, *Methods Appl. Fluoresc.* **2014**, *2*, DOI 10.1088/2050-6120/2/1/012001.

[64] M. L. Aulsebrook, B. Graham, M. R. Grace, K. L. Tuck, *Coord. Chem. Rev.* **2018**, *375*, 191–220.

[65] J. P. Leonard, T. Gunnlaugsson, *J. Fluoresc.* **2005**, *15*, 585–595.

[66] O. N. Okorie, P. Dellinger, *Crit. Care Clin.* **2011**, *27*, 299–326.

[67] X. Wang, H. Chang, J. Xie, B. Zhao, B. Liu, S. Xu, W. Pei, N. Ren, L. Huang, W. Huang, *Coord. Chem. Rev.* **2014**, *273–274*, 201–212.

[68] S. Shinoda, H. Tsukube, *Analyst* **2011**, *136*, 431–435.

[69] Z. Wang, J. Gao, K. Zhang, Z. Mai, Q. Wang, *Opt. Mater. (Amst).* **2018**, *81*, 1–6.

[70] Z. Zhou, C. C. Zhang, Y. Zheng, Q. Wang, *Dye. Pigment.* **2018**, *150*, 151–157.

[71] T. Xia, Y. Cui, Y. Yang, G. Qian, *ChemNanoMat* **2017**, *3*, 51–57.

[72] L. Zhang, A. F. Martins, P. Zhao, Y. Wu, G. Tircsó, A. D. Sherry, *Angew. Chemie - Int. Ed.* **2017**, *56*, 16626–16630.

[73] X. Wang, X. Wang, Y. Wang, Z. Guo, *Chem. Commun.* **2011**, *47*, 8127–8129.

[74] T. Hirayama, M. Taki, A. Kodan, H. Kato, Y. Yamamoto, *Chem. Commun.* **2009**, 3196–3198.

[75] A. M. Nonat, S. J. Quinn, T. Gunnlaugsson, *Inorg. Chem.* **2009**, *48*, 4646–4648.

[76] T. aki Uchida, K. Nozaki, M. Iwamura, *Chem. - An Asian J.* **2016**, *11*, 2415–2422.

[77] Z. Ye, G. Wang, J. Chen, X. Fu, W. Zhang, J. Yuan, *Biosens. Bioelectron.* **2010**, *26*, 1043–1048.

[78] D. Liu, K. Tang, W. Liu, C. Su, X. Yan, M. Tan, Y. Tang, *Dalt. Trans.* **2010**, *39*, 9763–9765.

[79] R. F. H. Viguier, A. N. Hulme, *J. Am. Chem. Soc.* **2006**, *128*, 11370–11371.

[80] X. Song, Y. Ma, X. Ge, H. Zhou, G. Wang, H. Zhang, X. Tang, Y. Zhang, *RSC Adv.* **2017**, *7*, 8661–8669.

[81] V. Borse, P. Jain, M. Sadawana, R. Srivastava, *Sensors Actuators, B Chem.* **2016**, *225*, 340–347.

[82] S. Nadella, J. Sahoo, P. S. Subramanian, A. Sahu, S. Mishra, M. Albrecht, *Chem. - A Eur. J.* **2014**, *20*, 6047–6053.

[83] A. T. Law Al, S. B. Adeloju, *Talanta* **2013**, *114*, 191–203.

[84] M. Leonzio, A. Melchior, G. Faura, M. Tolazzi, M. Bettinelli, F. Zinna, L. Arrico, L. Di Bari, F. Piccinelli, *New J. Chem.* **2018**, *42*, 7931–7939.

[85] R. P. Dellinger, M. M. Levy, A. Rhodes, D. Annane, H. Gerlach, S. M. Opal, J. E. Sevransky, C. L. Sprung, I. S. Douglas, R. Jaeschke, et al., *Intensive Care Med.* **2013**, *39*, 165–228.

[86] D. G. Smith, R. Pal, D. Parker, *Chem. - A Eur. J.* **2012**, *18*, 11604–11613.

[87] A. J. Harte, P. Jensen, S. E. Plush, P. E. Kruger, T. Gunnlaugsson, *Inorg. Chem.* **2006**, *45*, 9465–9474.

[88] R. S. Dickins, T. Gunnlaugsson, D. Parker, R. D. Peacock, *Chem. Commun.* **1998**, 1643–1644.

# Chapter 2

# Aim of this thesis

## 2.1. Aim

Trivalent lanthanide (Ln(III)) complexes present unique *f*→*f* transition properties. They can be used in complex biological matrices due to their long emission lifetimes, which permit the isolation of their emission from the undesired background fluorescence.[1]

Moreover, Eu(III) and mainly Tb(III) present low sensitivity to quenching caused by non-radiative absorbing species such as water, which makes them suitable for applications in aqueous media. Furthermore, the intensity of the luminescent response of these complexes is usually related to the concentration of target analyte,[2–7] and can be incremented by using ligands which promote the antenna effect.[2,3,8,9]

In view of all those particular proprieties, it is not surprising that Ln(III) complexes have been broadly studied for their use in several biomedical fields, such as medical diagnostics and luminescent sensing. Some of them, based on luminescent Eu(III) and Tb(III) complexes, have been successfully commercialized for the detection of relevant clinical biomarkers in biomedical diagnostics and imaging.[1]

The study of the stability, speciation and structure of these luminescent Ln(III) complexes in water is of main importance as:

- It is necessary to assure the stability of the proposed complexes in water, especially around pH 7.4, as probes have to be physiologically compatible.

- We have to guarantee that the luminescent Ln(III) complex is the predominant species in solution at pH 7.4 in order to assure that mostly all the luminescent response is due to that species.
- The structure of the Ln(III) complexes should present water molecules directly coordinated to the metal centre to permit the entrance of the anionic biomarkers into the inner coordination sphere by replacing the water molecules. This is of main importance, as it is actually how our biomarkers will be sensed, as already described in section 1.4.2..

In this work, a thoughtful library of Eu(III) and Tb(III) complexes has been studied potentiometrically, spectrophotometrically, calorimetrically and computationally in order to state their stability in water, their structure and their speciation at physiological pH. Furthermore, their viability as luminescent probes for the chosen anionic biomarkers has been studied by assessing their affinity for the target anions via calorimetric, luminescent and computational techniques, and their capacity for the actual sensing of these biomarkers by luminescent techniques.

## 2.2. References


[1] X. Wang, H. Chang, J. Xie, B. Zhao, B. Liu, S. Xu, W. Pei, N. Ren, L. Huang, W. Huang, *Coord. Chem. Rev.* **2014**, *273–274*, 201–212.

[2] M. H. V. Werts, *Sci. Prog.* **2005**, *88*, 101–131.

[3] S. Cotton, *Lanthanide and Actinide Chemistry*, John Wiley & Sons, Ltd, **2006**.

[4] J. C. G. Bünzli, S. Comby, A. S. Chauvin, C. D. B. Vandevyver, *J. Rare Earths* **2007**, *25*, 257–274.

[5] J.-C. G. Bünzli, *Coord. Chem. Rev.* **2015**, *293–294*, 19–47.

[6] S. A. Ansari, L. Liu, L. Rao, *Dalton Trans.* **2015**, *44*, 2907–14.

[7] G. Tian, L. R. Martin, L. Rao, *Inorg. Chem.* **2010**, *49*, 10598–10605.

[8] J. P. Leonard, T. Gunnlaugsson, *J. Fluoresc.* **2005**, *15*, 585–595.

[9] G. F. de Sá, O. L. Malta, C. de Mello Donegá, a. M. Simas, R. L. Longo, P. a. Santa-Cruz, E. F. da Silva, *Coord. Chem. Rev.* **2000**, *196*, 165–195.

# Chapter 3

# Instrumentation and techniques

## 3.1. Stock solutions and standardisation

### 3.1.1. Solvent

All the stock solutions were prepared with distilled water further purified with a Milli-Q system (>18 MΩ cm, ELGA Purelab Option-Q). Water was boiled before use in order to remove the solved atmospheric $CO_2$, which would act as a protolytic impurity (Equation 3.1.a and b).[1–4]

$$CO_{2(aq)} + H_2O_{(l)} \rightleftharpoons H_2CO_{3(aq)} \qquad \textit{Equation 3.1.a}$$

$$NaOH_{(aq)} + H_2CO_{3(aq)} \rightleftharpoons NaHCO_{3(aq)} + H_2O_{(l)} \qquad \textit{Equation 3.1.b}$$

### 3.1.2. Stock solutions

Fresh HCl and NaOH 0.1M stock solutions where prepared regularly with high purity commercial products. HCl was standardized by volumetric titration with the primary standard disodium tetraborate in the presence of methyl red indicator. NaOH was standardized with the freshly standardized HCl stock and phenolphthalein.

Eu(III) and Tb(III) stock solutions were prepared by dissolving their chloride hexahydrate salts. The lanthanide content in the stock solutions was determined by EDTA titration, using xylenol orange as indicator in a pH 5.5 acetic acid / acetate buffer.

The stock solution of L-lactate was prepared by diluting its sodium salt.

# 3.2. Determination of equilibrium constants

## 3.2.1. Principles and definitions

### 3.2.1.1. Activity and concentration

Given a generic species S, its activity and concentration can be related by using Equation 3.2., where $A_s$ is the activity of S, [S] is its concentration and $\gamma_s$ the activity coefficient of S, which is constant when the ionic strength (μ) and temperature ($T$) of the system are kept constant.[1,5]

$$A_s = \gamma_s \cdot [S] \qquad \textit{Equation 3.2.}$$

During the performance of our experiments, $T$ (298.15 K) and μ (0.1 M) are kept constant in order to deal with concentrations instead of activities. Thus, when we use some relevant concepts and equations, such as pH (Equation 3.3.a) and Nernst equation (Equation 3.4.a), we will take concentrations in consideration instead of activities. Therefore, instead of Equation 3.3.a we will use Equation 3.3.b (from now on, p[H] will be simply written as pH), and instead of Equation 3.4.a we will use Equation 3.4.b, where E is the observed emf, $E^0$ is the standard emf for the redox couple $S^{z+}/S^{(z-n)+}$, $n$ is the number of electrons involved in the reduction of S, R is the gas constant and F is the Faraday constant. $E^{0'}$ is a modified standard emf (Equation 3.4.c), and it will be written as $E^0$ from now on.

$$pH = -log\ a_{H^+} \qquad \textit{Equation 3.3.a}$$

$$p[H] = -log[H^+] \qquad \textit{Equation 3.3.b}$$

$$E = E^0 + \frac{RT}{nF} ln \frac{a_{S^{z+}}}{a_{S^{(z-n)+}}} \qquad \textit{Equation 3.4.a}$$

$$E = E^{0\prime} + \frac{RT}{nF} ln \frac{[S^{z+}]}{[S^{(z-n)+}]} \qquad \textit{Equation 3.4.b}$$

$$E^{0\prime} = E^0 + \frac{RT}{nF} ln \frac{\gamma_{S^{z+}}}{\gamma_{S^{(z-n)+}}} \qquad \textit{Equation 3.4.c}$$

### 3.2.1.2. Equilibrium constants

The equilibrium constant $K$ of a generic reaction (Equation 3.5.a) can be defined as the quotient between the activities of products and reactants (Equation 3.5.b) at equilibrium. But, as we have already discussed, as we are working at constant temperature and ionic strength, activities might be substituted by concentrations to give a modified $K'$ (Equation 3.5.c) which, from now on, will be simply called *K*.[1]

$$bB + cC \rightleftharpoons dD + eE \qquad \textit{Equation 3.5.a}$$

$$K = \frac{a_D^d \cdot a_E^e}{a_B^b \cdot a_C^c} \qquad \textit{Equation 3.5.b}$$

$$K' = \frac{[D^d] \cdot [E^e]}{[B^b] \cdot [C^c]} = K \qquad \textit{Equation 3.5.c}$$

Throughout this work, two different definitions of equilibrium constant will be used *K* (the already-defined stepwise equilibrium constant) and β (the overall equilibrium constant or formation constant). The former one is more intuitive and popular, and will be sometimes used for the comparison of the obtained results with bibliography. The latter one was used for computational purposes (definition required by the software used for the fitting of the constants) and will be defined hereafter.

Given a generic successive stepwise protonation, $K_1$, $K_2$ and $K_3$ can be defined (Equations 3.6.a-c).[1]

$$L^{3-} + H^+ \rightleftharpoons LH^{2-}\,; \quad K_1 = \frac{[LH^{2-}]}{[L^{3-}] \cdot [H^+]} \qquad \textit{Equation 3.6.a}$$

$$LH^{2-} + H^+ \rightleftharpoons LH_2^-\,; \quad K_2 = \frac{[LH_2^-]}{[LH^{2-}] \cdot [H^+]} \qquad \textit{Equation 3.6.b}$$

$$LH_2^- + H^+ \rightleftharpoons LH_3\,; \quad K_3 = \frac{[LH_3]}{[LH_2^-] \cdot [H^+]} \qquad \textit{Equation 3.6.c}$$

Given three overall protonation reactions for the same molecule, $\beta_1$, $\beta_2$ and $\beta_3$ can be defined (Equations 3.7.a-c). The mathematical relation between *K* and $\beta$ values are also shown in Equations 3.7.a-c. For simplicity, usually the logarithm of these constants is reported. The mathematical relation between *log K* and *log* $\beta$ values are easily deduced from Equations 3.7.a-c, and shown in Equations 3.8.a-c.[1]

$$L^{3-} + H^+ \rightleftharpoons LH^{2-}\ ; \quad \beta_1 = \frac{[LH^{2-}]}{[L^{3-}]\cdot[H^+]} = K \qquad \textit{Equation 3.7.a}$$

$$L^{3-} + 2H^+ \rightleftharpoons LH_2^-\ ; \quad \beta_2 = \frac{[LH_2^-]}{[L^{3-}]\cdot[H^+]^2} = K_1 \cdot K_2 \qquad \textit{Equation 3.7.b}$$

$$L^{3-} + 3H^+ \rightleftharpoons LH_3\ ; \quad \beta_3 = \frac{[LH_3]}{[L^{3-}]\cdot[H^+]^3} = K_1 \cdot K_2 \cdot K_3 \qquad \textit{Equation 3.7.c}$$

$$log\beta_1 = logK_1 \qquad \textit{Equation 3.8.a}$$

$$log\beta_2 = logK_1 + logK_2 \qquad \textit{Equation 3.8.b}$$

$$log\beta_3 = logK_1 + logK_2 + logK_3 \qquad \textit{Equation 3.8.c}$$

## 3.2.2. Acid-base titrations

### 3.2.2.1. Overview

Potentiometric and spectrophotometric acid-base titrations have been performed in order to obtain mostly all the equilibrium constants found during this work. When possible, potentiometry was used, as it is one of the most accurate and precise techniques for the determination of equilibrium constants, and one of the most used for this scope.[6] The recommended concentration of ligand to perform this technique with good results is around 1 mM.[1] Thus, when reaching the required concentration was not possible due to solubility problems or lack of the necessary amounts of ligand, spectrophotometric acid-base titrations where performed. The latter technique can also offer additional information about the protonation and complexation sites when the chromophore moieties of the molecule are involved (further explanation and examples in the forthcoming chapters).

### 3.2.2.2. Experimental

In order to keep ionic strength constant, all acid-base titrations were performed in 0.1 M NaCl. The titration cell was maintained at constant temperature (298.2 K ± 0.1 K) using a circulatory bath. The emf was collected by means of a combined glass electrode (Metrohm Unitrode 6.0259.100) connected to a computer-controlled potentiometer (Amel Instruments, 338 pH Meter). The initial solution was intensely bubbled with $N_2$ while the system was reaching thermal equilibrium. During experiments, a low $N_2$ flux was maintained over the closed system in order to avoid $CO_2$ from reaching the solution. The $N_2$ flux was previously passed through a NaOH trap in order to capture the eventual $CO_2$ present in the $N_2$. In the case of spectrophotometric titrations, also a fibre-optic probe, with a 10 mm path length, connected to a computer-controlled Varian Cary 50 instrument, was immersed into the solution in order to record absorbance data. NaOH was added by means of an automatic burette (Metrohm Dosimat 665) manually (spectrophotometry) or automatically (potentiometry). The solution was continuously gently stirred by means of a magnetic stirrer. The systems described have been schematized in Figure 3.1..

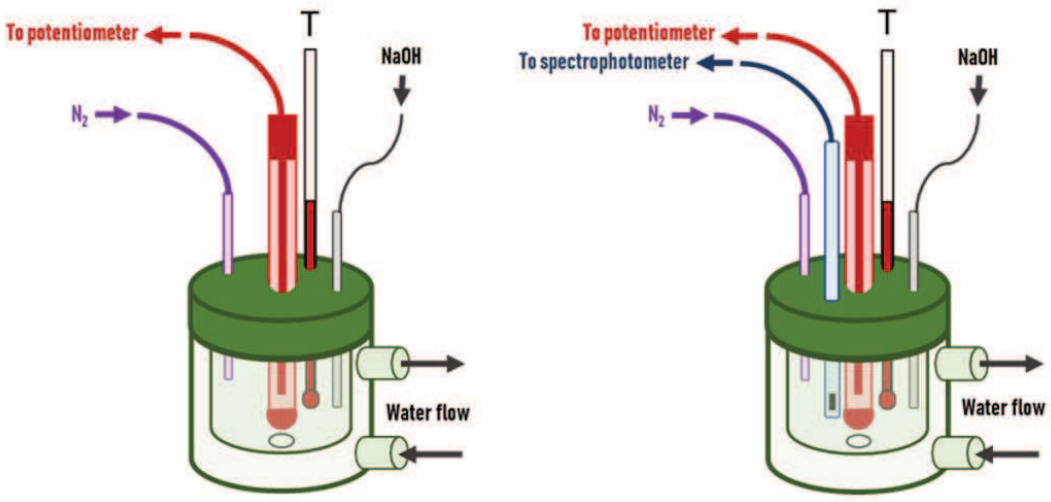


***Figure 3.1.*** *Schemes of the system for the performance of the a) potentiometric and b) spectrophotometric acid-base titrations.*

The electrode was calibrated potentiometrically (modified Nernst equation, Equation 3.4.b) before each titration by an acid-base titration with standard HCl and NaOH 0.1 M stock solutions and the carbon dioxide present in solution was checked by Gran method.[4,7] After calibration, the system was prepared for the protonation studies by reacidifying the system with HCl and adding the right amount of ligand. After this first acid-base titration, the solution was acidified again and the right amount of metal was added in order to prepare the system for the complexation studies (Figure 3.2.). This procedure was used in order to optimise the consumption of the precious ligands. In each titration, the solution was brought from an approximate pH value of 2.3 to about pH 11.5 (except in the case of earlier precipitation) by the addition of standard NaOH solution.

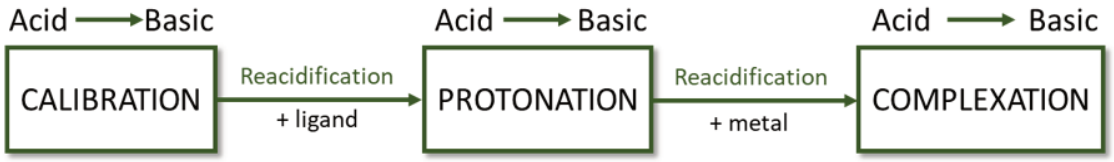


***Figure 3.2.*** *Overall scheme of the chain acid-base titrations performed for each complex.*

## 3.2.3. Potentiometric acid-base titrations

In potentiometry, the emf between two electrodes in contact with a solution is measured. This emf is affected by temperature and the species in solution, and is correlated to their activity. One of the electrodes is a reference one, which keeps its potential constant during the experiments. The other one is the indicator electrode, which has to be sensible towards the analyte of interest. Not always is possible to find an indicator electrode sensible towards the desired analyte but, fortunately, the system in equilibrium can usually be studied by following a competing species. For instance, in the case of the formation of a lanthanide complex, there will be competence between the $H^+$ and lanthanide cations during the acid-base titration toward ligand complexation and, thus, it is possible to study the system by following the $H^+$ cations instead of the lanthanide ones. As we have already mentioned, in this work a combined glass electrode has been used. It is both, the reference and the indicator electrode at the same time, and it is sensible towards the activity of $H^+$ cations.

Both the additions and the measurements where controlled by a personal computer. The inputs which defined the data acquisition where:

- Total volume of NaOH injected during the experiment.
- Volume step (fix or variable) and number of lectures.
- Dead time after the injection, before the reading.
- Delay time between readings (same injection).
- Maximum drift accepted between readings (same injection).
- Maximum number of readings for the same injection.

Titrations were performed on solutions containing the ligand (concentrations in the range 0.6-1 mM, depending on the experiment; for complexation studies, also 1:1 metal in solution) and an excess of HCl .

The emf data collected, the concentrations of the initial species (HCl, ligand and, eventually, metal), the initial volume, the temperature and the calibration data obtained previously are introduced in the Hyperquad program[8,9] in order to obtain the speciation model which better fits the experimental data. This program calculations are essentially based on a non-linear least-squares refinement, which minimizes the error ($U$) in each run ($i$) between calculated and experimental emf ($E$), giving less weight ($w$) to the data near the equivalence point (Equation 3.9.). $E_{calc}$ is obtained from Equation 3.4.b, where the modified standard emf and a slope factor, used to correct the deviation from the expected slope, $\left(\frac{RT}{nF}\right)$ are obtained from the previous calibration.

$$U = \sum_i [w_i \, (E_{calc,i} - E_{exp,i})^2] \qquad \textit{Equation 3.9.}$$

### 3.2.4. Spectrophotometric acid-base titrations

As already mentioned previously, potentiometic acid-base titrations are preferable for the study of systems in equilibrium due to its higher accuracy and precision. However, spectrophotometric acid-base titrations have been performed i) when the performance of potentiometric ones was not possible and ii) as a complementary technique for the acquisition of further information.

The change in the UV-Vis absorbance of our analytes along the acid-base titrations is used for the study of its chemical equilibria. Equation 3.10. shows the most used mathematical representation of the Beer-Lambert Law which relates absorbance and analyte concentration, where $A_\lambda$ is the absorbance at a certain $\lambda$ wavelength, d is the path length of the fibre-optic probe, [S] is the concentration of the absorbing analyte S and $\varepsilon_\lambda$ the molar absorbance at a certain $\lambda$ wavelength.[10] This expression can be used when working at low concentrations (< 0.02 M) and when the absorbing species does not go through chemical changes.

$$A_\lambda = d \cdot [S] \cdot \varepsilon_\lambda \qquad \textit{Equation 3.10.}$$

As our absorbent analytes form more than one absorbing species with diverse characteristic absorbance patterns during the experiments, the total absorbance of the system can be expressed as a sum of the separated contributions, as shown in Equation 3.11., where *n* would be the number of different absorbing species formed.

$$A_\lambda = d \cdot ([S]_0 \cdot \varepsilon_{\lambda,0} + [S]_1 \cdot \varepsilon_{\lambda,1} + \cdots + [S]_n \cdot \varepsilon_{\lambda,n}) \qquad \textit{Equation 3.11.}$$

The wavelength range investigated depended on the chromophore moieties presented by the ligand. The cell contained the ligand (concentrations between 0.03 and 0.13 mM, depending on the experiment) and, in the case of complexation studies, also the metal (1:1 ratio).

The emf data and absorbances collected (related to specific added volumes), the concentrations of the initial species (HCl, ligand and, eventually, metal), the initial volume, the temperature and the calibration data obtained previously are introduced in the HypSpec[8,9,11] program to obtain the speciation model which better fits the experimental data. Theoretically, the data obtained in one single wavelength (the one presenting the more marked change in absorbance during the titration) should be enough to perform the refinement, but it is better to pick some additional points around that chosen wavelength in order to reduce the effect of noise. However, it is advised to not use too many wavelengths.[9] Calculations are essentially based on a non-linear least-squares refinement but, in this case, it minimizes the error ($U$) in each run ($i$) between calculated and experimental absorbance ($A$) (Equation 3.12.).

$$U = \sum_i \left( \frac{A_{calc,i} - A_{exp,i}}{A_{exp,i}} \right)^2 \qquad \textit{Equation 3.12.}$$

### 3.2.5. Isothermal titration calorimetry

Isothermal Titration Calorimetry (ITC) was performed in order to determinate the constants and the related complexation enthalpy ($\Delta H^0$) for the formation of the L-lactate (Lac) ternary complex with [Tb(rac-bpcd)]$^+$. This technique has already been applied successfully to measure the heat involved in the species interaction.[12,13] The well-known thermodynamic equations 3.13. and 3.14. are used in order to get i) the free Gibbs energy ($\Delta G^0$) from $K$ and ii) the entropy ($\Delta S^0$) from $\Delta H^0$ and $\Delta G^0$.

$$\Delta G^0 = -RTlnK \qquad \textit{Equation 3.13.}$$

$$\Delta G^0 = \Delta H^0 - T\Delta S^0 \qquad \textit{Equation 3.14.}$$

The [Tb(rac-bpcd)]$^+$ complex solution was prepared by diluting together the stock solution of Tb and the $H_2$bpcd ligand in its racemic form. The ITC experiment was carried out at 298.15 K with a TA instruments TAM III thermostat equipped with a nanocalorimeter and an automatic titration syringe. The Lac solution (25 injections of 10 µL of Lac 80 mM) was added under constant stirring (60 rpm) to a 0.7 ml solution of [Tb(rac-bpcd)]$^+$ (0.63 mM). The delay time between two consecutive injections was set to 12 min, which was long enough to let the system reach thermal equilibrium. The reference cell was filled with MilliQ water.

$$Q_{corr,i,n} = -\sum_i (\Delta x_n) \Delta H_n^0 \qquad \textit{Equation 3.15.}$$

From this experiment we obtained the experimental heat ($Q_{exp}$). The same experiment was repeated in absence of Lac in order to obtain the dilution heat ($Q_{dil}$). The net reaction heat, or corrected heat ($Q_{corr}$), was obtained subtracting the $Q_{dil}$ to the $Q_{exp}$. The experiment was repeated per triplicate to check the reproducibility of the data. The $Q_{corr}$ data is directly correlated to the enthalpy, as presented in Equation 3.15., where $\Delta x_n$ is the change in the number of moles of the *n* species. $Q_{corr}$ and the experimental conditions were used as inputs for the Excel add-in cEST [14] (Section 3.5.2.) for the refinement of the formation constant of the ternary complex which better fit the experimental data.

## 3.3. Luminescence

### 3.3.1. Luminescence and decay kinetics

Luminescence was measured at room temperature with a Fluorolog 3 spectrofluorometer (Horiba-Jobin Yvon) equipped with a single-emission monochromator (Model HR320), a Xe lamp, a double-excitation monochromator and a photomultiplier in photon counting mode for the detection of the emitted signal. All spectra were corrected for the spectral distortions of the setup.

A xenon microsecond flashlamp was used for decay kinetics measurements. The signal was recorded by a multichannel scaling method. True decay times were obtained using the convolution of the instrumental response function with an exponential function and the least-squares-sum-based fitting program (SpectraSolve software package).

The total quantum yields ($\Phi_{tot}$) were obtained by measuring the visible emission spectrum of a fluorescence quantum yield reference sample (quinine in 1N $H_2SO_4$) presenting $\Phi_{tot}$ = 54.6% and using the Equation 3.16., where $\Phi$ is the quantum yield, *F* the integrated emission area across the band, *A* the absorbance at the excitation wavelength and *n* the index of refraction of the solvent. The subscript *u* refers to the unknown and *s* to the standard.[15]

$$\Phi_u = \frac{A_s \cdot F_u \cdot n_u^2}{A_u \cdot F_s \cdot n_s^2} \cdot \Phi_s \qquad \textit{Equation 3.16.}$$

One of the methods used to find the association constants of the adducts between Ln(III) complexes and the target biomarkers is the use of the Benesi-Hildebrand equation (Equation 3.17.), by means of a double reciprocal plot: the intensity (or ratio between intensities of interest) is plotted versus either the inverse of the analyte concentration or the inverse of its square concentration. The most linear plot indicates the ratio between the complex and the analyte, being 1:1 for the former and 1:2 for the latter. The overall stability constant is calculated from the ratio intercept/slope.[16,17]

$$\frac{I_0}{(I - I_0)} = \frac{I_0}{(I_\infty - I_0)} + \frac{I_0}{\{K \cdot (I_\infty - I_0) \cdot [BM]^n\}} \qquad \textit{Equation 3.17.a}$$

$I_0$, $I$ and $I_\infty$ are the emission intensities of Tb(III) at 546 nm in absence of analyte, intermediate analyte concentration and at concentration of complete complexation, respectively. $K$ is the stability constant of the adduct, $[BM]$ the concentration of the analyte (in our case, the target biomarker) and $n$ the number of analyte molecules bound to the metal centre.

'*I*' can be substituted by '*R*' when the ratio between two peaks (asymmetry ratio) is used. Also the MS Excel add-in cEST has been used for the refining of these constants (Section 3.5.2.).

$$R = \frac{I(\,^5D_0 \rightarrow\, ^7F_2)}{I(\,^5D_0 \rightarrow\, ^7F_0)} \qquad \textit{Equation 3.17.b}$$

The number of water molecules bound to the metal (*q*, hydration number) was determined using Horrock's equation (Equation 3.18.a).[18,19] The *A* constant is 1.2 for $Eu^{3+}$ and 5.0 for $Tb^{3+}$. τ is the radiative lifetime (lifetime of the radiation without non-radiative deactivation processes[20]) in water or heavy water. It is known that the X-H (i.e. X = N, O) oscillators nearby or in the first coordination sphere shorten luminescence lifetimes.[18] Thus, the correcting term $Q$ (Equation 3.18.b)[18] is added to Horrock's equation.

$$q = A\left[\frac{1}{\tau_{H_2O}} - \frac{1}{\tau_{D_2O}} - Q\right] \qquad \textit{Equation 3.18.a}$$

$$Q = \sum_n (Q_1 + Q_2 + \cdots + Q_n) \qquad \textit{Equation 3.18.b}$$

The radiative lifetimes have been obtained either by a) estimation by using Equation 3.19.a (*c* = speed of light in vacuous, in cm/s; $\tilde{\upsilon}$ = frequency of the transition in $cm^{-1}$; *n* = refractive index of the medium, $N_A$ = Avogadro's number; $\varepsilon(\upsilon)$ = absorption spectrum of the transition in $M^{-1}cm^{-1}$; $g_n$ = degeneracy of the state (n = 0 for ground state, n = exc for the excited one) or b) calculation with Equation 3.19.b. $\Phi_{Ln}$ is calculated either by using Equation 3.19.b or by using a reference standard.[21] The efficiency of the sensitization ($\eta_{sens}$) is calculated with Equation 3.19.c.

$$\frac{1}{\tau_{rad}} = 2303 \times \frac{8\pi c n^2 \tilde{\upsilon}_{ul}^2}{N_A} \frac{g_0}{g_{exc}} \int \varepsilon(\upsilon) d\upsilon \qquad \textit{Equation 3.19.a}$$

$$\Phi_{Ln} = \frac{\tau_{obs}}{\tau_{rad}} \qquad \textit{Equation 3.19.b}$$

$$\Phi_{tot} = \eta_{sens} \Phi_{Ln} \qquad \textit{Equation 3.19.c}$$

### 3.3.2. Circularly polarized light luminescence

Circularly polarized light luminescence (CPL) spectra were recorded with a homemade spectrofluoropolarimeter.[22] In order to measure the efficiency of the CPL the dissymmetry factor ($g_{lum}$) is used (defined in Equation 3.20., where $I_L$ and $I_R$ are the left- and right-polarized intensities).

$$g_{lum} = 2\frac{(I_L - I_R)}{(I_L + I_R)} \qquad \textit{Equation 3.20.}$$

The spectra were recorded in water or deuterated methanol at 2.0−3.0 mM (for Tb(bpcd)Cl) or 8.0 mM (for Eu(bpcd)Cl) concentrations, under 254 nm irradiation using a 90° geometry between the excitation and the detection directions. It was verified that the racemates provided 0-signal over each spectral window investigated before carrying out the measurements on the single enantiomers.

## 3.4. Characterization

### 3.4.1. CHNOS-Elemental analysis

Elemental analyses (EA) of the final products (ligands and complexes) and some of their intermediate products have been carried out by using a EACE 1110 CHNOS analyzer.

### 3.4.2. Electrospray ionization mass spectroscopy

The final products (ligands and complexes) and some of their intermediate products have been also analysed by electrospray ionization mass spectrometry (ESI-MS) with a Finnigan LXQ Linear Ion Trap (Thermo Scientific, San Jose, CA, USA) operating in positive mode. Xcalibur software (Thermo Scientific) was used for the data acquisition. For the acquisition of the spectra, a methanol solution of the sample was diluted and infused with a syringe pump at a flow rate of 10 μL/min into the ion source. The typical source conditions were transfer line capillary at 275 °C; ion spray voltage at 4.70 kV; sheath, auxiliary and sweep gas ($N_2$) flow rates at 10, 5 and 0 arbitrary units, respectively. Helium was used as the collision damping gas in the ion trap set at 1 mTorr.

## 3.5. Data analysis and computational calculations

### 3.5.1. Density functional theory

Density functional theory (DFT) calculations have been used to obtain the most probable structures of the complexes discussed in this work.

It is rather difficult to model Eu(III) and Tb(III) complexes computationally due to their open-shell electronic configuration. Thus, Y(III) analogues have been used in the DFT calculations for the complexes discussed in this work. The substitution of Eu(III) and Tb(III) by Y(III) in DFT computational studies has been proved to be a suitable approximation,[23] which is consistent with the fact that ionic radii of $Y^{3+}$, $Eu^{3+}$ and $Tb^{3+}$ are very similar (Table 1.5.) due to the lanthanide contraction.[24] Vibrational analysis was used to check all final geometries were minima. Solvent effects were considered by using the PCM model. Calculations have been carried out by using either Gaussian09 or Gaussian16.[25,26]

### 3.5.2. cEST and Solverstat

Equilibrium speciation tool (cEST)[14] is an Excel add-in for the simulation of chemical equilibria in solution. This software calculates the concentrations in equilibrium of species in non-aqueous and aqueous systems. It can be used for complexation, acid-base, redox and solubility equilibria. It can simulate or obtain chemical-physical parameters from experimental data (even heats from calorimetry experiments). The computational

methods developed in cEST are shown to be very reliable also when applied to homogeneous or heterogeneous equilibrium systems.[27,28]

The statistical analysis of the result is a crucial step to evaluate the reliability of the models. SolverStat[29] is an Excel add-in that performs advanced statistical tests on least squares regression data. Unlikely the Excel add-in Solver, SolverStat provides estimates of the precision of the fitted parameters and a complete and prompted analysis of fittings.

These Excel add-in have been used in this work for the fitting of the formation constants of some Ln(III) complexes with lactate, bicarbonate and citrate and for their statistical analysis. The refinement of the data has been achieved by minimizing the sum of the squares differences between the experimental and the calculated data (area of the selected luminescence peaks or asymmetry ratio, more details in Section 3.3.). In order to decide the most reliable model, some statistic parameters have been taken into account; the best model for each system should present the lowest confidence interval (obtained from the standard deviation of the refined constants, 95% confidence) and Akaike Information Criteria Corrected (AICc)[30]. The AICc parameter is a correction of the AIC parameter for small populations (<10) and is based on the least-squares approach. It permits comparison between models, being the model presenting a lower AICc (or AIC) value considered better.

## 3.6. Bibliography


[1] A. E. Martell, *Determination and Use of Stability Constants*, VCH, **1992**.

[2] A. Vesala, *J. Chem. Educ.* **1992**, *69*, 577–578.

[3] P. Sipos, P. M. May, G. T. Hefter, *Analyst* **2000**, *125*, 955–958.

[4] G. Gran, *Analyst* **1952**, *77*, 661.

[5] M. Ronteltap, M. Maurer, W. Gujer, *Water Res.* **2007**, *41*, 977–984.

[6] Anderegg G., *Anal. Chim. Acta* **1993**, *282*, 485–488.

[7] A. . Fallis, *J. Chem. Inf. Model.* **2013**, *53*, 1689–1699.

[8] L. Alderighi, P. Gans, A. Ienco, D. Peters, A. Sabatini, A. Vacca, *Coord. Chem. Rev.* **1999**, *184*, 311–318.

[9] P. Gans, A. Sabatini, A. Vacca, *Talanta* **1996**, *43*, 1739–1753.

[10] G. M. L. Donald L. Pavia, and J. R. V. George S. Kriz, *Introduction to Spectroscopy*, **2009**.

[11] P. Gans, A. Sabatini, A. Vacca, *Talanta* **1996**, *43*, 1739–53.

[12] A. Melchior, C. Gaillard, S. Gràcia Lanas, M. Tolazzi, I. Billard, S. Georg, L. Sarrasin, M. Boltoeva, *Inorg. Chem.* **2016**, *55*, 3498–3507.

[13] G. Tian, L. R. Martin, L. Rao, *Inorg. Chem.* **2010**, *49*, 10598–10605.

[14] P. Polese, M. Tolazzi, A. Melchior, *J. Therm. Anal. Calorim.* **2018**, *2*, DOI 10.1007/s10973-018-7409-2.

[15] D. F. Eaton, *Pure Appl. Chem.,* **1988**, *60*, 1107–1114.

[16] H. A. Benesi, J. H. Hildebrand, *J. Am. Chem. Soc.* **1949**, *71*, 2703–2707.

[17] E. Arunkumar, A. Ajayaghosh, J. Daub, *J. Am. Chem. Soc.* **2005**, *127*, 3156–3164.

[18] R. M. Supkowski, W. D. W. Horrocks, *Inorg. Chim. Acta* **2002**, *340*, 44–48.

[19] W. D. W. Horrocks, D. R. Sudnick, *J. Am. Chem. Soc.* **1979**, *101*, 334–340.

[20] A. Aebischer, F. Gumy, J.-C. G. Bünzli, *Phys. Chem. Chem. Phys.* **2009**, *11*, 1346–1353.

[21] M. H. V. Werts, R. T. F. Jukes, J. W. Verhoeven, *Phys. Chem. Chem. Phys.* **2002**, *4*, 1542–1548.

[22] F. Zinna, T. Bruhn, C. A. Guido, J. Ahrens, M. Bröring, L. Di Bari, G. Pescitelli, *Chem. - A Eur. J.* **2016**, *22*, 16089–16098.

[23] M. Soulié, F. Latzko, E. Bourrier, V. Placide, S. J. Butler, R. Pal, J. W. Walton, P. L. Baldeck, B. Le Guennic, C. Andraud, et al., *Chem. - A Eur. J.* **2014**, *20*, 8636–8646.

[24] S. Cotton, *Lanthanide and Actinide Chemistry*, John Wiley & Sons, Ltd, **2006**.

[25] M. J. Frisch, G. W. Trucks, H. B. Schlegel, G. E. Scuseria, M. A. Robb, J. R. Cheeseman, G. Scalmani, V. Barone, G. A. Petersson, H. Nakatsuji, et al., *Gaussian 16 Revis. A 03* **2016**.

[26] M. J. Frisch, G. W. Trucks, H. B. Schlegel, G. E. Scuseria, M. A. Robb, J. R. Cheeseman, G. Scalmani, V. Barone, B. Mennucci, G. A. Petersson, et al., **n.d.**

[27] H. Brandenburg, J. Krahmer, K. Fischer, B. Schwager, B. Flöser, C. Näther, F. Tuczek, *Eur. J. Inorg. Chem.* **2018**, *2018*, 576–585.

[28] S. G. Lanas, M. Valiente, M. Tolazzi, A. Melchior, *RSC Adv.* **2016**, *6*, 42288–42296.

[29] C. Comuzzi, P. Polese, A. Melchior, R. Portanova, M. Tolazzi, *Talanta* **2003**, *59*, 67–80.

[30] D. Posada, T. R. Buckley, *Syst. Biol.* **2004**, *53*, 793–808.

# Chapter 4

# Complexation and protonation

## 4.1. Library of ligands and complexes

When designing Ln(III) complexes for biomedical applications it is fundamental to find an adequate ligand. It has to strongly absorb the exciting UV-Vis light and efficiently transfer it to the Ln(III) ion (antenna effect, refer to Chapter 1). Moreover, it has to be stable in water (biocompatibility) and should present a high overall brightness, as well as leaving some space for the coordination of additional target molecules (i.e. biomarkers).

We have already discussed in Chapter 1 that Polyamino-polycarboxylate ligands are great candidates for the formation of highly stable Ln(III) complexes, which makes them specially suitable for biomedical applications.[1–4]

The ligand should also present a chromophore moiety (antenna group).[5–7] In literature we can find several examples of luminescent Ln(III) complexes presenting amino heteroaromatic antenna, such as pyridine[8–13], quinoline[14,15], isoquinoline[2] and acridone[16–18]. Also the preorientation of a favorable geometry generated by rigidity and steric constrains may increase the overall binding affinity.[11]

In this study we propose some Ln(III) (Ln = Eu, Tb) polyamino-polycarboxilate complexes of ligands with either pyridine or quinoline chromophore moieties (antenna) (Figure 4.1.). All the ligands present a 1,2-diaminocyclohexane backbone (DACH, Figure 4.1.) which confers them both, rigidity and chirality.

The complexes formed with these four ligands differ in charge, steric hindrance and lipophilicity since i) Ln(PyC3A) and Ln(QC3A) are neutral, while $Ln(bpcd)^+$ and $Ln(bQcd)^+$ are cationic; ii) each complex presents diverse steric hindrance at the metallic

center, depending on the antenna moieties, being quinoline-functionalized and diacetate complexes bulkier, and pyridine-functionalized and triacetate complexes less busy; iii) the complexes presenting quinoline moieties are more lipophilic. The lipophilicity and charge strongly affect theirmobility/location in the organism and the performance of *in vitro* experiments in terms of cell viability and cell association.[19,20]

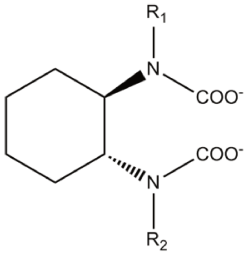


***'DACH' BACKBONE***

| | PYRIDINE (less lipophilic) | QUINOLINE (more lipophilic) |
|---|---|---|
| TRIACETATE (neutral) | 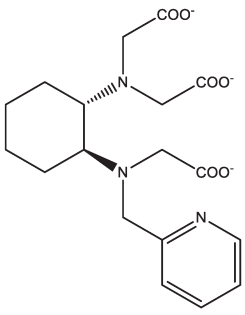 | 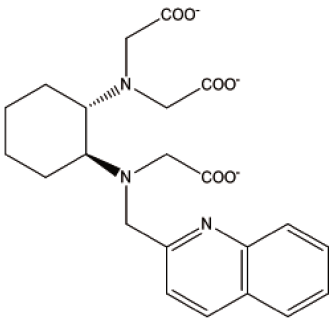 |
| | **$[PyC3A]^{3-}$** | **$[QC3A]^{3-}$** |
| BIACETATE (Cationic) | 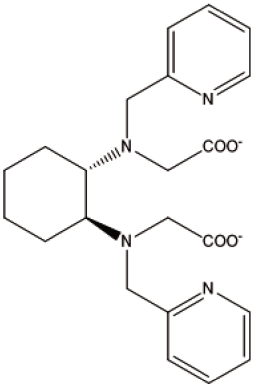 | 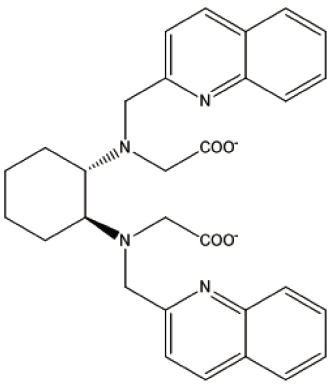 |
| | **$[bpcd]^{2-}$** | **$[bQcd]^{2-}$** |

***Figure 4.1.*** *Ligands discussed in this chapter. Depending on the experiment, the S,S, R,R or racemic forms of the ligands have been studied. For clarity, just one stereoisomer for each ligand.*

This modulation of the DACH backbone by functionalizing it with diverse moieties will facilitate the study of the selectivity towards diverse target analytes, as previously stated in literature,[21,22] since we expect steric hindrance and charge to strongly influence the stability of both the Ln(III) complexes and their adducts with the target biomarkers (as already discussed in Chapter 1). Moreover, all the presented complexes show less steric hindrance around the metal center in comparison with other luminescent Ln(III) anion probes found in literature. This might facilitate the coordination of more than one target anion to the first coordination sphere, which would lead to a higher affinity between the complex and the target biomarker.

## 4.2. Stability, speciation and structure

### 4.2.1. Protonation constants

The protonation constants of the ligands used during this work have been determined by acid-base potentiometric titration. The best fit of the experimental emf data for all ligands was reached with the Hyperquad program by using a four species model. For more experimental details, refer to Chapter 3.

The constants obtained are reported in Table 4.1. along with additional protonation data from literature for the ligand PyC3A and 1,2-cyclohexanediaminetetraacetic acid (CDTA, Figure 4.3.), which also presents the DACH backbone. The titration curve for all the ligands is displayed in Figure 4.2. along with its speciation, calculated with the Hyss program[23] by using the experimental conditions and the protonation constants found. In this figure we observe very similar trends in speciation for all the ligands, with two clear inflection points at 2 and 3 equivalents of free $OH^-$ and concurring with the maximum concentration for the species $LH_2$ and LH respectively. The log*K* values reported indicate the presence of two fairly strong acidic and two weakly basic sites in each ligand. Even if the ligands present six groups presenting acid/base properties, the protonation constants of the two remaining groups could not be determined, as they did not present acid/base activity in the pH range of study. As previously reported for CDTA[24], the first protonation constant can be assigned for all the ligands to an aliphatic amine group (log*K* ~6.9 - 10.7, depending on the substituents[25]).

***Table 4.1.*** *Protonation constants ($logK_i$) of all the ligands used in this work (Figure 4.1.), with their confidence intervals (95% confidence), found by potentiometry at T = 298.2 K ± 0.1 K and μ = 0.1 M NaCl. Additional protonation data from another work (μ = 0.15 M NaCl) has also been reported for comparison. Charges omitted for clarity.*

| | bpcd | bQcd | PyC3A | QC3A | PyC3A[26] | CDTA[26] |
|---|---|---|---|---|---|---|
| $\log K_1$ | 9.72 ± 0.02 | 9.37 ± 0.03 | 10.26 ± 0.02 | 10.53 ± 0.03 | 10.16 ± 0.02 | 9.43 ± 0.02 |
| $\log K_2$ | 5.87 ± 0.07 | 5.85 ± 0.07 | 6.33 ± 0.07 | 6.29 ± 0.09 | 6.39 ± 0.04 | 6.01 ± 0.02 |
| $\log K_3$ | 2.94 ± 0.12 | 3.46 ± 0.10 | 3.67 ± 0.11 | 3.60 ± 0.16 | 3.13 ± 0.03 | 3.68 ± 0.02 |
| $\log K_4$ | 2.22 ± 0.17 | 1.79 ± 0.31 | 2.01 ± 0.14 | 2.81 ± 0.16 | - | 2.51 ± 0.05 |

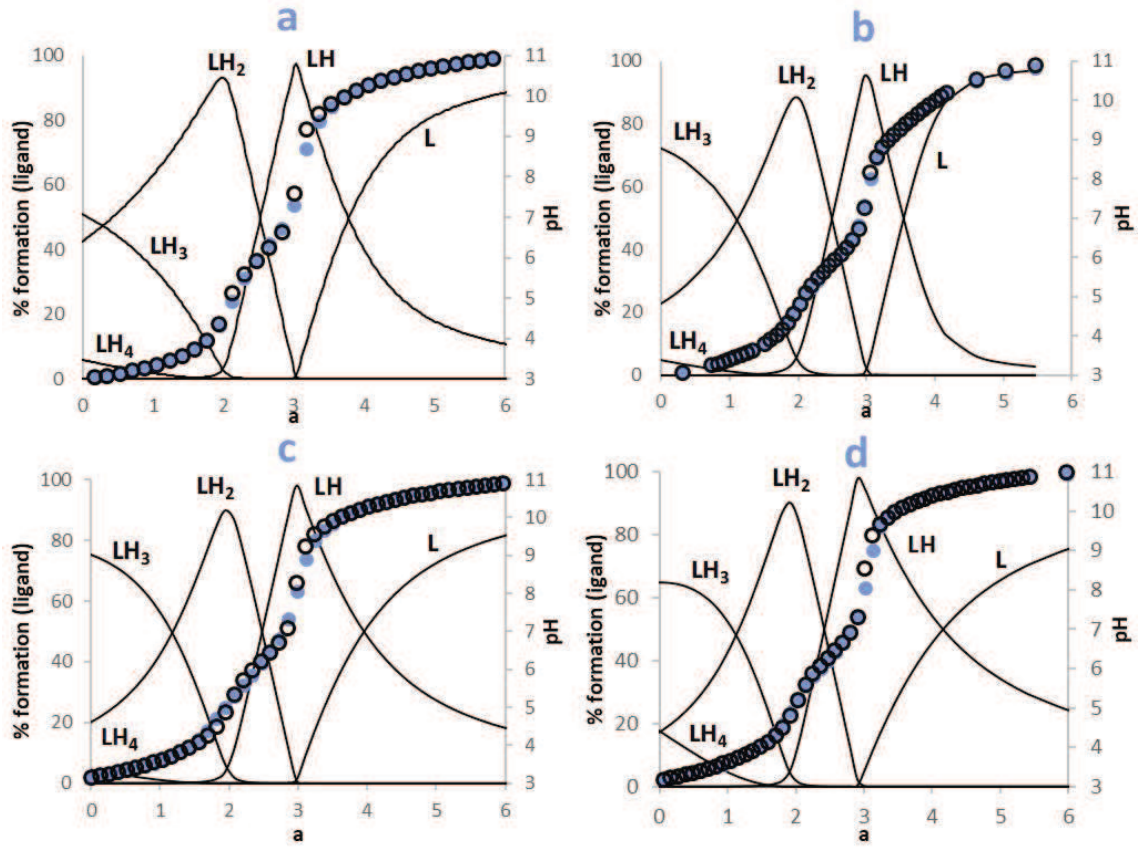


***Figure 4.2.*** *Titration curve (● observed and ○ calculated pH) for the ligand (L) a) bpcd (0.95 mM), b) bQcd (0.94 mM), c) PyC3A (0.6 mM) and d) QC3A (0.7 mM) obtained by acid-base potentiometric titration at T = 298.2 K ± 0.1K and μ=0.1 M NaCl. a = (moles of free $OH^-$) / (moles of L). Charges omitted for clarity.*

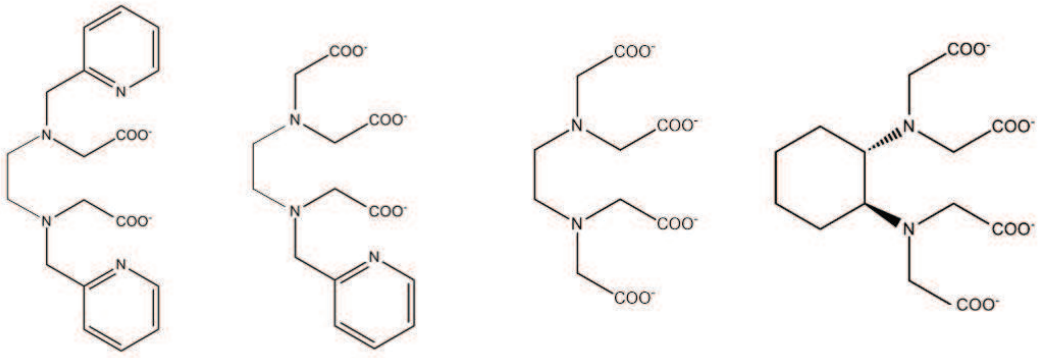


***Figure 4.3.*** *From left to right, ligands bped* [27], *PEDTA*[28], EDTA[29] and CDTA[24].

Further data were needed to assign the other protonation constants to specific sites. Thus, acid-base spectrophotometric titrations were performed in the same conditions of the protonation titrations in order to follow the deprotonation of the pyridine and quinoline moieties during the titration. The protonation of the nitrogen present in pyridine and quinoline moieties increases the molar absorbance of the ligand, which permits the assignation of some protonation constants to the protonation of the heterocycles. The molar absorbances obtained (at $\lambda$ = 265 nm for pyridine-functionalized and at $\lambda$ = 318nm for quinoline-functionalized ligands are reported in Figure 4.4. along with the speciation calculated with the Hyss program[23] by using the experimental conditions and the protonation constants found. By observing the trends of molar absorbance and speciation together, we may assign the $K_3$ constants of the triacetate ligands and all $K_2$ constants to the protonation of the heterocyclic nitrogen. This is in agreement with the protonation constants found in literature for quinoline ($\log K = 4.97$)[30] and picoline ($\log K = 6.06$)[31]. The remaining protonation constants may be assigned to the protonation of acetates. The protonation sequence we propose is in agreement with the one suggested by Caravan[27] for bped (Figure 4.3.), a ligand similar to bpcd but with an ethylene substituting the DACH backbone.

## 4.2.2. Stability constants

The stability constants of the complexes used during this work at T = 298.2 K and μ = 0.1 M NaCl have been determined by acid-base potentiometric (bpcd) or spectrophotometric (bQcd, PyC3A, QC3A) titrations. The best fit of the data was obtained by either Hyperquad or Hypspec program (for potentiometries or spectrophotometries respectively). (for more experimental details, check Chapter 3).

Two typical UV-Vis titrations are shown in Figure 4.5. as representative examples: very similar plots are obtained for the complexes presenting the same chromophore, though the intensity of the signal is higher for the species presenting more than one chromophore moiety. The stability constants obtained are reported in Table 4.2. along with additional constants from literature for the similar ligands bped[27], PEDTA[28], EDTA[29] and CDTA[29] (Figure 4.3.).

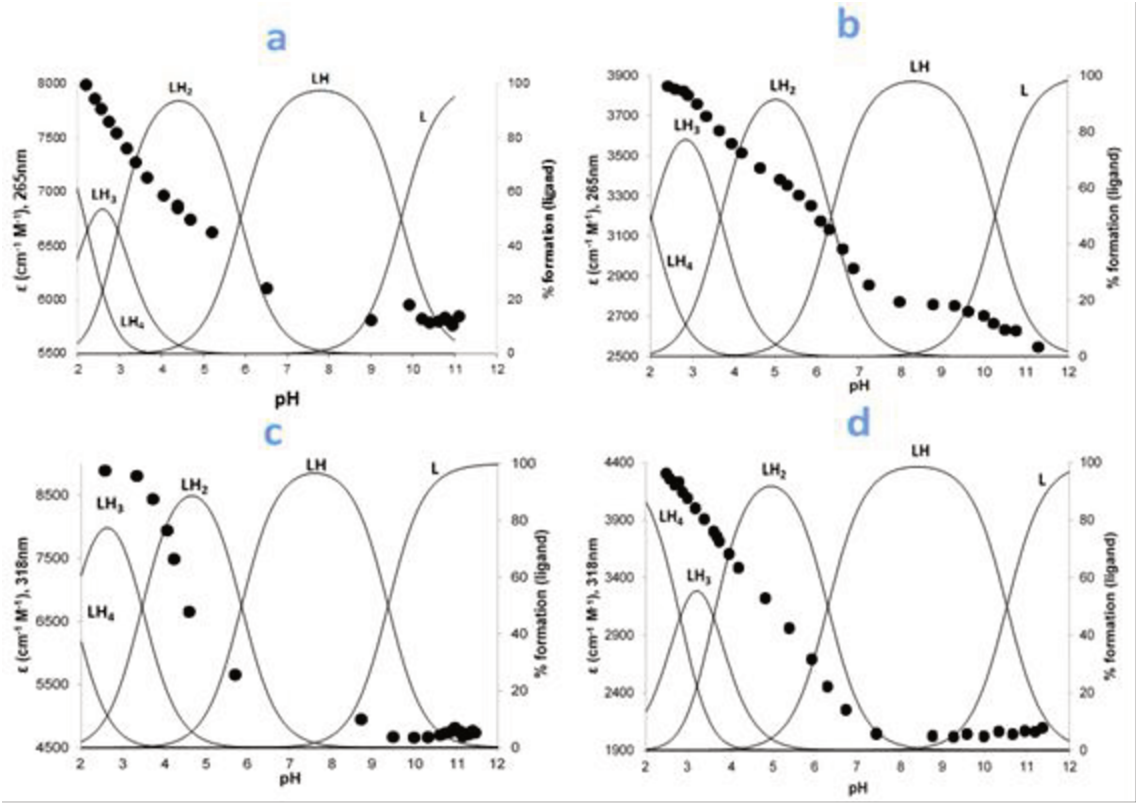


***Figure 4.4.*** *Species distribution of the complexes for the ligands (L) a) bpcd (0.04 mM), b) PyC3A (0.13 mM), c) bQcd (0.08 mM) and d) QC3A (0.09 mM) along with the molar absorbance values at λ=318 nm (for the pyridine- functionalized ligands) and λ=265 nm (for the quinolone-functionalized ligands) obtained by acid-base spectrophotometric titration at T = 298.2 K ± 0.1K and μ = 0.1 M NaCl. Charges omitted for clarity.*

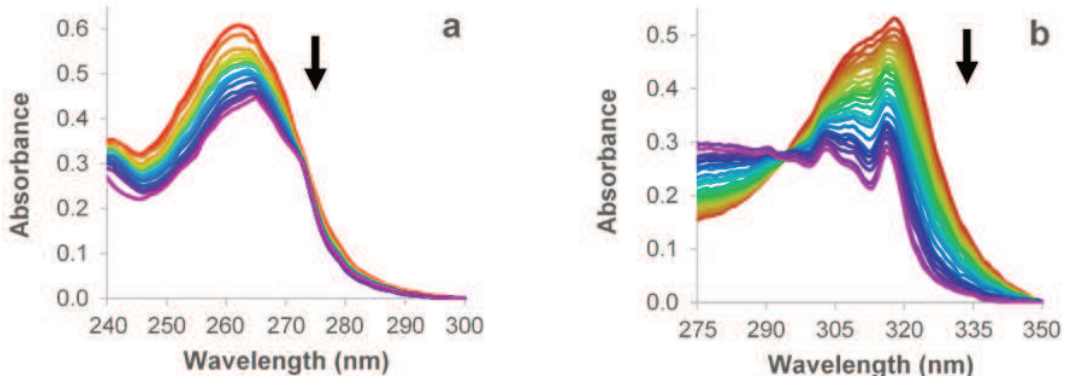


***Figure 4.5.*** *UV-Vis absorption spectra changes during the acid-base titration (in the pH range 2.3-11.5) for the ligands a) PyC3A (0.13 mM) and b) QC3A (0.09 mM), in the presence of equimolar Eu(III). T = 298.2 K and μ = 0.1 M NaCl.*

***Table 4.2.*** *Stepwise formation constants (logβ) of all the complexes discussed in this work with their confidence intervals (95% confidence), found by acid-base titration at T = 298.2 K ± 0.1 K and μ = 0.1 M NaCl. Other similar complexes have also been reported for comparison. Charges omitted for clarity.*

| | bpcd | bQcd | PyC3A | QC3A | bped[27] | PEDTA[28] | EDTA[29] | CDTA[29] |
|---|---|---|---|---|---|---|---|---|
| **Eu(III)L** | 11.19 ± 0.32 | 9.97 ± 0.08 | 15.68 ± 0.01 | 12.55 ± 0.16 | - | - | 17.3 | 19.6 |
| **Eu(III)L(OH)** | 2.18 ± 0.57 | - | - | - | - | - | - | - |
| **Tb(III)L** | 11.36 ± 0.15 | 9.80 ± 0.13 | 15.70 ± 0.02 | 12.08 ± 0.28 | - | - | 17.9 | 20.0 |
| **Tb(III)L(OH)** | 2.04 ± 0.33 | - | - | - | - | - | - | - |
| **Gd(III)L** | - | - | - | - | 12.37* | 15.56 | 17.4 | 19.6 |
| **Gd(III)L(OH)** | - | - | - | - | 2.1* | - | - | - |

**** μ = 0.16 M NaCl***

If we check the stability constants presented in Table 4.2., it can be observed that complexes with quinoline moieties (bQcd and QC3A) present lower stability constants than their pyridine analogues (bpcd and PyC3A respectively). This behavior is not surprising, since bulkier quinoline moieties cause stronger steric hindrance than pyridine ones.

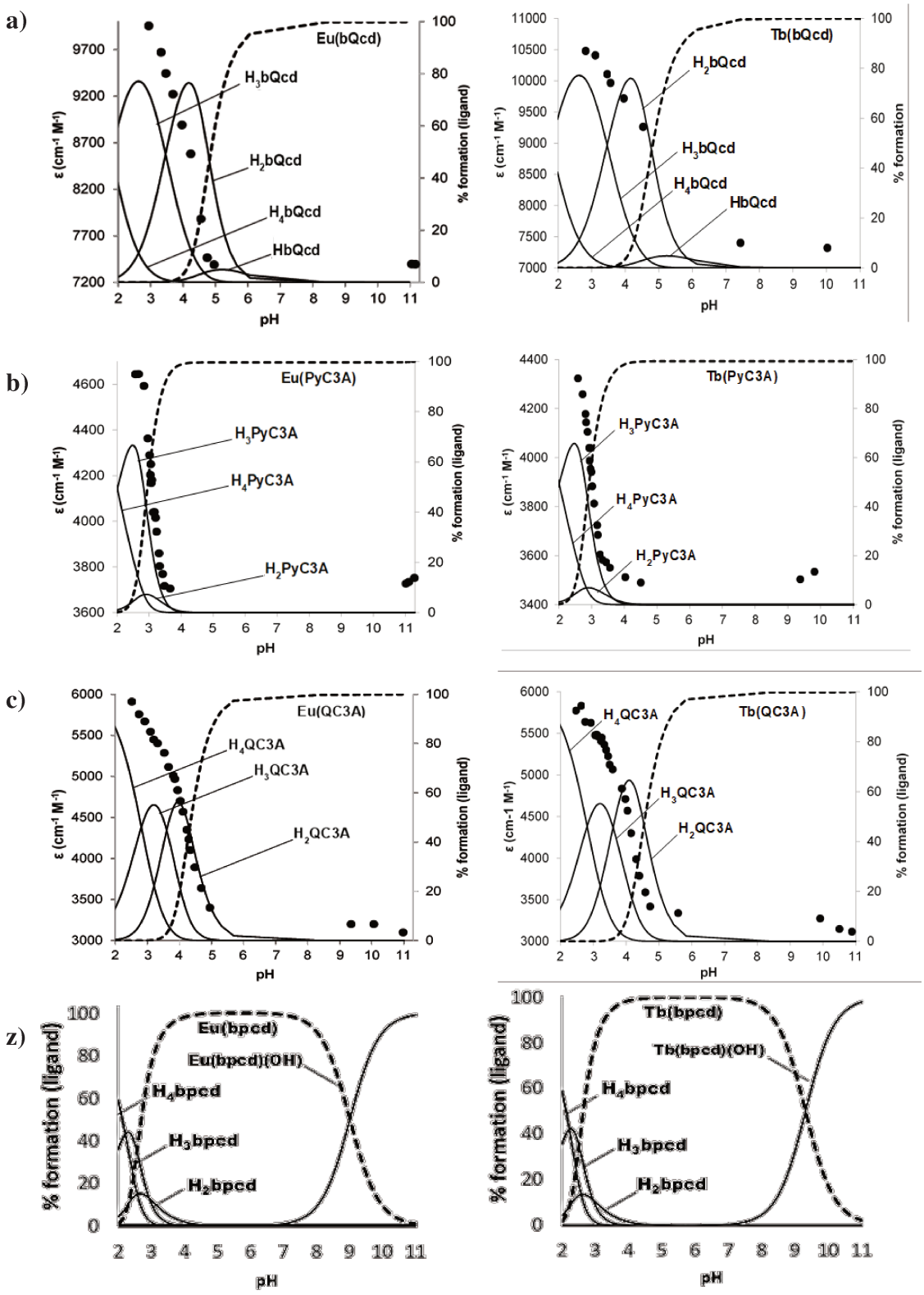


***Figure 4.6.*** *Species distribution of the ligands a) bQcd (0.08 mM left, 0.03mM right), b) PyC3A (0.13 mM left, 0.15 mM right), c) QC3A (0.09 mM) and z) bpcd (0.2 mM) in the presence of either, Eu(III) (left) or Tb(III) (right), ratio 1:1 M:L, with a little excess of metal. Also the molar absorbance values (•) at λ=318nm (for bQcd and QC3A) and λ=265 nm (for PyC3A) obtained by acid-base spectrophotometric titration at T = 298.2 K and μ = 0.1 M are reported. Charges and negligible species (below 5%) omitted for clarity.*

On the other hand, triacetate complexes (PyC3A and QC3A) present higher stability constants than their diacetate analogues (bpcd and bQcd respectively). This trend can be easily explained by the noted strong interaction between oxygen donors and Ln(III), and is also observed for the similar ligands bped[27], PEDTA[28] and EDTA[29] (bi- , tri- and tetra-acetate respectively) with Gd(III), and for the tetra-acetate CDTA[29] (Figure 4.3.), which presents the highest stability constants for Eu(III), Tb(III) and Gd(III). Besides, as expected and currently observed in literature[29], the stability of the Eu(III) and Tb(III) complexes with the same ligand are analogous, due to the very similar radii properties among this close Ln(III).[7]

The species distribution of the ligands bpcd, bQcd, QC3A and PyC3A in water in the presence of Eu(III) or Tb(III) at 298.2 K has been calculated with the program Hyss[23] by using the found protonation and stability constants. The speciations are represented in Figure 4.6. along with the molar absorbances from pH 2 to 11. We can observe that, in all cases, the luminescent L-Ln(III) species is the most abundant species at pH around 7.4, representing near the 100% of the total L species at that pH. We can also observe that the molar absorbance decreases with the formation of the Ln(III) complex. Since molar absorbance is higher for the protonated heteroaromatic antenna, we may assume the coordination of Ln(III) with the heterocyclic nitrogen/s.

### 4.2.3. Structure

It was not possible to obtain single crystals suitable for X-ray diffraction from our Ln(III) complexes, thus their structure was studied by density functional theory (DFT) calculations. As we have already discussed in Chapter 3, this computational method has been previously applied successfully to obtain structural and thermochemical data for f-block metal complexes.[32–34] It is very difficult to fit the models for Eu(III) and Tb(III) complexes since these metals are paramagnetic. Thus, the Y(III) analogue has been used instead, as the radii of Eu(III) (94.7 pm), Tb(III) (92.3 pm) and Y(III) (90.0 pm) are quite similar due to the lanthanide contraction.[7,8,10,35]

An 8-fold coordination was obtained for all the Y(III) complexes (including water molecules). Moreover, an equilibrium between two isomers in solution was found in all

cases, with *trans-N,N* and *trans-O,O* structures for the cationic diacetate complexes ([Ln-bpcd]$^+$ and [Ln-bQcd]$^+$) and *trans-O,O* and *trans-N,O* structures for the neutral triacetate ones (Ln-PyC3A and Ln-QC3A), all of them presenting two water molecules in the first coordination sphere (Figure 4.7.). Comparable geometries have been previously seen in literature for analogous complexes, such as Gd(III)-bpcd[36], M(III)-bped[27] (M = Al, Ga, In) and other similar complexes[37].

Unfortunately, it was not possible to confirm these structures via nuclear magnetic resonance (NMR), as the spectra of the complexes present hardly-assignable broad resonances. The wide lines obtained are in agreement with the proposed solution equilibria between isomers. We present one of the NMR spectrum in Figure 4.8. as a representative example.

If we go back to Figure 4.6., we said that the contemporaneous decreasing in the molar absorbance and formation of the Ln(III) complex may indicate the coordination of Ln(III) with the heterocyclic nitrogen/s, which is in accordance with the structures proposed. Moreover, the number of water molecules close to the metal (hydration number, Table 3.4.) was also determined by luminescent experiments and using Horrock's equation (Equation 3.18.a),[38,39] where $q$ is the hydration number and $\tau$ are the radiative lifetimes in water and heavy water (Section 3.3.1.). The obtained values (from 2.4 to 2.8) are partially in accordance with the structures proposed by DFT calculations. But it has to be emphasized that i) Horrock's equation usually overestimates the number of waters directly coordinated to the metal, as also outer sphere waters are slightly considered[39] and ii) the structures proposed by DFT calculations may also be in equilibrium with analogous structures presenting three waters, as additional water molecules where also assessed in the second coordination sphere near the metal centre (Figure 4.9).

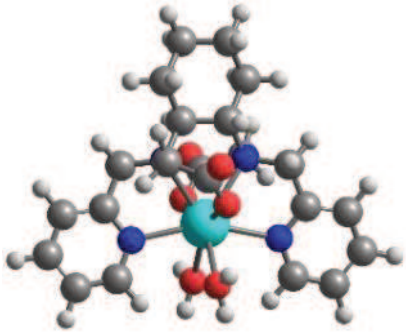

$[Y(trans\text{-}O,O\text{-}bpcd)(H_2O)_2]^+$

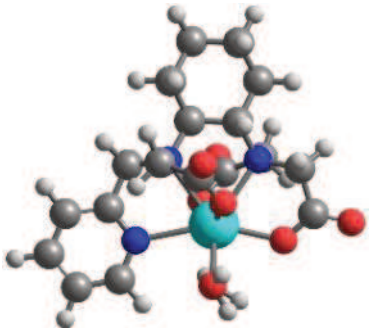

$[Y(trans\text{-}O,O\text{-}PyC3A)(H_2O)_2]^+$

$[Y(trans\text{-}N,N\text{-}bpcd)(H_2O)_2]^+$

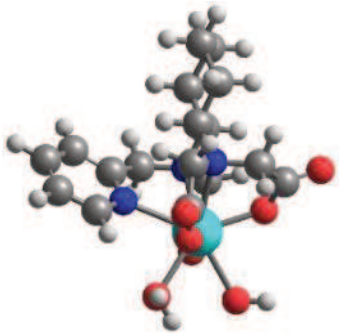

$[Y(trans\text{-}N,O\text{-}PyC3A)(H_2O)_2]^+$

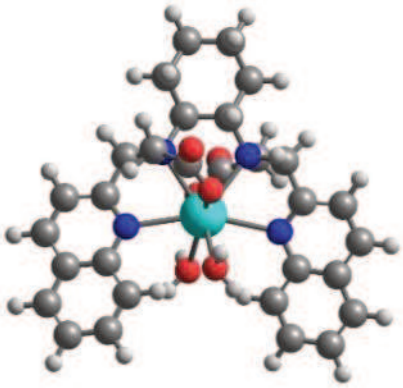

$[Y(trans\text{-}O,O\text{-}bQcd)(H_2O)_2]^+$

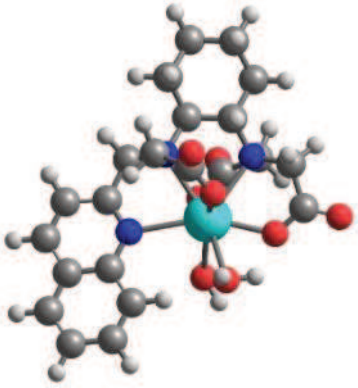

$[Y(trans\text{-}O,O\text{-}QC3A)(H_2O)_2]^+$

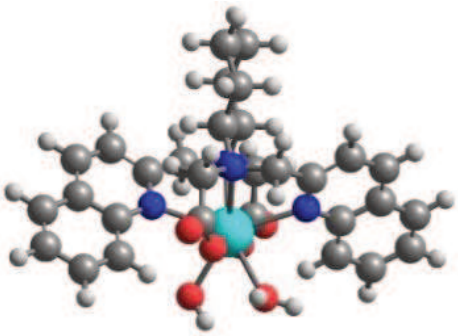

$[Y(trans\text{-}N,N\text{-}bQcd)(H_2O)_2]^+$

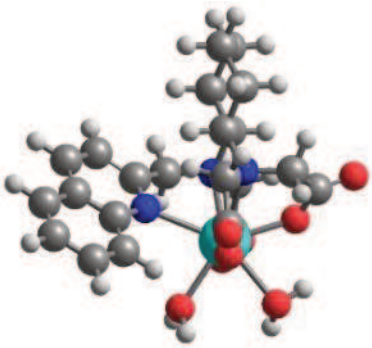

$[Y(trans\text{-}N,O\text{-}QC3A)(H_2O)_2]^+$

***Figure 4.8.*** *Minimum energy structures found for the Y(III) complexes by DFT calculations.*

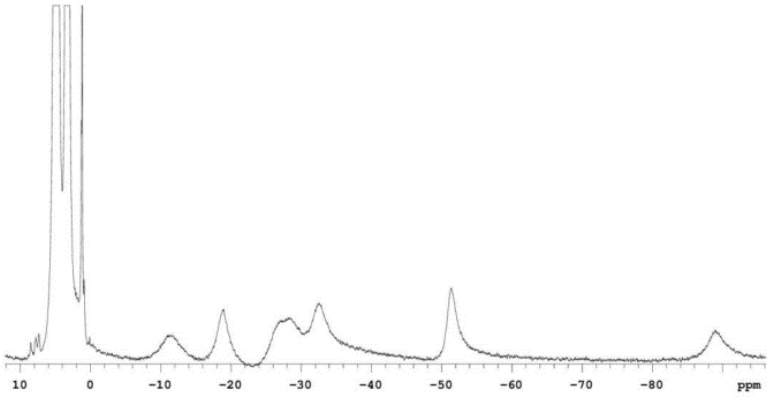


***Figure 4.7.*** *$^{1}$H-NMR spectrum (600MHz, CD3OD) of the Tb(bpcd)Cl complex.*

The Y-$N_{heterocyclic}$ distances found for pyridine-based complexes are shorter than those found for the quinoline-based ones (Table 4.3.), which is in accordance with the higher stability constants found for the pyridine-based complexes (Table 4.2.).

***Table 4.3.*** *Representative bond distances (Å) found by DFT calculations for the complexes represented in Figure 4.7..*

| Complex | Y-$O_{acetate}$ | Y-$N_{amine}$ | Y-$N_{heterocycle}$ | Y-$O_{water}$ |
|---|---|---|---|---|
| **[Y(*trans*-O,O bpcd)$(H_2O)_2$]$^+$** | 2.262 | 2.550 | 2.525 | 2.448 |
| **[Y(*trans*-N,N bpcd)$(H_2O)_2$]$^+$** | 2.292 | 2.610 | 2.503 | 2.492 |
| **[Y(*trans*-O,O bpcd)$(H_2O)_2$]$^+$** | 2.268 | 2.557 | 2.661 | 2.464 |
| **[Y(*trans*-N,N bpcd)$(H_2O)_2$]$^+$** | 2.284 | 2.567 | 2.594 | 2.482 |
| **Y(*trans*-O,O PyC3A)$(H_2O)_2$** | 2.286 | 2.568 | 2.550 | 2.474 |
| **Y(*trans*-N,O PyC3A)$(H_2O)_2$** | 2.300 | 2595 | 2.546 | 2.539 |
| **Y(*trans*-O,O QC3A)$(H_2O)_2$** | 2.286 | 2.574 | 2.654 | 2.458 |
| **Y(*trans*-N,O QC3A)$(H_2O)_2$** | 2.290 | 2.576 | 2.642 | 2.478 |

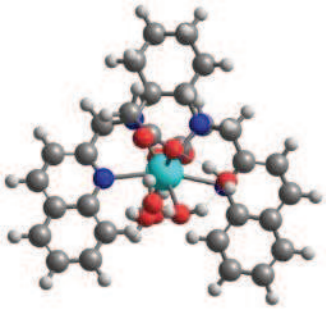

**[Y(*trans*-O,O-bQcd)$(H_2O)_5]^+$**

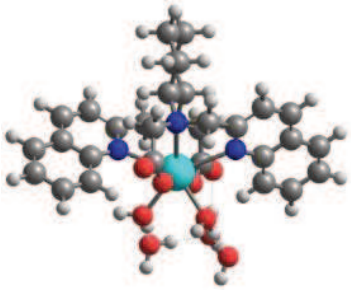

**[Y(*trans*-N,N -bQcd)$(H_2O)_5]^+$**

**[Y(*trans*-O,O-PyC3A)$(H_2O)_3$]**

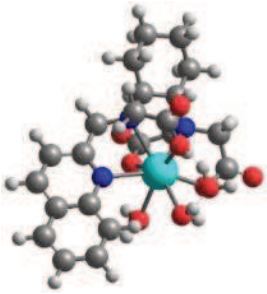

**[Y(*trans*-O,O-QC3A)$(H_2O)_3$]**

***Figure 4.9**. Minimum energy structures found for the Y(III) complexes by DFT calculations including 2nd sphere water molecules*

## 4.2.4. Luminescent characterization

The excitation spectra in aqueous solution for the Eu(III) complexes with $bpcd^{2-}$, $bQcd^{2-}$, $PyC3A^{3-}$ and $QC3A^{3-}$, and the Tb(III) complex with $PyC3A^{3-}$ are shown in Figures 4.10.a-b, left part of the graphs. For Eu complexes, the $^5D_0 \rightarrow {}^7F_2$ transition of Eu(III) has been monitored ($\lambda_{em}$ = 612-615 nm); for Tb complexes, the $^5D_4 \rightarrow {}^7F_5$ transition of Tb(III) has been monitored ($\lambda_{em}$ = 545 nm).

The ligand to metal energy transfer is confirmed when the excitation spectra and their equivalent absorption ones (Figure 4.11.) are superimposable. In the absorption graph, we may also notice that the spectra for complexes presenting the same kind of antenna moiety (either, pyridine or quinoline) are also superimposable, and the complexes presenting two antenna moieties show, as expected, nearly double of the molar absorbance than their one-antenna equivalents.

The luminescent emission spectra obtained by excitation of either the pyridine ($\lambda_{exc}$ = 265 nm) or the quinoline ($\lambda_{exc}$ = 319 nm) antenna for all the complexes present the typical *f-f* transition luminescence for Eu(III) (red); the same happens for Tb(III) (green), but just in the case of pyridine-functionalized complexes (Figure 4.10a-b, right part of the graphs). Thus, we may say that the latter are good sensitizers for both, Eu(III) and Tb(III); on the other hand, quinoline-functionalized complexes efficiently transfer the energy to Eu(III), but not to Tb(III). This fact could be explained by an excessively small energy gap between the triplet excited state of the quinoline ligands and the highest luminescent excited state of Tb(III), which may cause a back energy transfer (Section 1.2.).[40]

The luminescent decay curves in aqueous solution for Eu(III) ($^5D_0$ excited state) and Tb(III) ($^5D_4$ excited state) were recorded for all the complexes studied. Some of the curves are presented in Figure 4.12. as a representative example. All the obtained curves fit by a single exponential function (1:1 ratio ligand:Ln(III)). In Table 4.5. the lifetimes observed ($\tau_{obs}$) in both water and heavy water are represented, along with the hydration number ($q$), the radiative lifetime ($\tau_{rad}$), the intrinsic quantum yield ($\Phi_{Ln}$), the total quantum yield ($\Phi_{tot}$) and the sensitization of the Ln(III) luminescence by the ligand ($\eta_{sens}$). All the Equations and information about the calculations performed to get this data can be found in Section 3.3.1..

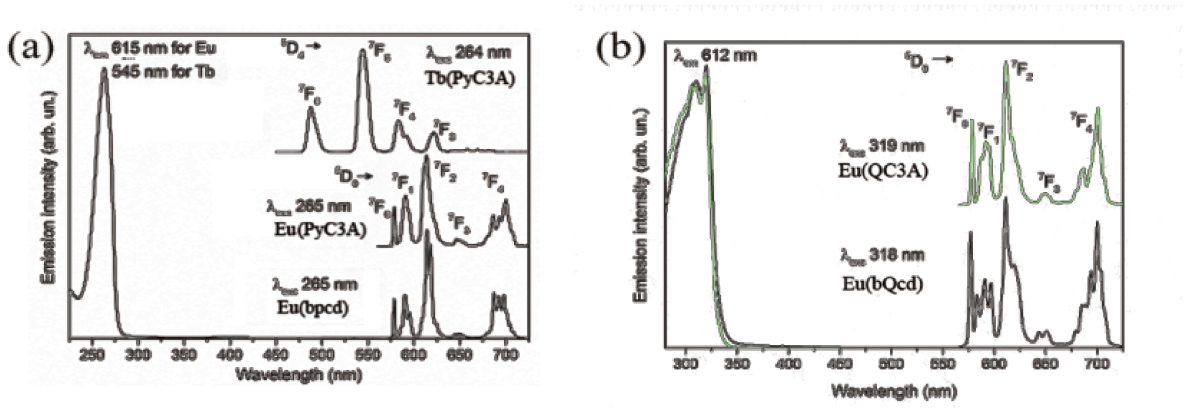


***Figure 4.10.*** *Luminescence excitation (left part of the plots) and emission (right part of the plots) spectra for some a) pyridine- and b) quinoline-functionalized Ln(III) complexes (0.1 mM, T = 298.2 K).*

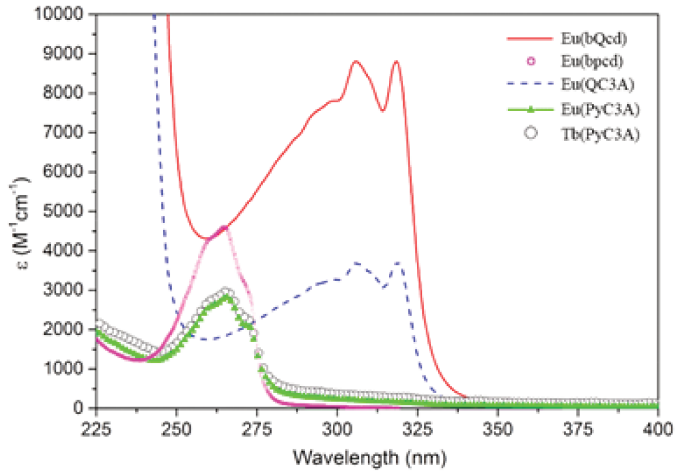


***Figure 4.11.*** *Absorbance spectra for some Ln(III) complexes in water.*

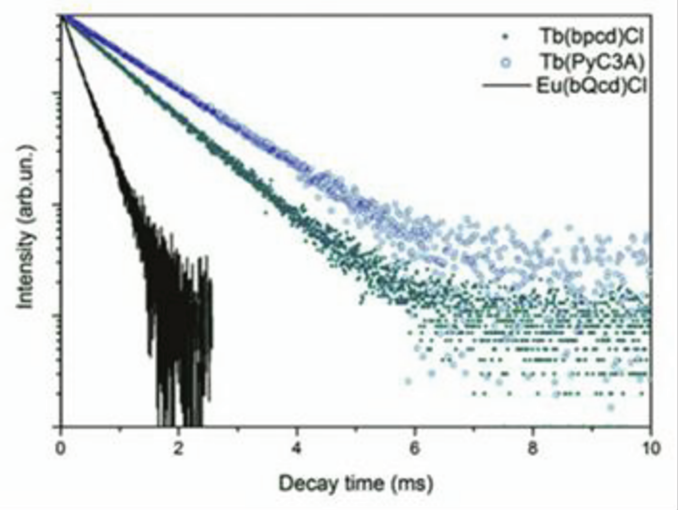


***Figure 4.12.*** *Luminescent decay times (ms) for some representative Eu(III) and Tb(III) complexes.*

$\Phi_{Ln}$ is the ratio between the number of emitted and absorbed photons upon Ln(III) direct excitation. It is not surprising that Tb(III) displays higher $\Phi_{Ln}$ values (~16% in front of ~10% for Eu(III)), since this cation presents bigger energy gap between the emitting state and the lower ones, which hinders the multiphonon relaxation process (non-radiative relaxation).

***Table 4.4.*** *Observed lifetimes ($\tau_{obs}$), in either water or heavy water; radiative lifetimes ($\tau_{rad}$), estimated or *calculated with Equation 3.4.b; hydration number (**q**); intrinsic quantum yield ($\Phi_{Ln}$), estimated in water using Equation 3.4.b or **determined by means of a reference standard; total quantum yield ($\Phi_{tot}$) and sensitization ($\eta_{sens}$) of the Eu(III) and Tb(III) complexes under study.*

| Complex | $\tau_{obs}$ (ms) | | $\tau_{rad}$ (ms) | *q* | $\Phi_{Ln}$ (%) | $\Phi_{tot}$ (%) | $\eta_{sens}$ (%) |
|---|---|---|---|---|---|---|---|
| | $H_2O$ | $D_2O$ | | | | | |
| **[Eu(bpcd)]$^+$** | 0.30 ± 0.01 | 1.70 ± 0.01 | 3.00 | 2.7 ± 0.1 | 10.0 | 6.1 | 61 |
| **[Eu(bQcd)]$^+$** | 0.29 ± 0.01 | 1.68 ± 0.01 | 3.22 | 2.8 ± 0.1 | 9.0 | 2.6 | 29 |
| **Eu(PyC3A)** | 0.33 ± 0.01 | 3.56 ± 0.01 | 3.66 | 2.7 ± 0.1 | 9.0 | 5.67 | 63 |
| **Eu(QC3A)** | 0.33 ± 0.01 | 2.15 ± 0.01 | 3.34 | 2.5 ± 0.1 | 9.9 | 4.0 | 40 |
| **[Tb(bpcd)]$^+$** | 0.94 ± 0.01 | 2.15 ± 0.01 | 5.98* | 2.6 ± 0.1 | 15.7** | 10.0 | 64 |
| **Tb(PyC3A)** | 1.16 ± 0.01 | 3.53 ± 0.01 | 6.86* | 2.4 ± 0.1 | 16.9** | 11.2 | 66 |

$\Phi_{tot}$ is the ratio between the photons emitted by the Ln(III) and the ones absorbed by the ligand. It is calculated by means of a reference standard presenting a known Φ (refer to Section 3.3.1. for experimental details). The apparently low $\Phi_{tot}$ values are in fact in a range typically seen in literature for cell imaging with either lanthanide or d-block complexes (4-10% range)[19,41–44]. Moreover, we are expecting a rise in this value with the formation of the adduct with the target biomarker, since the quenching water molecules in the inner sphere will be displaced.

The $\eta_{sens}$ value is calculated by using Equation 3.4.c. As it can be seen in Table 4.4., it results much higher for the pyridine-functionalized complexes (61-66%) than for the quinoline-functionalized ones (29-40%). This may be attributed to the shorter Ln-$N_{heterocycle}$ distances in the case of quinoline-based complexes (DFT calculations), since the energy transfer from the antenna to the Ln(III) depends on the distance between them: the shorter is the distance, the more efficient is the energy transfer and, consequently, the higher is $\eta_{sens}$.[45]

## 4.3. Conclusions

### PROTONATION OF THE LIGANDS

- The proposed ligands are stable in water at the studied pH range (from 2 to 11), temperature (298 K) and ionic strength (0.1 M NaCl).
- The protonation constants obtained are in accordance with values found in literature for similar ligands and conditions.
- They all present four dissociable protons assigned to either acetate, heteroaromatic nitrogen or ternary nitrogen positions.

### FORMATION OF THE COMPLEXES

- The Eu(III) and Tb(III) complexes studied are very stable at the proposed pH range (from 2 to 11), temperature (298 K) and ionic strength (0.1 M NaCl).
- The overall stability constants found are high and in accordance with values found in literature for similar complexes and conditions.
- The pyridine-functionalized ligands present higher affinity for the lanthanide cations due to the higher steric hindrance of the bulkier quinoline moieties.
- The tri-acetate ligands form more stable lanthanide complexes than the di-acetate ones due to the higher negative charge of the former ones and the oxyfilicity of lanthanide cations.
- The predominant species in solution at pH 7.4 is in all cases the luminescent lanthanide complex, with around 100% prevalence.
- All complexes are octacoordinated, presenting 2 waters in the first coordination sphere. The presence of these coordinated waters, which quench the luminescent signal, can be substituted by the target biomarker, which would cause a rising in the luminescent response.

## LUMINESCENCE OF THE COMPLEXES

- Eu(III) is sensitized by all the ligands in study. On the other hand, Tb(III) is sensitized just by the ligands presenting pyridine antenna.
- The 1:1 ligand-Ln(III) stoichiometry is confirmed by the fitting of the luminescent decay curves in single exponential functions.
- Less multiphonon relaxation is observed in Tb(III) complexes due to smaller energy gaps between excited and ground levels.
- Total quantum yields are in the range of values frequently found in literature for cell imaging with either lanthanide or d-block complexes. Moreover we expect the rise of these values due to the substitution of the quenching coordinated waters by the target biomarker.
- $\eta_{sens}$ are higher for pyridine- (61-66%) than for quinoline-based (29-40%) complexes, which may be attributed to the longer Ln(III)-$N_{heterocyclic}$ bonds in the latter ones (DFT).

## 4.4. Bibliography


[1] R. Janicki, A. Mondry, P. Starynowicz, *Coord. Chem. Rev.* **2017**, *340*, 98–133.

[2] F. Caillé, C. S. Bonnet, F. Buron, S. Villette, L. Helm, S. Petoud, F. Suzenet, É. Tóth, *Inorg. Chem.* **2012**, *51*, 2522–2532.

[3] J. M. Couchet, J. Azéma, C. Galaup, C. Picard, *J. Lumin.* **2011**, *131*, 2735–2745.

[4] E. Brunet, O. Juanes, R. Sedano, J. C. Rodríguez-Ubis, *Tetrahedron Lett.* **2007**, *48*, 1091–1094.

[5] C. Picard, N. Geum, I. Nasso, B. Mestre, P. Tisnès, S. Laurent, R. N. Muller, L. Vander Elst, *Bioorganic Med. Chem. Lett.* **2006**, *16*, 5309–5312.

[6] M. H. V. Werts, *Sci. Prog.* **2005**, *88*, 101–131.

[7] S. Cotton, *Lanthanide and Actinide Chemistry*, John Wiley & Sons, Ltd, **2006**.

[8] M. Leonzio, A. Melchior, G. Faura, M. Tolazzi, M. Bettinelli, F. Zinna, L. Arrico, L. Di Bari, F. Piccinelli, *New J. Chem.* **2018**, *42*, 7931–7939.

[9] C. C. McLauchlan, J. Florián, D. S. Kissel, A. W. Herlinger, *Inorg. Chem.* **2017**, *56*, 3556–3567.

[10] M. Leonzio, A. Melchior, G. Faura, M. Tolazzi, F. Zinna, L. Di Bari, F. Piccinelli, *Inorg. Chem.* **2017**, *56*, 4413–4422.

[11] M. D. Ogden, S. I. Sinkov, G. P. Meier, G. J. Lumetta, K. L. Nash, *J. Solution Chem.* **2012**, *41*, 2138–2153.

[12] N. Chatterton, C. Gateau, M. Mazzanti, J. Pécaut, A. Borel, L. Helm, A. Merbach, *Dalton Trans.* **2005**, 1129–1135.

[13] P. Caravan, P. Mehrkhodavandi, C. Orvig, **1997**, *1669*, 1316–1321.

[14] C. M. G. dos Santos, A. J. Harte, S. J. Quinn, T. Gunnlaugsson, *Coord. Chem. Rev.* **2008**, *252*, 2512–2527.

[15] J. P. Leonard, T. Gunnlaugsson, *J. Fluoresc.* **2005**, *15*, 585–595.

[16] X. Wang, H. Chang, J. Xie, B. Zhao, B. Liu, S. Xu, W. Pei, N. Ren, L. Huang, W. Huang, *Coord. Chem. Rev.* **2014**, *273–274*, 201–212.

[17] Y. Bretonniere, M. J. Cann, D. Parker, R. Slater, *Org. Biomol. Chem.* **2004**, *2*, 1624–1632.

[18] Y. Bretonnière, M. J. Cann, D. Parker, R. Slater, *Chem. Commun.* **2002**, *8*, 1930–1931.

[19] K. L. Peterson, J. V. Dang, E. A. Weitz, C. Lewandowski, V. C. Pierre, *Inorg. Chem.* **2014**, *53*, 6013–6021.

[20] B. S. Murray, E. J. New, R. Pal, D. Parker, *Org. Biomol. Chem.* **2008**, *6*, 2085–2094.

[21] D. G. Smith, R. Pal, D. Parker, *Chem. - A Eur. J.* **2012**, *18*, 11604–11613.

[22] C. P. Montgomery, E. J. New, D. Parker, R. D. Peacock, *Chem. Commun.* **2008**, 4261–4263.

[23] L. Alderighi, P. Gans, A. Ienco, D. Peters, A. Sabatini, A. Vacca, *Coord. Chem. Rev.* **1999**, *184*, 311–318.

[24] R. Ferreirós-Martínez, D. Esteban-Gómez, C. Platas-Iglesias, A. de Blas, T. Rodríguez-Blas, *Dalton Trans.* **2008**, 5754–65.

[25] A. V. Rayer, K. Z. Sumon, L. Jaffari, A. Henni, *J. Chem. Eng. Data* **2014**, *59*, 3805–3813.

[26] E. M. Gale, S. Mukherjee, C. Liu, G. S. Loving, P. Caravan, *Inorg. Chem.* **2014**, *53*, 10748–10761.

[27] P. Caravan, S. J. Rettig, C. Orvig, *Inorg. Chem.* **1997**, *36*, 1306–1315.

[28] M. Wagner, R. Ruloff, E. Hoyer, W. Gründer, *Z.Naturforsch.* **1997**, *52c*, 508–515.

[29] R. M. Smith, A. E. Martell, *Sci. Total Environ.* **1987**, *64*, 125–147.

[30] G. Anderegg, *Helv. Chim. Acta* **1974**, *57*, 1340–1346.

[31] K. Kahmann, H. Sigel, H. Erlenmeyer, *Helv. Chim. Acta* **1964**, *47*, 1754–1763.

[32] A. C. Mendonça, A. F. Martins, A. Melchior, S. M. Marques, S. Chaves, S. Villette, S. Petoud, P. L. Zanonato, M. Tolazzi, C. S. Bonnet, et al., *Dalt. Trans.* **2013**, *42*, 6046.

[33] F. Endrizzi, A. Melchior, M. Tolazzi, L. Rao, *Dalton Trans.* **2015**, *44*, 13763–14180.

[34] F. Piccinelli, M. Bettinelli, A. Melchior, C. Grazioli, M. Tolazzi, *Dalt. Trans.* **2015**, *44*, 182–192.

[35] M. Soulié, F. Latzko, E. Bourrier, V. Placide, S. J. Butler, R. Pal, J. W. Walton, P. L. Baldeck, B. Le Guennic, C. Andraud, et al., *Chem. - A Eur. J.* **2014**, *20*, 8636–8646.

[36] J. Florián, C. C. McLauchlan, D. S. Kissel, C. C. Eichman, A. W. Herlinger, *Inorg. Chem.* **2015**, *54*, 10361–10370.

[37] G. Tircsó, M. Regueiro-Figueroa, V. Nagy, Z. Garda, T. Garai, F. K. Kálmán, D. Esteban-Gómez, É. Tóth, C. Platas-Iglesias, *Chem. - A Eur. J.* **2016**, *22*, 896–901.

[38] W. D. W. Horrocks, D. R. Sudnick, *J. Am. Chem. Soc.* **1979**, *101*, 334–340.

[39] R. M. Supkowski, W. D. W. Horrocks, *Inorg. Chim. Acta* **2002**, *340*, 44–48.

[40] M. Mihorianu, M. Leonzio, M. Monari, L. Ravotto, P. Ceroni, M. Bettinelli, F. Piccinelli, *ChemistrySelect* **2016**, *1*, 1996–2003.

[41] M. Chen, Y. Wu, Y. Liu, H. Yang, Q. Zhao, F. Li, *Biomaterials* **2014**, *35*, 8748–8755.

[42] C. Li, Y. Liu, Y. Wu, Y. Sun, F. Li, *Biomaterials* **2013**, *34*, 1223–1234.

[43] S. P. Y. Li, A. M. H. Yip, H. W. Liu, K. K. W. Lo, *Biomaterials* **2016**, *103*, 305–313.

[44] D. Parker, P. K. Senanayake, J. A. Gareth Williams, *J. Chem. Soc. Perkin Trans. 2* **1998**, 2129–2140.

[45] D. L. Dexter, *J. Chem. Phys.* **1953**, *21*, 836–850.

# Chapter 5

# Luminescent sensing of relevant biomarkers

## 5.1. Background: sensing of biomarkers

As already discussed in Chapter 1, luminescent Ln(III) complexes have been broadly used for sensing due to their exceptional optical properties, which make them potentially more interesting than other probe concepts. We have also briefly presented the high variety of target ions and molecules which may be sensed by this complexes, from small anions such as chlorides to big molecules such as proteins. In this chapter we will evaluate the viability of the lanthanide complexes presented in Chapter 4 as luminescent sensors for some crucial anionic biomarkers (L-lactate, bicarbonate and citrate). We will discuss their affinity with the target analytes, the structure of the adducts and their luminescent response. We will also discuss their potential as bioprobes for practical applications in terms of selectivity and mobility/localization in the organism.

## 5.2. Lactate sensing

### 5.2.1. Introduction

Lactic acid (Figure 5.1.) is a weak acid with a p*K*a of 3.69 at 298.15 K and an ionic strength ($\mu$) of 0.1 M in water[1]. This $pK_a$ is much lower than that of cells and extracellular fluids (physiologic pH is around 7.4, and the lowest limits of pH compatible with life over a prolonged period is 6.8). If we use the Henderson-Hasselbalch equation (Equation 5.1.), we can easily calculate the approximated ratio lactate/lactic acid expected under physiological pH (Equation 5.2.a) and critically low pH (Equation 5.2.b). Regarding the high ratios obtained in this calculations (over 800) we can state that mostly all lactic acid will be in the form of lactate in physiological conditions.[2] Thus, in lactic acid/lactate

studies for biomedical applications, the lactate form will be considered (more specifically, L-lactate[3], figure 5.1. left).

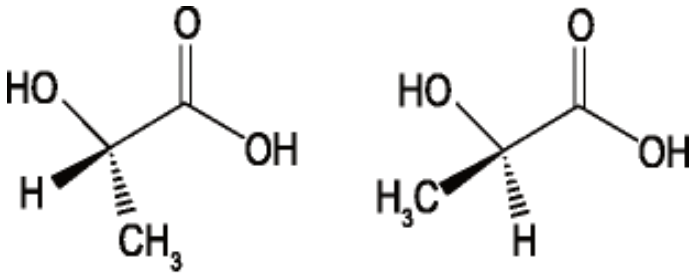


***Figure 5.1.*** *L-lactic acid (left) and D-lactic acid (right).*

$$pH = pKa + \log([A^-]/[HA]) \qquad \textit{(Equation 5.1.)}$$

$$7.4 = 3.85 + \log(\text{[lactate]} / [\text{lactic acid}]) \rightarrow \mathbf{3548}{:}1 \qquad \textit{(Equation 5.2.a)}$$

$$6.8 = 3.85 + \log(\text{[lactate]} / [\text{lactic acid}]) \rightarrow \mathbf{891}{:}1 \qquad \textit{(Equation 5.2.b)}$$

Hyperlactatemia (excess of lactate, check usual lactate concentrations in diverse physiological fluids in Table 5.1.) is related to an increase in the anaerobic metabolism, which may be caused by extensive physical exercise or by several pathological conditions, such as respiratory, renal or liver failure.[2,4] The detection and monitoring of lactate concentration has indeed become of great importance due to its crucial role in many fields such as sports medicine (i.e. brain function during exercise and lactate threshold)[3,6,7], food industry (i.e. microbial contamination and food adulteration)[8] and clinical diagnostics (i.e. liver and respiratory failure, sepsis, Parkinson's disease, prostate cancer and colon cancer)[2,3,5,9–12]. Thus, high lactate concentration (>4.0 mM) is prognostic in prehospital, emergency departments and intensive care unit settings, as it may act as an alarm signal for the diagnosis of patient conditions, and can be used to guide early resuscitation therapy in critical situations.[2,3,13]

During the last decades many lactate sensors have been developed. Currently, the predominant lactate sensors in the market are electrochemical, as they are user-friendly,

sensitive, economic and portable, but they do not permit the convenient monitoring of the lactate concentration through time, as the implanted sensors get coated by body defense mechanisms. Implanted biosensors have been tested with no commercial success due to biocompatibility issues.[3] For instance, vascular sensors may cause thrombosis or embolism.[14] Many attempts have been made to monitor lactate in other fluids/tissues. To do so, it is important to choose matrices whose lactate content correlates with its concentration in blood (Table 5.1.).[3] As an example, an electrochemical non-invasive sensor has been developed for the quantification of lactate in exhaled breath, with a low detection limit of 150 nM and good selectivity toward common interferences in this matrix, but no validation with real samples was reported.[15]

***Table 5.1.*** *Amount of lactate found in different body fluids.*[3][16]

| MATRIX | Blood | Extracellular fluid | Intracellular fluid | Tears | Exhaled breath | Saliva |
|---|---|---|---|---|---|---|
| **[Lactate] (mM)** | 0.5-2* | 0.6-2.3 | 3-22 | 1-5 | 0.014-0.022 | 0.1-2.5 |

***** It may be higher during exercise (12 mM)[17] or extreme exercise (25 mM)[18].

Optical lactate sensors have also been developed from the 60's. In 1964, an absorbance-based sensor (and the first optical sensor developed for lactate detection reported in literature) was developed by Broder and Weil.[13] But absorbance techniques were gradually replaced by fluorescence techniques, due to their independence from the light pathway and their lower detection limits.[3] Conveniently, the luminescence intensity of the luminescent substances is usually correlated to their concentration. Thus, many fluorescent sensors have been developed for the detection of lactate. For instance, Groegel et al. reported in 2011 an enzymatic biosensor capable of detecting L-lactate with a detection limit of 164 nM,[19]

Even if there already exist some commercial sensors for the determination of lactate at abnormally-high concentrations, the achievement of miniaturizable, more robust, and more selective probes is still a challenge.[4] Luminescent sensors may permit the development of valuable non-invasive and miniaturized sensors, which would lead to the commercialization of biocompatible lactate sensors with the capability of constantly monitoring the concentration of this relevant biomarker.

## 5.2.2. Stability

The stability constants (Table 5.2.) for the adduct between $[Tb(bpcd)]^+$ and L-lactate (from now on Lac) has been determined via two independent experiments: luminescent titration (LT, Figure 5.2.) and isothermal titration calorimetry (ITC, Figure 5.3.). For experimental and calculation details, please refer to Chapter 2. The data from LT experiments were processed by using the Benesi-Hildebrand equation (Section 3.3.1.); the data from the ITC experiments were processed with Excel add-in cEST [20] (Section 3.5.2.).

We obtained very similar stability constants via both ITC and LT experiments and for either the racemic or the pure enantiomers of the lanthanide complex. The constants are also similar to that found for the formation of $[Ln(Lac)_3]$, which would be an analogue for [Tb(bpcd)(Lac)], as in both complexes Ln(III) is coordinated by three carboxylate moieties. The enthalpy and the entropy for the adduct formation are both positive. Unfavorable enthalpies are typical in charge-neutralization reactions in water; entropy may be favorable due to i) the substitution of the water molecules coordinated to the Ln(III) by Lac and ii) the increment of the disorder in the water molecules present in the second coordination sphere, which will be less attracted by the neutral ligand.

***Table 5.2.*** *Stability constants and thermodynamic parameters for the formation of the adduct [bpcd-Tb-Lac] and stepwise formation constants for the reaction [Ln-(Lac)$_2$] +Lac ⇌ [Ln-(Lac)$_3$] at T = 298.15 K and $\mu$ = 0.1 M NaCl..*

| Technique | log *K* | Δ*G* (kJ/mol) | Δ*H* (kJ/mol) | Δ*S* (J/mol·K) |
|---|---|---|---|---|
| **[Tb(bpcd)(Lac)]** | | | | |
| ITC (racemic isomer) | 1.30 ± 0.09 | -7.0 ± 0.1 | 14.44 ± 0.05 | 72.4 ± 0.1 |
| LT (S,S isomer) | 1.35 ± 0.01 | -7.7 | - | - |
| LT (racemic and R,R isomer) | 1.45 ± 0.01 | -8.3 | - | - |
| **[Ln(Lac)$_3$]** | | | | |
| Potentiometry (Ln=Tb) | 1.1[21]*/ 1.15[22] | - | - | - |
| Potentiometry (Ln=Eu) | 1.06[21]* / 1.26[22] | - | - | - |
| Spectroscopy (Ln=Eu) | 1.38[23] | - | - | - |

* (0.1 M $NaClO_4$)

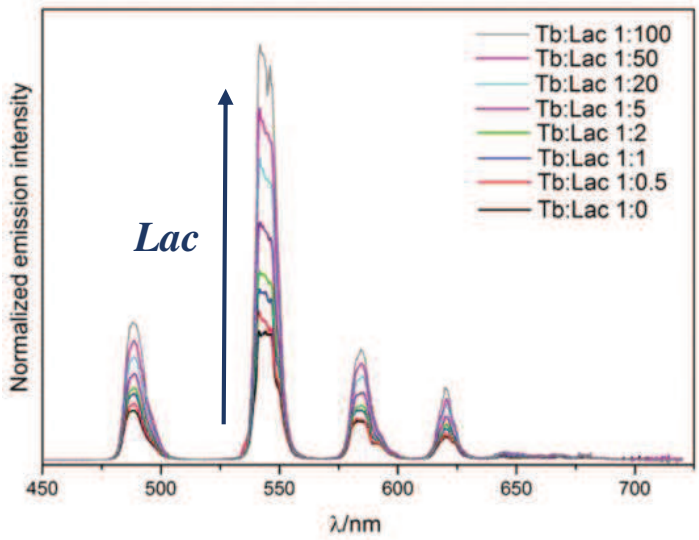


***Figure 5.2.*** *Luminescent titration of the [Tb(R,R-bpcd)(H$_2$O)$_x$]$^+$ complex (0.03 mM) under addition of Lac ($\lambda_{exc}$=270 nm).*

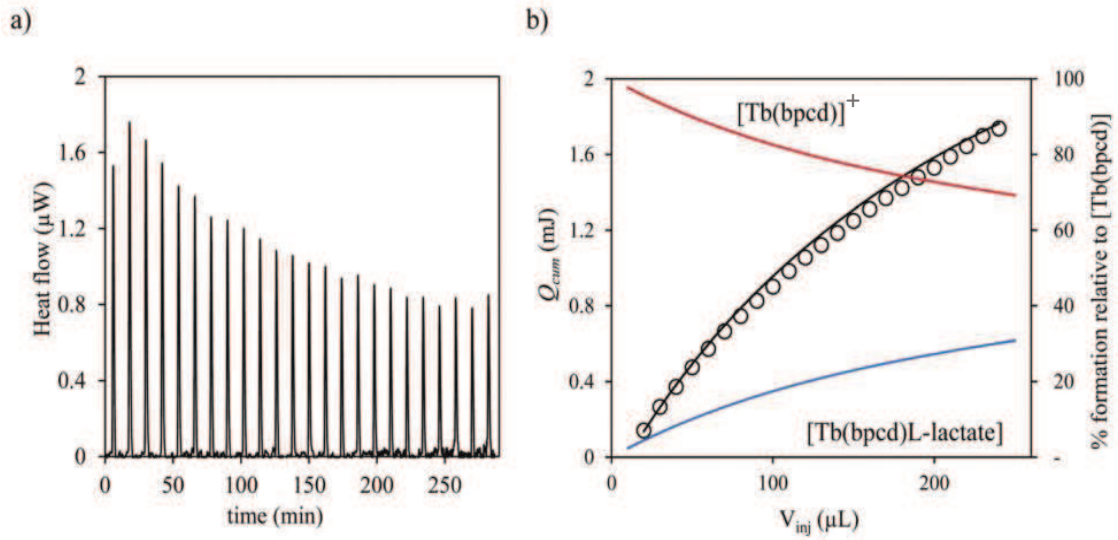


***Figure 5.3.*** *a) Raw ITC output signal for the formation of the [Tb(bpcd)(Lac)] adduct; b) observed (circles) and calculated (solid line) cumulative heat ($Q_{cum}$, stepwise sum of the $Q_{corr}$) along with the calculated speciation.*

## 5.2.3. Structure

The lower energy structures for the [Y(S,S-bpcd)(Lac)] adduct have been determined by DFT calculations (Figure 5.4.) in either, gas phase or using a polarizable continuum model (PCM), which simulates the solvent as a polarizable continuum medium.[24] Structures e and f are, respectively, structures a and b optimized with four additional solvating water molecules. More details in DFT calculations and the choice of the Y(III) anion for their performance can be found in Sections 3.4.1. and 4.2.3..

The trans-O,O and trans-Npy,Npy isomers of the $[Y(bpcd)]^+$ complex, determined previously (Section 4.2.3.), where considered for the calculations. As we have already mentioned, $[Ln(Lac)_3]$ can be considered an analogue complex for [Tb(bpcd)(Lac)], as in both complexes Ln(III) is coordinated by three carboxylate moieties. Thus, as suggested in literature for the coordination of three Lac with Ln(III) in the $[Ln(Lac)_3]$ complex,[23,25] the hydroxyl group of Lac was considered to be protonated, and we contemplated the coordination of Lac through either the carboxylate group or the hydroxo/carboxylate oxygens in DFT calculations.

In Table 5.3. the calculated energy differences for the a-f isomers in either, gas phase or PCM, are presented. As it can be observed, the lower values by using PCM (either with or without using additional solvating water molecules) are found for both, the trans-O,O isomer and the trans-Npy,Npy isomer with Lac coordinating through both, the hydroxo and the carboxylate oxygens, which is in agreement with the results found previously in literature for the $[Ln(Lac)_3]$ complex.[23,25]

***Table 5.3.*** *Relative energies (kcal/mol) of the [Y(bpcd)(Lac)] isomers studied by DFT calculations (Figure 3.5.) in gas phase and PCM, where $E_a$ is the reference energy for $E_{a-d}$ and $E_e$ for $E_{e-f}$.*

| Structure | a | b | c | d | e | f |
|---|---|---|---|---|---|---|
| $\Delta E_{gas}$ | 0.0 | 4.3 | 6.3 | 9.7 | 0.0 | 13.6 |
| $\Delta E_{PCM}$ | 0.0 | 4.7 | -0.2 | 1.5 | 0.0 | 9.1 |

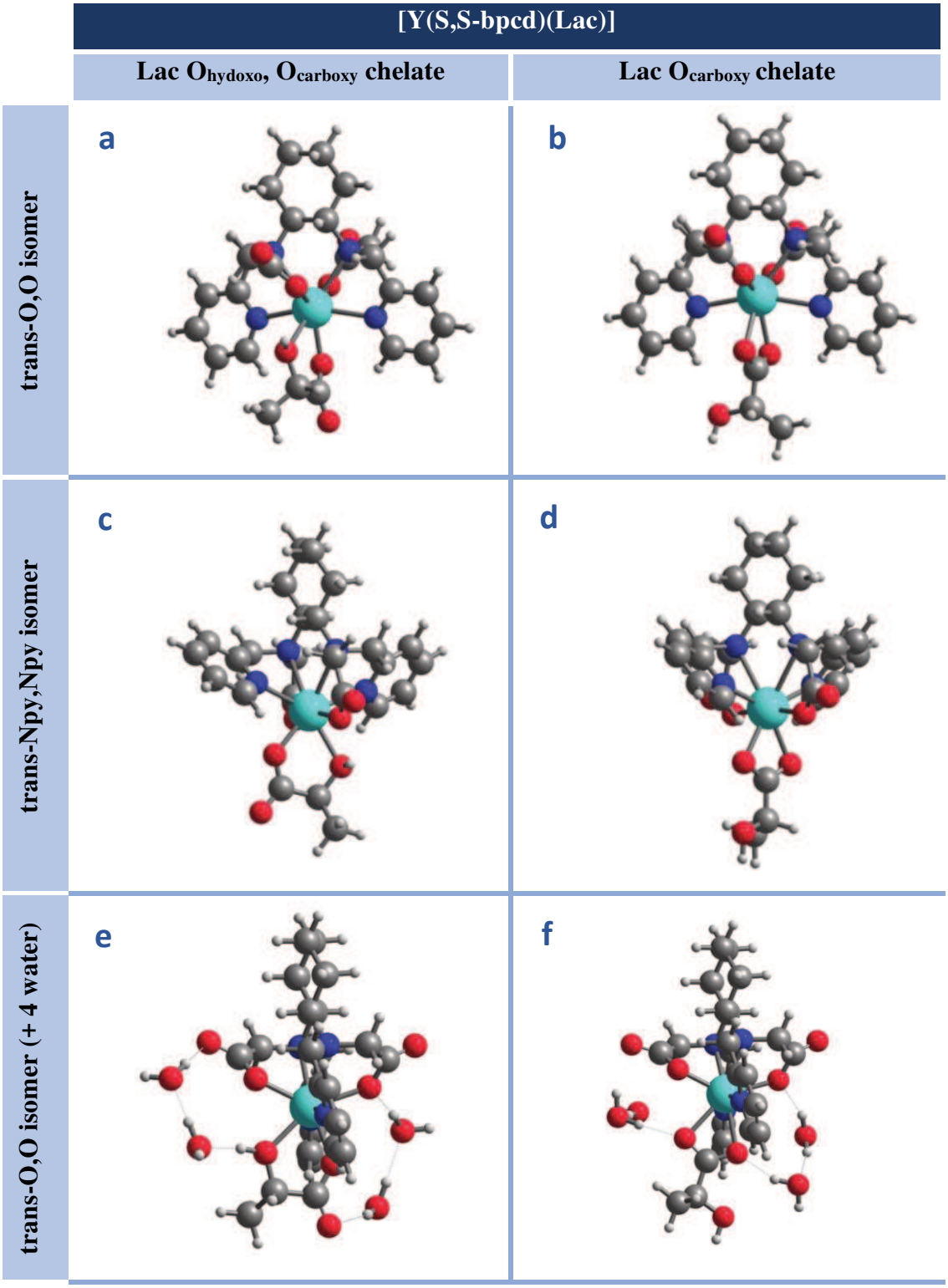


***Figure 5.4.*** *DFT minimum energy structures for the [Y(S,S-bpcd)(Lac)] adduct.*

## 5.2.4. Luminescence and sensing

The luminescence of the $[Eu(bpcd)]^+$ and $[Tb(bpcd)]^+$ complexes has been studied either in the presence of Lac, with total luminescence and circularly polarized light luminescence (CPL), and has been compared with the luminescent response of the $[Tb(bped)]^+$ complex, the achiral version of $[Tb(bpcd)]^+$ (Figure 4.3.). Refer to Section 3.3. for details in the experimental conditions.

### 5.2.4.1. Total luminescence response with L-lactate

As it has already been shown in Figure 5.2., the luminescence of the Tb(III) complex with R,R-bpcd increases with the successive addition of Lac, until arriving at a plateau at very high Lac concentrations (1:100 complex:Lac molar ratio). The same experiments were also performed for the S,S isomer and for the achiral Tb(III) complex with bped (Figure 4.3.). In Figure 5.5.a, the relative intensities (experimental intensity/intensity without the presence of Lac) at 546 nm (maximum intensity for the $^5D_4 \rightarrow {}^7F_5$ band) for both enantiomers and the achiral complex are represented as a function of the Lac/Tb(III) molar ratio. In Figure 5.5.b., the lifetimes of the same Tb(III) complexes are represented as a function of the Lac/Tb(III) molar ratio. Both, the luminescent response (sensitivity towards the presence of Lac) and the observed lifetimes, are higher for the chiral complexes than for the achiral one, with slightly higher values for the S,S enantiomer.

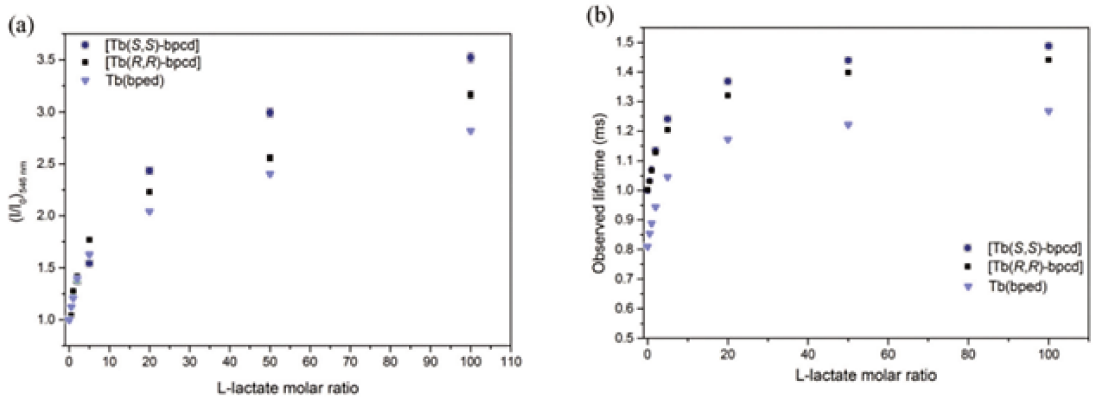


***Figure 5.5.*** *a) Relative emission intensity (546 nm) and b) lifetime as a function of Lac/Tb(III) molar ratio.*

As we have already mentioned, water molecules near the metal center quench the luminescent signal and cause shorter lifetimes. Thus, the increase in the luminescence and lifetimes can be explained by the substitution of the water molecules present in the first coordination sphere by the incoming Lac anion.[26,27] The fact that these values are lower for the achiral complex than for the chiral ones might have been explained by a higher number of water molecules in the first coordination sphere in the former one, but that hypothesis was immediately discarded, as the hydration number for all chiral and achiral Tb(III) complexes discussed in this section are very similar ($2.5 < q < 2.7$). Thus, another explanation should be found.

### 5.2.4.2. CPL

CPL is a chiroptical technique which is attracting a great interest due to its wide range of applications in technological and biomedical fields.[26,28–30] Very interestingly, this phenomenon may be displayed by Ln(III) in chiral environments, with high dissymmetry factors ($g_{lum}$, refer to Section 3.3.2.). It is very important, as high $g_{lum}$ values are required for real applications, such as bioanalysis[31], the developing of cutting-edge technology LEDs[32] or the selective sensing of chiral analytes (such as lactate) by inducing a CPL response via the binding of this chiral analyte to the Ln(III) complex.[29,30,33–36]

High $g_{lum}$ values are reported in literature for Ln(III) complexes presenting the DACH backbone (Figure 4.1.).[30] Some of them are very similar to the $bpcd^{2-}$ complexes we propose, for instance $cddadp^{2-}$ (Figure 5.6.).[37] But, in the design of $bpcd^{2-}$, the carboxylic moieties linked to the pyridine antenna where eliminated in order to leave additional space for the binding of the target biomarker.

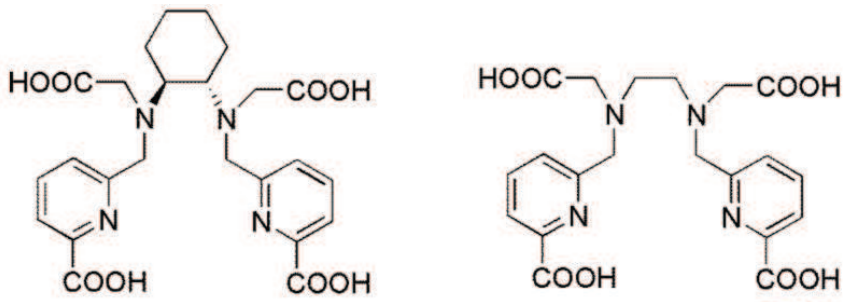


***Figure 5.6.*** *Ligands $H_4cddadp$ (left) and $H_4bpeda$ (right) proposed in literature*[37].

During CPL experiments in $CD_3OD$ we confirmed high $g_{lum}$ for our Eu and Tb complexes (Tables 5.4. and 5.5.). The results for the Tb isomers turned out to be specially promising, as their $g_{lum}$ values are even higher than those reported in literature for other chiral Tb(III) complexes (|0.044| < glum < |0.082|)[31,38,39] and similar to those found for cyclen-based (|0.22|)[40] and DACH-based (|0.20|)[30] Tb complexes. We would like to emphasize that, as also observed in our results, Eu complexes usually display higher $g_{lum}$ values than Tb complexes. Considering these promising results, CPL spectra in water were recorded for the main band of the Tb(bpcd)Cl complex for the two enantiomers. The values obtained (Table 5.5. in parenthesis) were still high, which makes this Tb complex potentially suitable as a CPL sensing probe in aqueous solution.

***Table 5.4.*** *$g_{lum}$ values for the R,R, and S,S enantiomers of Eu(bpcd)Cl in $CD_3OD$, calculated on minima or maxima of the CPL curves.*

| Wavelength (nm) | (R,R) | (S,S) |
|---|---|---|
| **598** | -0.9 | +0.18 |
| **607** | +2.3 | -0.28 |
| **625** | -0.14 | -0.14 |

***Table 5.5.*** *$g_{lum}$ values for the R,R, and S,S enantiomers of Tb(bpcd)Cl in $CD_3OD$, calculated on minima or maxima of the CPL curves.*

| Wavelength (nm) | (R,R) | (S,S) |
|---|---|---|
| **546** | +0.11 (+0.07) | -0.11 (-0.06) |
| **586** | +0.16 | -0.15 |
| **594** | -0.70 | +0.70 |
| **616** | +0.31 | -0.31 |
| **625** | -0.11 | -0.09 |

### 5.2.4.3. CPL sensing of L-lactate

Regarding the good results obtained in the CPL experiments with the Tb(bpcd)Cl complex in water, we studied the CPL response of the complex in the presence of lactate. CPL titrations for both enantiomers were performed separately at 546 nm upon the addition of Lac, from 0 to 100 equivalents (Figure 5.7.), and we observed that the enantiomers presented diverse trends. The (R,R) enantiomer presented a 50% variation from 0 to 100 equivalents of Lac, while the (S,S) enantiomer presented a lower variation

of 17%. The stability constants of the adducts between Lac and both enantiomers are, as we have already discussed (Table 5.2.), very similar. Actually, we observed that the racemic complex show CPL activity in the presence of Lac, as the CPL signals from the enantiomers do not cancel out (Figure 5.8.a). Also the response of the achiral complex $[Tb(bped)]^+$ in the presence of Lac was studied (Figure 4.8.b), but no CPL signal was observed.

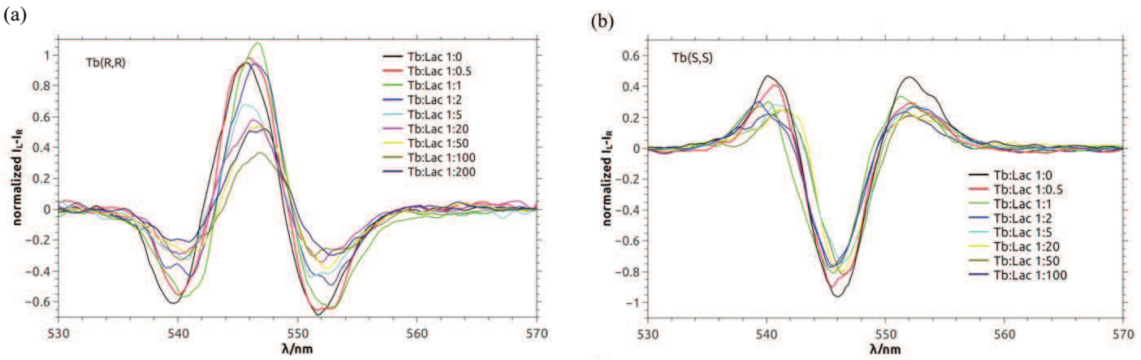


***Figure 5.7.*** *CPL titration at 546 nm, normalized to the first titration point, for the a) (R,R) and the b) (S,S) enantiomer of the $[Tb(bpcd)]^+$ complex upon addition of Lac.*

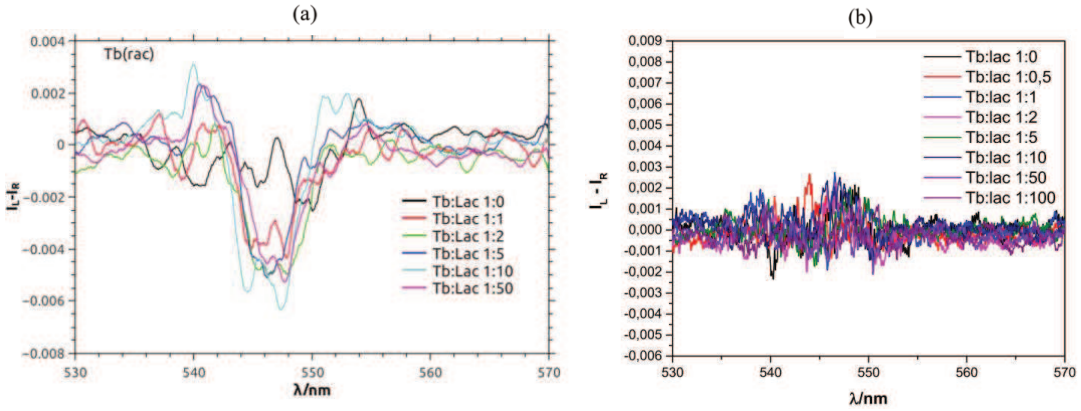


***Figure 5.8.*** *CPL titration at 546 nm, normalized to the first titration point, for a) the racemic $[Tb(bpcd)]^+$ and b) the racemic $[Tb(bped)]^+$ complex upon addition of Lac.*

Regarding the good results obtained for our chiral Tb complex, we decided to study its CPL response in a more complex matrix including Lac, in order to assess the viability of this potential probe for practical applications. The commercial solution Ringer's lactate[41] was chosen due to its current application in hospitals for the treatment of metabolic acidosis and for the replacement of electrolytes and fluids after blood loses. This solution contains, apart from L-lactate (28.3 mM), $CaCl_2 \cdot 2H_2O$ (0.27 g/L), KCl (0.40 g/L) and NaCl (6.0 g/L). The CPL spectra were recorded in the commercial solution containing the racemic [Tb(bpcd) ]$^+$ complex 5 mM), with the ratio Tb:Lac being 1:5.4. As expected, we observed CPL activity (Figure 5.9.), and it was in agreement with the previous CPL experiments performed with our complex in the presence of Lac (Figure 5.8.a) regarding both, shape and intensity. We would like to point out the fact that Lac is the only chiral species in the commercial solution and, consequently, the only one capable of inducing the CPL activity observed.

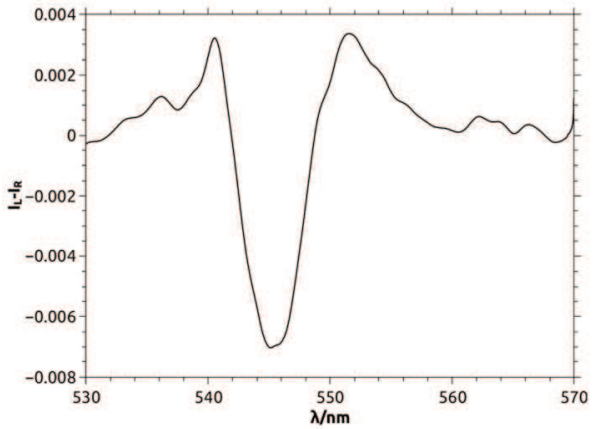


***Figure 5.9.*** *CPL spectrum at 546 nm for the racemic [Tb(bpcd)]$^+$ (5 mM) in a commercial Ringer's lactate solution.*

## 5.2.5. Conclusions

### STABILITY AND STRUCTURE OF THE LACTATE ADDUCT

- The adduct between L-lactate and the Tb(III) complex is stable at temperature $T$ = 298.15 K and ionic strength μ = 0.1 M NaCl.
- Similar stability constants are found either via ITC or LT for the (R,R) and (S,S) isomers and for the racemic forms of the complex. The obtained stability constants are also similar to those presented by $Eu(Lac)_3$ and $Tb(Lac)_3$.
- The trans-O,O isomer and the trans-Npy,Npy isomer coexist in equilibrium, with Lac coordinating through both, the hydroxo and the carboxylate oxygens, which is in agreement with the results found previously in literature for the $[Ln(Lac)_3]$ complex.[23,25]

### SENSING OF LACTATE

- The racemic form of $[Tb(bpcd)]^+$ exhibits CPL activity in the presence of L-lactate due to the diverse trends displayed by the (R,R) and (S,S) isomers.
- The luminescent response of the Tb(III) complex rises in the presence of L-lactate until reaching a plateau at 100 equivalents of lactate.
- L-lactate was detected by the racemic $[Tb(bpcd)]^+$ in a commercial solution in the presence of other electrolytes.

## 5.3. Sensing of bicarbonate

### 5.3.1. Introduction

Carbonate presents the protonation constants p$K_{a1}$ = 9.87 and p$K_{a2}$ = 6.11 at 298.15 K, and p$K_{a1}$ = 9.67 and a p$K_{a2}$ = 6.04 at 323 K, all under $\mu$ = 0.1 M (Equations 5.3.a and b).[42]

$$pK_{a1} = \frac{[HCO_3^-]}{[CO_3^{2-}][H^+]} \qquad \textit{(Equation 5.3.a)}$$

$$pK_{a2} = \frac{[H_2CO_3]}{[HCO_3^-][H^+]} \qquad \textit{(Equation 5.3.a)}$$

If we use the Henderson-Hasselbalch equation (Equation 5.1.), we can easily calculate the approximated ratios of carbonate/bicarbonate and bicarbonate/carbonic acid expected under physiological pH (Equations 5.4.a and b) and critically low pH (Equations 5.4.c and d) at 298.15 K (calculations at 323 K omitted, as the constants for both temperatures are comparable).

7.4 = 6.11 + log ( **[bicarbonate]** / [carbonic acid] ) → **20**:1 *(Equation 5.4.a)*

7.4 = 9.87 + log ( [carbonate] / **[bicarbonate]** ) → 1:**295** *(Equation 5.4.b)*

6.8 = 6.11 + log ( **[bicarbonate]** / [carbonic acid] ) → **5**:1 *(Equation 5.4.c)*

6.8 = 9.87 + log ( [carbonate] / **[bicarbonate]** ) → 1:**1174** *(Equation 5.4.d)*

Even considering this equation as an approximation, we may affirm that carbonate will be usually in the form of bicarbonate in physiological conditions. Thus, in carbonate/bicarbonate/carbonic acid studies for biomedical applications, the bicarbonate form will be considered (figure 5.10.).

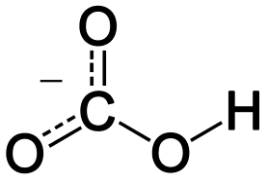

***Figure 5.10.*** *Bicarbonate (hydrogen carbonate) anion.*

Abnormal bicarbonate concentrations may be related to irregular pH homeostasis and, consequently, to many diseases. For instance, metabolic acidosis (abnormally high hydrogen ion concentration) may indicate the presence of solid tumors[43] or cause chronic kidney disease – it has been observed that patients with chronic kidney diseases caused by metabolic acidosis show low serum bicarbonate concentration.[44]

Other many physiological processes, apart from pH homeostasis and kidney function, depend on this equilibrium, such as sperm maturation and blood flow.[16,45,46] Moreover, bicarbonate is 10 times more concentrated than other anions present in human body's fluids and tissues (except within cells, where lactate could compete with bicarbonate in specific cell types) (Table 5.6.).[16] Thus, the development of sensors for bicarbonate quantification at physiological conditions is of main importance for the study, detection and treatment of many diseases related to this anion and its physiological processes.

***Table 5.6.*** *Typical concentrations (mM) of selected anions in humans.*[16]

| Anion | Extracellular fluid | Intracellular fluid* | Cerebrospinal fluid |
|---|---|---|---|
| **Bicarbonate** | 24-27 | 10-12 | 20-23 |
| **Lactate** | 0.6-2.3 | 3-22 | 0.5-2.2 |
| **Citrate** | 0.1-0.3 | 2-4 | 0.05-0.25 |
| **Phosphate** | 1.2-1.3 | 0.8-1.2 | 0.15 |
| **Chloride** | 104-115 | 3-15 | 115-130 |
| **Sulfate** | 0.4-0.6 | 0.3-04 | 0.06-0.2 |

* Concentrations may vary considerably depending on the cell type.

As previously discussed for lactate, fluorimetric sensors are especially convenient as they facilitate the development of non-invasive and miniaturized sensors, which may permit the commercialization of biocompatible devices with the capability of constantly checking the concentration of relevant biomarkers. In literature we may find many examples of Eu(III) and Tb(III) complexes which successfully quantify bicarbonate in 'physiological' conditions.[16] Bretonniere *et al.*[47,48] report Eu(III) complexes, all containing acridone as chromophore moieties (Figure 5.11.), which present a good luminescent response for bicarbonate concentrations between 5 and 25 mM.

Moreover, they can selectively bind bicarbonate (log$K$ = 0.8-2.3, depending on the ligand) in the presence of chloride, phosphate, lactate, citrate and protein. Murray *et al.*[49] report a non-toxic (to several cell types, with an $IC_{50}$ > 200 µM) Eu(III) complex (Figure 5.12., R = phenyl) selective for bicarbonate (log$K$ = 3.50) and citrate (log$K$ = 6.02), which may allow the monitoring of local changes of this anions within the mitochondrial region. This same complex and two analogues (Figure 5.12., R = phenyl, ester, carboxylate respectively) have also been reported by Smith *et al.*[50,51]; they monitored *in vivo* for the first time the concentration of bicarbonate in the mitochondria of cells. Imperio *et al.*[52] present an Eu(III) luminescent complex which selectively binds bicarbonate in the presence of competing anions, such as lactate and citrate. However, the stability of the adduct does not accomplish the conditions required in the applications. In 2013, Butler *et al.*[53] reported Eu(III) complexes capable of selectively binding bicarbonate in a complex medium when found in a concentration >10 mM (log$K$ between 3 and 4, 295 K, 50% MeOH / 0.1 M NaCl).

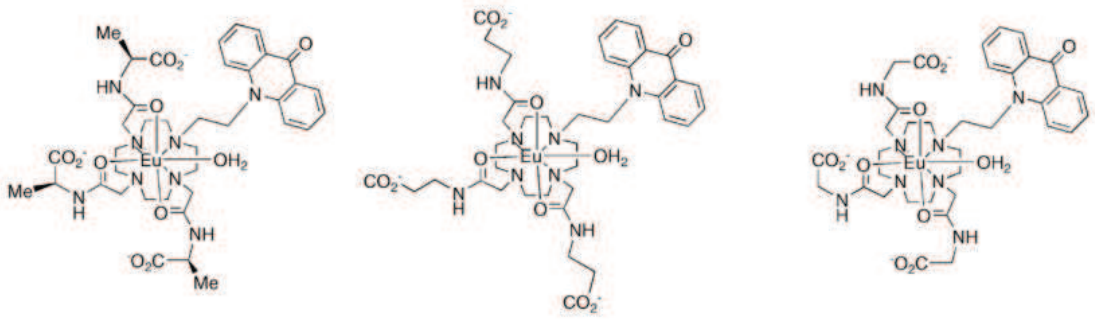

***Figure 5.11.*** *Three representative Eu(III) complexes presenting acridone chromophore moieties.*[47,48]

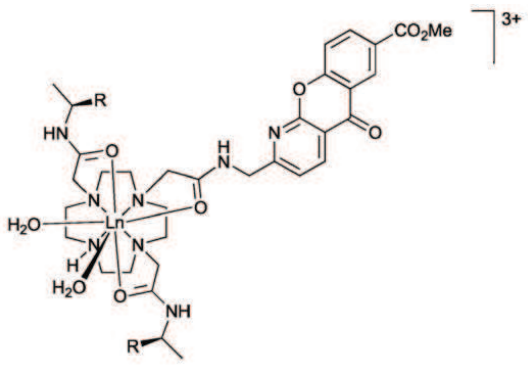


***Figure 5.14.*** *Ln(III) (Ln = Eu, Tb) complex, R = phenyl, ester, carboxylate.*[49–51]

As already described in Chapter 4, the complexes we present in this work differ in charge, steric hindrance and lipophilicity. It is expected that these differences will confer them different affinity towards diverse analytes (selectivity towards diverse target biomarkers), and lipophilicity strongly affect the mobility of the complexes in the organism, which is a very important fact to take into account for medical sensors. Moreover, the complexes proposed present a 6-fold coordination (ignoring water molecules) in comparison to that commonly found in literature (7-fold coordination, ignoring water molecules, strongly pre-oriented)[16,35,47–50,52–54] which may allow them the reversible binding of more than one target analyte at the same time (higher affinity) when the target molecule is small enough, such as in the case of bicarbonate. We continued our sensing studies with the small, relevant biomarker bicarbonate with the library of Eu and Tb complexes introduced in Chapter 3, in order to not just studying their viability as bicarbonate sensors, but also to begin a broader study about the selectivity of these complexes towards diverse analytes and interferings.

## 5.3.2. Stability

The binding constants of the adduct between bicarbonate and some Ln(III) complexes with bpcd, bQcd, QC3A and PyC3A (Table 5.7.) where obtained via LT upon the addition of bicarbonate (Figure 5.13. as an example) to a solution containing the Ln(III) complex (40 μM) at $T$ = 298.15 K, pH = 7.4 and μ = 0.1 M NaCl. The data was treated with the cEST program for MS Excel (Section 3.4.3.) and/or by using the Benesi-Hildebrand equation (B-H, Section 3.3.1.).

***Table 5.7.*** *Apparent binding constants found via luminescent titration upon the addition of bicarbonate for the adducts between bicarbonate and the lanthanide complexes (40 μM) at T = 298.15 K, pH = 7.4 and μ = 0.1 M NaCl. # is the number of bicarbonates coordinated to the metal center.*

| Complex | # | log *K (B-H)* | log *K (cEST)* |
|---|---|---|---|
| **[Eu(bpcd)]$^+$** | 2 | 5.76 ± 0.08 | 5.83 ± 0.07 |
| **[Tb(bpcd)]$^+$** | 2 | 5.94 ± 0.08 | - |
| **[Eu(bQcd)]$^+$** | 2 | 4.62 ± 0.08 | - |
| **Eu(PyC3A)** | 1 | 2.06 ± 0.08 | 2.09 ± 0.04 |
| **Eu(QC3A)** | 1 | 3.11 ± 0.08 | - |

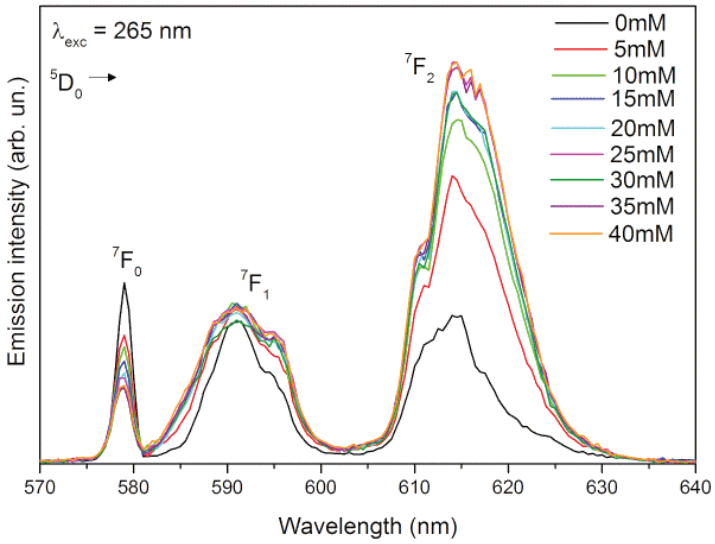


***Figure 5.13.*** *Total luminescence titration of [Eu(PyC3A)] upon addition of bicarbonate.*

The results obtained using both data treatment methods are comparable. We also observe that the cationic Ln(III) complexes show higher affinity towards bicarbonate, which makes sense taking into account the positive charge of the former and the negative charge of the latter. Interestingly, their affinity constants (4.62 - 5.94) are higher than those found in literature for other luminescent Eu and Tb complexes with bicarbonate (usually in the 2.6 - 3.85 range, to the best of our knowledge).

In addition, and as we have already mentioned, the unusual 'open concept' of the Ln(III) complexes presented in this work, with 6-fold coordination (ignoring water molecules in the first coordination sphere), may permit the entrance of more than one target molecule into the first coordination sphere, which would be much difficult for complexes similar to those presented in literature, usually presenting strongly pre-oriented environments with higher coordination numbers.[16,35,47–53] And we actually do observe that up to two bicarbonate anions can enter the first coordination sphere of the cationic Ln(III) complexes. We do not observe that behavior for the neutral complexes, which is reasonable, as the negative charge generated by the first coordinating bicarbonate would hamper the binding of an additional anion due to coulombic repulsion.

### 5.3.3. Structure

The possible structures of the 2:1 bicarbonate:complex adduct where studied by DFT calculations for the [Y(*trans*-O,O-bpcd)$(H_2O)_2]^+$ complex, as the bpcd-based adducts are the ones presenting the highest affinity constants with bicarbonate (Figure 5.14.). The most stable coordination mode of the bicarbonate is the bis-monodentate one, which presents 10.3 kcal/mol less than the bis-bidentate isomer.

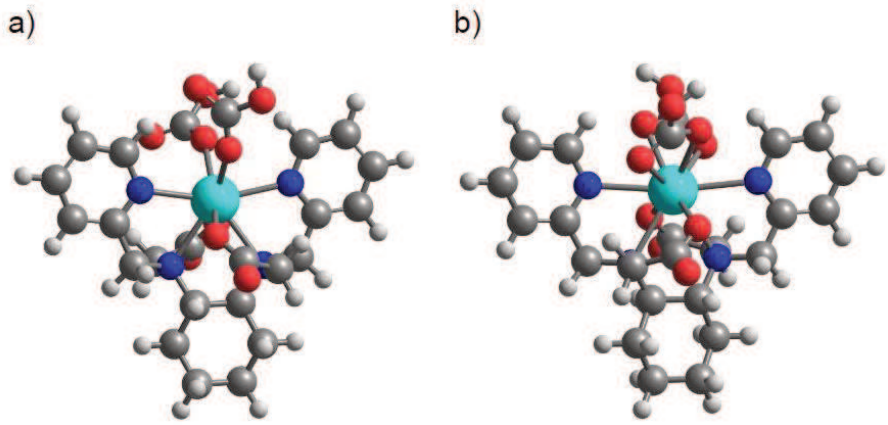


***Figure 5.14.*** *DFT minimum energy structures in PCM water for the [Y(trans-O,O-bpcd)$(H_2O)_2]^+$ adduct with bicarbonate considering either a)bis-monodentate or b) bis-bidentate bicarbonate coordination modes.*

### 5.3.4. Luminescent sensing

As we have already seen in Section 5.3.2., the luminescent emission of the complexes changes with the stepwise addition of bicarbonate. In Figure 5.13. (as a representative example) we can observe that the intensity of the $^5D_0 \rightarrow {}^7F_0$ and $^5D_0 \rightarrow {}^7F_2$ transition peaks decrease and increase respectively. This indicates a change in the symmetry of the Eu(III) environment, which can be represented by using the asymmetry ratio (*R*, ratio between the intensity values for both transitions, Equation 3.17.b.).

In Figure 5.15., the *R* values for all the Eu(III) complexes are represented upon the addition of bicarbonate. We observe a logarithmic increase of *R* with the addition of this anion until the reach of a plateau. The most sensitive complex towards the addition of bicarbonate is $[Eu(bpcd)]^+$, which presents the steepest slope from 0 to 10 mM bicarbonate concentration. Very interestingly, this concentration range is of great interest for the diagnosis of metabolic acidosis.

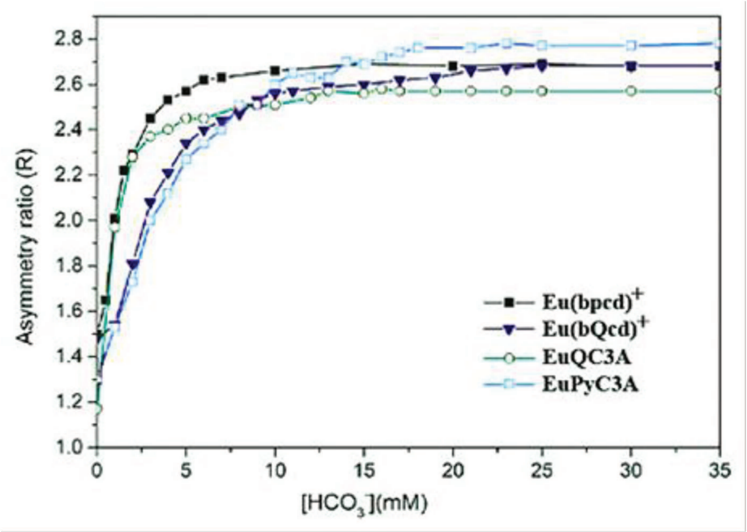


***Figure 5.15.*** *R for the Eu(III) complexes under study upon addition of bicarbonate.*

## 5.3.5. Conclusions

### STABILITY AND STRUCTURE OF THE BICARBONATE ADDUCTS

- The adducts between bicarbonate and the studied Ln(III) complexes are stable at temperature $T$ = 298.15 K, pH = 7.4 and ionic strength μ = 0.1 M NaCl.
- The highest affinity constants have been found for the bicarbonate adducts with the cationic Ln(III) complexes, in part due to coulombic attraction.
- The cationic Ln(III) complexes can bind up to two bicarbonate molecules.
- The coordination mode of the bicarbonates in the 1:2 adducts is bis-monodentate (DFT).

### SENSING OF BICARBONATE

- The increase in the bicarbonate concentration leads to a clear change in the luminescent intensity of the Ln(III) complexes.
- The asymmetry ratio ($R$) of all the complexes increases upon the addition of bicarbonate until reaching a plateau (10 - 20 mM bicarbonate).
- The Ln(III) complexes with bpcd present the most sensitive response towards bicarbonate concentration, especially in the range 0 - 10 mM, a decisive bicarbonate concentration range for the diagnosis of metabolic acidosis.

## 5.4. First steps towards the sensing of citrate

### 5.4.1. Introduction

Citrate has the p*K*a values 3.13, 4.76 and 6.40 at $T = 298.15$ K.[16] Thus, we expect to find it as a trianion at a physiological pH around 7.4 (Figure 5.16.).

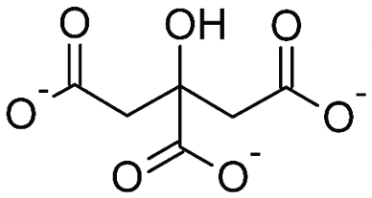


***Figure 5.16.*** *Citrate trianion.*

This anion is one of the key intermediates in the Krebs cycle of anaerobic cells and plays an important role in glycolysis.[16,55] Therefore, it is not difficult to deduce that it may be a good biomarker for certain anomalies in the organism. In fact, it is well known that low levels of citrate in urine (usually around 10 - 12 µmol/g) may diagnose diverse kidney dysfunctions and even prostate cancer (1 - 3 µmol/g).[55] This fact alone would already be a good pretext for the development and study of potential citrate probes but, furthermore, the assessment of the affinity for citrate of probes initially developed for the sensing of other biomarkers is also interesting in order to study the possible competence between potentially-interfering molecules currently found in the fluids of interest.

In literature we find several examples studying citrate as either just a mere potential interfering[35,47,48,52,56–60] or by actually quantifying its affinity towards the studied probe[16,49–51,53,61,62]. In Table 5.8. we present some affinity constants found in literature for luminescent lanthanide complexes towards citrate. Also the charges of the binary complexes are reported, as the coulombic interactions between complex and citrate strongly affect the stability of these ternary complexes. It can be appreciated that the affinity constants are higher for the positively-charged Ln(III) complexes, which makes sense, since the interaction of the positively-charged Ln(III) complexes with citrate (with three negative charges) would be favoured by coulombic attraction.

***Table 5.8.*** *Apparent affinity constants of some luminescent Ln(III) complexes towards citrate, T = 298.15 K, μ = 0.1 M NaCl, pH = 7.4. The highest value found in each reference is reported. Also the total charge of the adducts is reported * T = 295 K, ** 0.1 M NaCl, 4 mM KCl, 0.1 M HEPES and 0.9 mM $NaH_2PO_4$, *** 10 mM $ZnCl_2$*

| REF. | Murray[49] 2008 | Pal[62] 2009 | Smith[51] 2011 | Smith[50] 2012 | Butler[53] 2013 | Mc Mahon[61] 2014 |
|---|---|---|---|---|---|---|
| **log *K*** | 6.02 | 5.26** | 5.21 | 4.80* | 3.65 | 3.95*** |
| **Q binary complex** | +3 | +3 | +3 | +3 | -1 | +1 |

Recently, we have begun our studies with citrate by using the Ln(III) complexes already discussed in this thesis. The first step has been assessing the luminescent response and affinity of some of these complexes upon increasing concentration of citrate.

## 5.4.2. First results

Emission luminescence batch analyses were performed with $[Tb(bpcd)]^+$, Tb(PyC3A) ($\lambda_{exc}$ = 265 nm ) and Eu(QC3A) ($\lambda_{exc}$ = 318 nm ) complexes (0.1 mM) at diverse citrate concentration (typically around 20 points from 0.001 mM to 7 mM). All experiments have been performed at pH 7.4 in 3-(N-morpholino)propanesulfonic acid (MOPS) buffer and 0.9% NaCl. The data treatment has been performed with the cEST program for MS excel (Section 3.4.3.). The constants found for the three adducts with citrate are presented in Table 5.9..

***Table 5.9.*** *Apparent affinity constants found for some Ln(III) complexes with citrate at room temperature, pH = 7.4, in MOPS buffer, 0.9% NaCl.*

| Complex | $[Tb(bpcd)]^+$ | [Tb(PyC3A)] | [Eu(QC3A)] |
|---|---|---|---|
| **log *K*** | 5.31 ± 0.30 | 3.76 ± 0.13 | 4.31 ± 0.08 |

The highest affinity constant with citrate was obtained, as expected (coulombic attraction), by the cationic complex but, surprisingly, the value is comparable with the constants found in literature for more positively-charged Ln(III) complexes. That may be

due to the lower steric hindrance present in the complex we propose in comparison with those in literature, with more rigid, pre-organized coordination sites.

### 5.4.3. First conclusions

Regarding the luminescent response of the complexes upon diverse citrate concentrations and the relatively high affinity constants obtained for the citrate adducts, we may say that they are, especially the cationic $[Tb(bpcd)]^{+}$, promising probes for the sensing of this biomarker.

## 5.5. Comparison of the results obtained

Even if the luminescent response and stability of the studied Ln(III) complexes seems adequate for their use as either, lactate, bicarbonate or citrate probes, at physiological pH and ionic strength, it is also important to consider that these molecules are not found isolated in real matrices. Hence, we should also take into account i) which molecules are usually present in the concerned matrix, ii) their concentration in that medium and iii) their affinity towards the studied probe.

***Table 5.10.*** *Apparent affinity constants found for the Ln(III) complexes proposed in this work with the studied biomarkers, at T = 298.15 K, pH = 7.4 and μ = 0.1 M NaCl. *When more than a constant value was reported for the same adduct (different data processing or technique, diverse isomers), the mean value is reported.* §2:1 adducts (biomarker : Ln(III) complex)

| Complex | Lac | Bic | Cit |
|---|---|---|---|
| **Eu(bpcd)$^+$** | - | 5.80*§ | - |
| **Tb(bpcd)$^+$** | 1.35* | 5.94 § | 5.31 |
| **Eu(bQcd)$^+$** | - | 4.62 § | - |
| **Eu(PyC3A)** | - | 2.08* | - |
| **Tb(PyC3A)** | - | - | 3.76 |
| **Eu(QC3A)** | - | 3.11 | 4.31 |

As a first approximation, we will discuss the viability of our Ln(III) complexes as potential probes for either of the biomarkers already discussed in view of the results and conclusions obtained so far. In order to ease the discussion, all the apparent stability constants obtained for L-lactate (Lac), bicarbonate (Bic) and citrate (Cit) with the Ln(III) complexes of study have been collected in Table 5.10.. The [Tb(bpcd)]$^+$ complex has presented the best results in terms of both luminescent response and affinity towards the target biomarker. Thus, we will focus on it for this comparative analysis.

In order to estimate the possible speciation of the [Tb(bpcd)]$^+$ complex in the presence of Lac, Bic and Cit in real matrices, some speciation simulations have been performed using the Hyss program. We have studied the potential speciation in intra and extracellular fluids by using the adequate concentrations for all the biomarkers (Table 5.6.) and a model of study considering the expected species and their stability constants (Table 5.11.).

***Table 5.11.*** *Model used for the speciation simulation. The logβ are the overall formation constants of the species at T = 298.15 K and μ = 0.1 NaCl. *Values determined in this work. Charges omitted for clarity.* [63] *μ = 0.7 $NaClO_4$.*

| *log*β | bpcd | Lac | Bic | Cit | H | Tb |
|---|---|---|---|---|---|---|
| 9.72* | 1 | 0 | 0 | 0 | 1 | 0 |
| 15.59* | 1 | 0 | 0 | 0 | 2 | 0 |
| 18.53* | 1 | 0 | 0 | 0 | 3 | 0 |
| 20.75* | 1 | 0 | 0 | 0 | 4 | 0 |
| 3.86[16] | 0 | 1 | 0 | 0 | 1 | 0 |
| 2.95[22] | 0 | 1 | 0 | 0 | 0 | 1 |
| 5.21[22] | 0 | 2 | 0 | 0 | 0 | 1 |
| 6.36[22] | 0 | 3 | 0 | 0 | 0 | 1 |
| 6.4[16] | 0 | 0 | 0 | 1 | 1 | 0 |
| 11.16[16] | 0 | 0 | 0 | 1 | 2 | 0 |
| 14.29[16] | 0 | 0 | 0 | 1 | 3 | 0 |
| 7.15[64] | 0 | 0 | 0 | 1 | 0 | 1 |
| 12.18[64] | 0 | 0 | 0 | 2 | 0 | 1 |
| 5.73[63] | 0 | 0 | 1 | 0 | 0 | 1 |
| 10.26[63] | 0 | 0 | 2 | 0 | 0 | 1 |
| 9.87[42] | 0 | 0 | 1 | 0 | 1 | 0 |
| 15.98[42] | 0 | 0 | 1 | 0 | 2 | 0 |
| 11.36* | 1 | 0 | 0 | 0 | 0 | 1 |
| 2.04* | 1 | 0 | 0 | 0 | -1 (OH) | 1 |
| 12.71* | 1 | 1 | 0 | 0 | 0 | 1 |
| 17.3* | 1 | 0 | 2 | 0 | 0 | 1 |
| 16.67* | 1 | 0 | 0 | 1 | 0 | 1 |
| 13.78 | 0 | 0 | 0 | 0 | -1 (OH) | 0 |

In literature we find several studies regarding *in vivo* sensing experiments with Ln(III) complexes, and the concentrations of complex in this works typically range from 0.02 mM to 10 mM,[47,49–51,53,65–67] Thus, all the simulations have been studied at diverse concentrations of complex in the range 0.02 - 10 mM. As it can be seen in Table 5.6., the concentration of Lac may vary considerably depending on the cell of study or the extracellular fluid, therefore calculations have been done considering diverse Lac concentrations. For Bic and Cit, the mean concentration in intracellular or extracellular fluids has been considered.

In Figures 5.17. and 5.18., ten estimations of the speciation in intra and extracellular fluids (respectively), taking into account the cited considerations, are presented. The highly-emitting species (the ones containing the complex, i.e. both the antenna and the emitting lanthanide) are represented with solid lines, and the colours represent the diverse species of Bic (blue), Lac (green) and Cit (orange). The pairs of Figures 5.17.a-b (intracellular, 0.02 mM complex), 5.17.c-d (intracellular, 2.5 mM complex), 5.18.a-b (extracellular, 0.02 mM complex) and 5.18.c-d (extracellular, 2.5 mM complex) are, respectively, very

similar between them (independently from the Lac concentration used), especially around pH 7.4. On the other hand, we observe important differences between Figures 5.17.e-f (intracellular, 10 mM complex) and, in addition, more than one emitting species is present at notable concentration at pH 7.4.

In Figures 5.17. a-b and 5.18.a-b, both predominant species at pH 7.4 are Cit species, but just one of them, the Cit adduct with the Tb complex, is a strongly-emitting species. In figures 5.17.c-d, this Cit adduct is clearly predominant at that pH. Thus, we may say that, so far, the $[Tb(bpcd)]^+$ complex would seem a promising probe for Cit under the studied conditions, but it would be necessary to avoid high complex concentrations in order to evade the lack of selectivity observed in Figures 5.17.e-f and the predominance of the binary complex observed in Figures 5.18.c-d.

The luminescent response of the complex in the presence of Cit has been studied for a concentration of complex of 0.04 mM and concentrations of Cit in the range 0.001-3 mM (Figure 5.19.). The response is sensitive towards Cit concentration up to 0.5 mM. Regarding that the typical concentrations of Cit in intracellular fluids go from 2 to 4 mM, it would be useful to sense concentrations up to, at least, 2-3 mM, in order to unambiguously diagnose potential metabolic problems directly linked to low Cit concentrations (Section 5.4.1.).

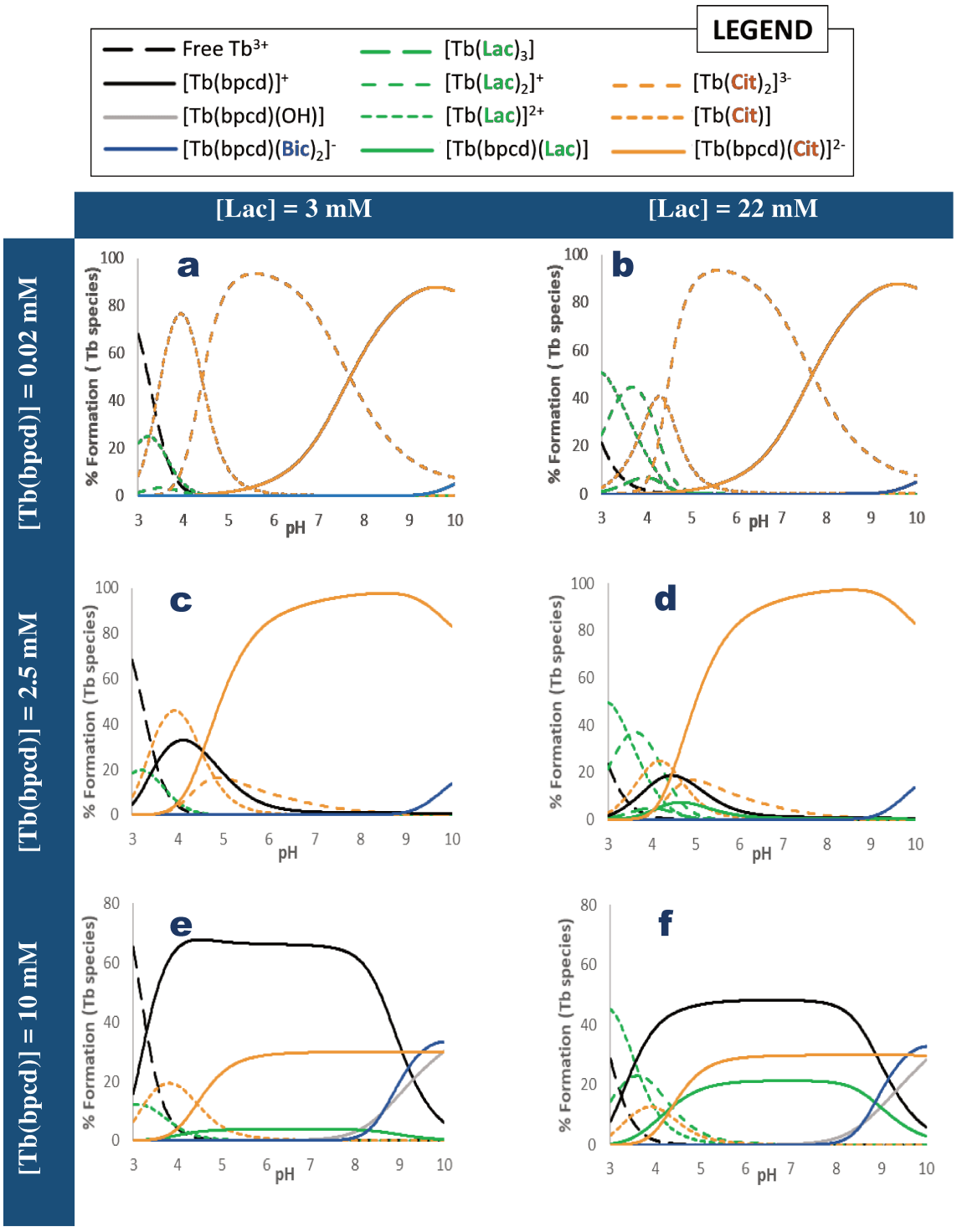


***Figure 5.17.*** *Estimated speciation of the Tb(III) species in intracellular fluid considering the* $[Tb(bpcd)]^+$ *complex, Lac (concentrations reported in the figure), Bic (11 mM) and Cit (3 mM) species. The solid lines correspond to highly-luminescent emitting species (containing both, the pyridine antenna and the emitting Tb(III)). Charges and species below 4% formation omitted for clarity.*

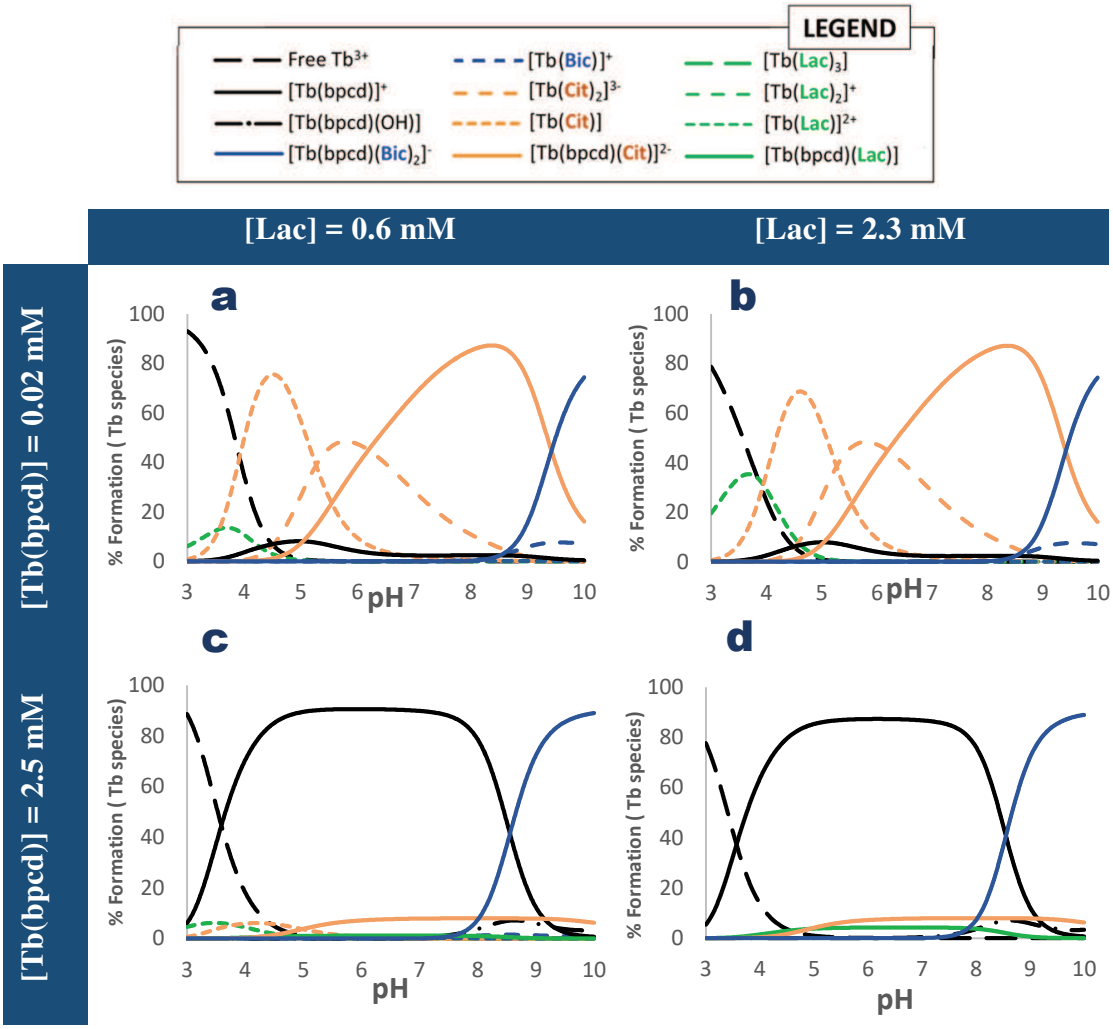


***Figure 5.18.*** *Estimated speciation of the Tb(III) species in extracellular fluid considering the* $[Tb(bpcd)]^+$ *complex, Lac (concentrations reported in the figure), Bic (25.5 mM) and Cit (0.2 mM) species. The solid lines correspond to highly-luminescent emitting species (containing both, the pyridine antenna and the emitting Tb(III)). Charges and species below 4% formation omitted for clarity.*

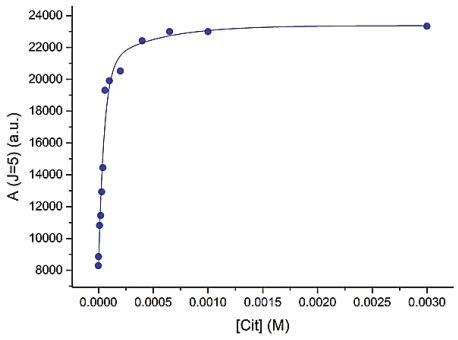


***Figure 5.19.*** *Luminescent response (area under the* $^5D_4 \rightarrow {}^7F_j$ *peak, j=5) of the* $[Tb(bpcd)]^+$ *complex (0.04 mM) in the presence of diverse concentrations of Cit. Dots represent the experimental points, the solid line represents the fitting obtained by the cEST program.*

## 5.6. Bibliography


[1] K. Gajda-Schrantz, L. Nagy, T. Fiore, L. Pellerito, T. Gajda, *J. Chem. Soc. Dalt. Trans.* **2002**, 152.

[2] O. N. Okorie, P. Dellinger, *Crit. Care Clin.* **2011**, *27*, 299–326.

[3] L. Rassaei, W. Olthuis, S. Tsujimura, E. J. R. Sudhölter, A. Van Den Berg, *Anal. Bioanal. Chem.* **2014**, *406*, 123–137.

[4] F. Alam, S. RoyChoudhury, A. H. Jalal, Y. Umasankar, S. Forouzanfar, N. Akter, S. Bhansali, N. Pala, *Biosens. Bioelectron.* **2018**, *117*, 818–829.

[5] R. P. Dellinger, M. M. Levy, A. Rhodes, D. Annane, H. Gerlach, S. M. Opal, J. E. Sevransky, C. L. Sprung, I. S. Douglas, R. Jaeschke, et al., *Intensive Care Med.* **2013**, *39*, 165–228.

[6] J. J. Todd, *Biosci. Horizons* **2014**, *7*, 1–7.

[7] N. Nikolaus, B. Strehlitz, *Microchim. Acta* **2008**, *160*, 15–55.

[8] S. Q. Liu, *Int. J. Food Microbiol.* **2003**, *83*, 115–131.

[9] A. G. Feldman, R. J. Sokol, R. M. Hardison, E. M. Alonso, R. H. Squires, M. R. Narkewicz, Pediatric Acute Liver Failure Study Group, *J. Pediatr.* **2017**, *182*, 217–222.e3.

[10] P. Sundaramoorthy, J. J. Sim, Y. S. Jang, S. K. Mishra, K. Y. Jeong, P. Mander, O. B. Chul, W. S. Shim, S. H. Oh, K. Y. Nam, et al., *PLoS One* **2015**, *10*, 1–15.

[11] J. M. Lupo, A. P. Chen, M. L. Zierhut, R. A. Bok, C. H. Cunningham, J. Kurhanewicz, D. B. Vigneron, S. J. Nelson, *Magn. Reson. Imaging* **2010**, *28(2)*, 153–162.

[12] C. Henchcliffe, D. C. Shungu, X. Mao, C. Huang, M. J. Nirenberg, B. G. Jenkins, M. F. Beal, *Ann. N. Y. Acad. Sci.* **2008**, *1147*, 206–220.

[13] G. Broder, M. H. Weil, *Am. Assoc. Adv. Sci.* **1964**, *143*, 1457–1459.

[14] J. P. and P. V. A. M. Spehar-Deleze, S. Anastasova, in *2012 Ninth Int. Conf. Wearable Implant. Body Sens. Networks*, **2012**, pp. 17–21.

[15] T. Shimomura, T. Sumiya, M. Ono, T. Itoh, T. Hanaoka, *Procedia Chem.* **2012**, *6*, 46–51.

[16] S. J. Butler, D. Parker, *Chem. Soc. Rev.* **2013**, *42*, 1652–1666.

[17] W. C. Stanley, E. W. Gertz, J. a Wisneski, D. L. Morris, R. a Neese, G. a Brooks, *Am. J. Physiol.* **1985**, *249*, E595–E602.

[18] M. L. Goodwin, J. E. Harris, A. Hernández, L. B. Gladden, *J. Diabetes Sci. Technol.* **2007**, *1*, 558–569.

[19] D. B. M. Groegel, M. Link, A. Duerkop, O. S. Wolfbeis, *ChemBioChem* **2011**, *12*, 2779–2785.

[20] P. Polese, M. Tolazzi, A. Melchior, *J. Therm. Anal. Calorim.* **2018**, *2*, DOI 10.1007/s10973-018-7409-2.

[21] H. Deelstra, F. Verbeek, *Anal. Chim. Acta* **1964**, *31*, 251–257.

[22] M. Nilsson, K. L. Nash, *Solvent Extr. Ion Exch.* **2007**, *25*, 665–701.

[23] A. Barkleit, J. Kretzschmar, S. Tsushima, M. Acker, *Dalt. Trans.* **2014**, *43*, 11221–11232.

[24] J. Tomasi, B. Mennucci, R. Cammi, *Chem. Rev.* **2005**, *105*, 2999–3093.

[25] L. E. Roy, L. R. Martin, *Dalt. Trans.* **2016**, *45*, 15517–15522.

[26] C. M. G. dos Santos, A. J. Harte, S. J. Quinn, T. Gunnlaugsson, *Coord. Chem. Rev.* **2008**, *252*, 2512–2527.

[27] M. H. V. Werts, *Sci. Prog.* **2005**, *88*, 101–131.

[28] T. Wu, X. Z. You, P. Bouř, *Coord. Chem. Rev.* **2015**, *284*, 1–18.

[29] T. aki Uchida, K. Nozaki, M. Iwamura, *Chem. - An Asian J.* **2016**, *11*, 2415–2422.

[30] A. P. S. Samuel, J. L. Lunkley, G. Muller, K. N. Raymond, *Eur. J. Inorg. Chem.* **2010**, 3343–3347.

[31] S. Petoud, G. Muller, E. G. Moore, J. Xu, J. Sokolnicki, J. P. Riehl, U. N. Le, S. M. Cohen, K. N. Raymond, *J. Am. Chem. Soc.* **2007**, *129*, 77–83.

[32] J. R. Brandt, X. Wang, Y. Yang, A. J. Campbell, M. J. Fuchter, *J. Am. Chem. Soc.* **2016**, *138*, 9743–9746.

[33] M. L. Aulsebrook, B. Graham, M. R. Grace, K. L. Tuck, *Coord. Chem. Rev.* **2018**, *375*, 191–220.

[34] E. R. Neil, D. Parker, *RSC Adv.* **2017**, *7*, 4531–4540.

[35] R. Carr, R. Puckrin, B. K. McMahon, R. Pal, D. Parker, L. O. Pålsson, *Methods Appl. Fluoresc.* **2014**, *2*, DOI 10.1088/2050-6120/2/2/024007.

[36] F. Zinna, T. Bruhn, C. A. Guido, J. Ahrens, M. Bröring, L. Di Bari, G. Pescitelli, *Chem. - A Eur. J.* **2016**, *22*, 16089–16098.

[37] G. Tircsó, M. Regueiro-Figueroa, V. Nagy, Z. Garda, T. Garai, F. K. Kálmán, D. Esteban-Gómez, É. Tóth, C. Platas-Iglesias, *Chem. - A Eur. J.* **2016**, *22*, 896–901.

[38] J. Gregoliński, J. Lisowski, *Angew. Chemie - Int. Ed.* **2006**, *45*, 6122–6126.

[39] J. Yuasa, T. Ohno, H. Tsumatori, R. Shiba, H. Kamikubo, M. Kataoka, Y. Hasegawa, T. Kawai, *Chem. Commun.* **2013**, *49*, 4604.

[40] R. S. Dickins, J. A. K. Howard, C. L. Maupin, J. M. Moloney, D. Parker, J. P. Riehl, G. Siligardi, J. A. G. Williams, *Chem. - A Eur. J.* **1999**, *5*, 1095–1105.

[41] E. De Madaria, I. Herrera-Marante, V. González-Camacho, L. Bonjoch, N. Quesada-Vazquez, I. Almenta-Saavedra, C. Miralles-Maciá, N. G. Acevedo-Piedra, M. Roger-Ibáñez, C. V Sánchez-Marin, et al., *United Eur. Gastroenterol. J.* **2016**, *6*, 63–72.

[42] S. He, J. W. Morse, *Geochim. Cosmochim. Acta* **1993**, *57*, 3533–3554.

[43] M. Damaghi, J. W. Wojtkowiak, R. J. Gillies, *Front. Physiol.* **2013**, *4*, 1–10.

[44] J. D. Kopple, K. Kalantar-Zadeh, R. Mehrotra, *Kidney Int. Suppl.* **2005**, *67*, 21–27.

[45] J. Buck, L. R. Levin, *Sensors* **2011**, *11*, 2112–2128.

[46] E. Boedtkjer, V. V. Matchkov, D. M. B. Boedtkjer, C. Aalkjaer, *Physiology* **2016**, *31*, 370–383.

[47] Y. Bretonniere, M. J. Cann, D. Parker, R. Slater, *Org. Biomol. Chem.* **2004**, *2*, 1624–1632.

[48] Y. Bretonnière, M. J. Cann, D. Parker, R. Slater, *Chem. Commun.* **2002**, *8*, 1930–1931.

[49] B. S. Murray, E. J. New, R. Pal, D. Parker, *Org. Biomol. Chem.* **2008**, *6*, 2085–2094.

[50] D. G. Smith, R. Pal, D. Parker, *Chem. - A Eur. J.* **2012**, *18*, 11604–11613.

[51] D. G. Smith, G. L. Law, B. S. Murray, R. Pal, D. Parker, K. L. Wong, *Chem. Commun.* **2011**, *47*, 7347–7349.

[52] D. Imperio, G. B. Giovenzana, G. L. Law, D. Parker, J. W. Walton, *Dalt. Trans.* **2010**, *39*, 9897–9903.

[53] S. J. Butler, B. K. McMahon, R. Pal, D. Parker, J. W. Walton, *Chem. - A Eur. J.* **2013**, *19*, 9511–9517.

[54] R. M. Smith, A. E. Martell, *Sci. Total Environ.* **1987**, *64*, 125–147.

[55] J. C. G. Bünzli, *Chem. Rev.* **2010**, *110*, 2729–2755.

[56] G. Tircsó, Z. Garda, F. K. Kálmán, Z. Baranyai, I. Pócsi, G. Balla, I. Tóth, *J. Inorg. Biochem.* **2013**, *127*, 53–61.

[57] S. Comby, S. A. Tuck, L. K. Truman, O. Kotova, T. Gunnlaugsson, *Inorg. Chem.* **2012**, *51*, 10158–10168.

[58] X. L. Du, T. L. Zhang, L. Yuan, Y. Y. Zhao, R. C. Li, K. Wang, S. C. Yan, L. Zhang, H. Sun, Z. M. Qian, *Eur. J. Biochem.* **2002**, *269*, 6082–6090.

[59] R. S. Dickins, T. Gunnlaugsson, D. Parker, R. D. Peacock, *Chem. Commun.* **1998**, 1643–1644.

[60] D. G. Smith, B. K. McMahon, R. Pal, D. Parker, *Chem. Commun.* **2012**, *48*, 8520–8522.

[61] B. K. McMahon, D. Parker, *RSC Adv.* **2014**, *4*, 37649–37654.

[62] R. Pal, D. Parker, L. C. Costello, *Org. Biomol. Chem.* **2009**, *7*, 1525–1528.

[63] X. Liu, R. H. Byrne, *J. Solution Chem.* **1998**, *27*, 803–815.

[64] A. OHYOSHI, **1972**, *34*, 1955–1960.

[65] J. W. Walton, A. Bourdolle, S. J. Butler, M. Soulie, M. Delbianco, B. K. McMahon, R. Pal, H. Puschmann, J. M. Zwier, L. Lamarque, et al., *Chem. Commun.* **2013**, *49*, 1600–1602.

[66] J. Vuojola, T. Soukka, *Methods Appl. Fluoresc.* **2014**, *2*, DOI 10.1088/2050-6120/2/1/012001.

[67] M. Sy, A. Nonat, N. Hildebrandt, L. J. Charbonnière, *Chem. Commun.* **2016**, *52*, 5080–5095.

# Chapter 6

# General conclusions and future outlook

The luminescent Ln(III) (Ln= Eu, Tb) complexes proposed in this work are stable at physiological ionic strength and pH, and are the predominant species in solution at pH 7.4. The pyridine-based ligands efficiently sensitize both, Eu(III) and Tb(III), and the former lanthanide is also sensitized by the quinoline-functionalized ones. Moreover, their total quantum yields are in the range of values found in literature for cell imaging, with higher values found for the Tb(III) complexes. In addition, all of them present quenching water molecules in the first coordination sphere, which we expected to be substituted by the target biomarkers, with the resulting rise in the luminescent response. And we actually observed this behavior in the presence of L-lactate (Lac), bicarbonate (Bic) and citrate (Cit).

The Lac adduct with $[Tb(bpcd)]^+$ is stable under physiological conditions and, as expected, the luminescent response of the complex increased upon addition of Lactate. The racemic complex exhibits CPL activity in the presence of Lac, which permitted the sensing of this biomarker in a commercial medical solution containing Lac among other non-chiral electrolytes.

The Bic adducts with the Ln(III) complexes of study are stable under physiological conditions. The cationic complexes $[Eu(bpcd)]^+$, $[Tb(bpcd)]^+$ and $[Eu(bQcd)]^+$ are the most stable ones, and can bind up to two bicarbonate molecules. As in the case of Lac, the luminescence response of the Ln(III) complexes proposed clearly changes upon the addition of Bic, and the asymmetry ratio increases. The most sensitive response is achieved by the $[Tb(bpcd)]^+$ complex, especially in the range 0-10 mM of Bic, whith is particularly interesting for the diagnosis of metabolic acidosis.

Some preliminary studies have been performed regarding the sensing of Cit. The Ln(III) complexes studied form stable adducts with this biomarker, being the $[Tb(bpcd)]^+$ complex the most stable. The luminescent response of this complex also increased upon addition of Cit.

Speciation simulations have been performed by using the constants obtained during this work and in literature, the usual concentrations of the biomarkers under study in cells and the typical concentrations of complex used in *in vivo* luminescent experiments. We observed that the $[Tb(bpcd)]^+$ complex may selectively sense Cit in the presence of Lac and Bic, which makes this complex a very promising probe for the sensing of this biomarker.

In regard of the results obtained, it would be interesting to perform further luminescent titrations of the Tb complex in the presence of Cit, but using higher concentration of complex, which might increase the sensibility of the response. In addition, supplementary experiments should be performed in order to complete an extensive study on the affinity and luminescent response of all the complexes proposed with Lac, Bic, Cit and further biomarkers and interfering molecules, for instance phosphate and ATP. Also additional CPL studies may be performed for the adducts with the chiral molecules under study, such as citrate.After that, the next step would be to test the most promising probes *in vivo*, in order to test cell viability and permeability towards the selected sensors, which would lead our luminescent probes one step closer to their actual application in diagnosis.

# Annex

# List of publications and communications

## PUBLICATIONS

2018 Dalton Transactions (Pending publication with **intern front cover**)

*F. Piccinelli, C. de Rosa, A. Melchior, G. Faura, M. Tolazzi, M. Bettinelli*

**Eu(III) and Tb(III) complexes of 6-fold coordinating ligands showing high affinity for bicarbonate ion: a spectroscopic and thermodynamic study**

2018 New Journal of Chemistry, 42, 7931-7939 (DOI: 10.1039/c7nj04640e)

*M. Leonzio, A. Melchior, G. Faura, M. Tolazzi, M. Bettinelli, F. Zinna, L. Arrico, L. Di Bari and F. Piccinelli*

**A chiral lactate reporter based on total and circularly polarized Tb(III) luminescence**

2017 Inorganic Chemistry, 56, 4413-4422 (DOI: 10.1021/acs.inorgchem.7b00430)

M. Leonzio, A. Melchior, G. Faura, M. Tolazzi, F. Zinna, L. Di Bari and F. Piccinelli

**Strongly Circularly Polarized Emission from Water-Soluble Eu(III)- and Tb(III)-Based Complexes: A Structural and Spectroscopic Study**

2016 Inorganica Chimica Acta, 453, 751-756 (DOI: 10.1016/j.ica.2016.09.047)

F. Piccinelli, M. Leonzio, M. Bettinelli, A. Melchior, G. Faura and M. Tolazzi

**Luminescent $Eu^{3+}$ complexes in acetonitrile solution: Anion sensing and effect of water on the speciation**

## COMMUNICATIONS

9-12/09/2018 XI CONVEGNO NAZIONALE AICIng - *Bologna, Italy*

Poster: M. Tolazzi*, F. Piccinelli, C. de Rosa, A. Melchior, G. Faura, Marco Bettinelli

***Spectroscopic and Thermodynamic Studies on Complexes of Eu (III) and Tb (III) with Affinity for the Bicarbonate Ion***

3-6/09/2018 10th INTERNATIONAL CONFERENCE ON f-ELEMENTS - *Lausanne, Switzerland* ***[JUNIOR GRANT]***

Poster: G. Faura*, F. Piccinelli, C. de Rosa, A. Melchior, M. Tolazzi and M. Bettinelli

***Putting some light on sensing of biomarkers; trivalent lanthanide complexes as luminescent bioprobes***

3-7/06/2018 INTERNATIONAL SYMPOSIUM ON METAL COMPLEXES – Florence (Italy)

Poster: F. Piccinelli, C. de Rosa, A. Melchior, G. Faura, M. Tolazzi*, and M. Bettinelli

**$Eu^{3+}$ and $Tb^{3+}$ complexes with polyaminocarboxylate ligands: a spectroscopic and thermodynamic study**

16-18/05/2018 5th INTERNATIONAL CONFERENCE ON RARE EARTH MATERIALS - *Wrocław, Poland*

Invited speaker: F. Piccinelli*, C. De Rosa, A. Melchior, M. Tolazzi, G. Faura, L. Arrico, L. Di Bari and M. Bettinelli

**Chiral anion reporters based on total and circularly polarized Eu(III) and Tb(III) luminescence**

12-13/06/2017 VII WORKSHOP AICIng - *Milan, Italy*

Poster: G. Faura*, A. Melchior and M. Tolazzi,
**Synthesis of $Fe_3O_4$@$SiO_2$-DFO Nanoparticles for Lanthanide(III) recovery.**

7-10/06/2017 INTERNATIONAL SYMPOSIUM ON METAL COMPLEXES - *Dijon, France*

Oral communication: A. Melchior*, F. Piccinelli, L. Di Bari, G. Faura, M. Leonzio, F. Zinna, M. Tolazzi, M. Bettinelli
**Luminescent lanthanide(III) complexes for anions sensing: Spectroscopy, speciation and modelling studies**

11-14/09/2016 X CONVEGNO NAZIONALE AICIng - *Udine, Italy*

* Member of the organizing committee

Poster: F. Piccinelli, M. Trevisani, M. Leonzio, M. Bettinelli, A. Melchior, G. Faura*, and M. Tolazzi
***Luminescent Eu3+ complexes in acetonitrile solution: anions sensing and effect of water on the speciation.***